

AEDC-TR-95-18

TECHNICAL REPORT
FEB 1996

OCT 28 1996

**A Comparison of an AEDC and a Russian Developed
Pressure Sensitive Paint in the AEDC
Propulsion Wind Tunnel 16T**

M. E. Sellers
Micro Craft Technology/AEDC Operations

PROPERTY OF U.S. AIR FORCE
AEDC TECHNICAL LIBRARY

December 1995

Final Report for Period April 23-28, 1995

Approved for public release; distribution is unlimited.

**ARNOLD ENGINEERING DEVELOPMENT CENTER
ARNOLD AIR FORCE BASE, TENNESSEE
AIR FORCE MATERIEL COMMAND
UNITED STATES AIR FORCE**



NOTICES

When U. S. Government drawings, specifications, or other data are used for any purpose other than a definitely related Government procurement operation, the Government thereby incurs no responsibility nor any obligation whatsoever, and the fact that the Government may have formulated, furnished, or in any way supplied the said drawings, specifications, or other data, is not to be regarded by implication or otherwise, or in any manner licensing the holder or any other person or corporation, or conveying any rights or permission to manufacture, use, or sell any patented invention that may in any way be related thereto.

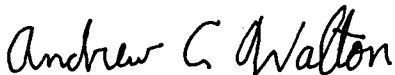
Qualified users may obtain copies of this report from the Defense Technical Information Center.

References to named commercial products in this report are not to be considered in any sense as an endorsement of the product by the United States Air Force or the Government.

This report has been reviewed by the Office of Public Affairs (PA) and is releasable to the National Technical Information Service (NTIS). At NTIS, it will be available to the general public, including foreign nations.

APPROVAL STATEMENT

This report has been reviewed and approved.



ANDREW C. WALTON, 1st Lt, USAF
Technology Project Manager
Applied Technology Division
Test Operations Directorate

Approved for publication:

FOR THE COMMANDER



ROBERT T. CROOK
Assistant Chief, Applied Technology Division
Test Operations Directorate

REPORT DOCUMENTATION PAGE			Form Approved OMB No. 0704-0188	
Public reporting burden for this collection of information is estimated to average 1 hour per response, including the time for reviewing instructions, searching existing data sources, gathering and maintaining the data needed, and completing and reviewing the collection of information. Send comments regarding this burden estimate or any other aspect of this collection of information, including suggestions for reducing this burden, to Washington Headquarters Services, Directorate for Information Operations and Reports, 1215 Jefferson Davis Highway, Suite 1204, Arlington, VA 22202-4302, and to the Office of Management and Budget, Paperwork Reduction Project (0704-0188), Washington, DC 20503.				
1. AGENCY USE ONLY (Leave blank)		2. REPORT DATE December 1995		3. REPORT TYPE AND DATES COVERED Final Report for Period April 23 - 28, 1995
4. TITLE AND SUBTITLE A Comparison of an AEDC and a Russian Developed Pressure Sensitive Paint in the AEDC Propulsion Wind Tunnel 16T			5. FUNDING NUMBERS PE - 65130D	
6. AUTHOR(S) Sellers, M.E., Micro Craft Technology/AEDC Operations				
7. PERFORMING ORGANIZATION NAME(S) AND ADDRESS(ES) Arnold Engineering Development Center/DOF Air Force Materiel Command Arnold Air Force Base, TN 37389-6000			8. PERFORMING ORGANIZATION (REPORT NUMBER) AEDC-TR-95-18	
9. SPONSORING/MONITORING AGENCY NAME(S) AND ADDRESS(ES) Arnold Engineering Development Center/DOT Air Force Materiel Command Arnold Air Force Base, TN 37389-9011			10. SPONSORING/MONITORING AGENCY REPORT NUMBER	
11. SUPPLEMENTARY NOTES Available in Defense Technical Information Center (DTIC).				
12A. DISTRIBUTION/AVAILABILITY STATEMENT Approved for public release; distribution is unlimited.			12B. DISTRIBUTION CODE	
13. ABSTRACT (Maximum 200 words) A comparison of a pressure sensitive paint (PSP) developed at Arnold Engineering Development Center (AEDC) with a PSP developed in Russia was performed in the AEDC Propulsion Wind Tunnel 16T. A Generic Wall Interference Model similar to an old AEDC model used to study wall interference effects was fabricated at the Central Aerohydrodynamics Institute (TsAGI) in Zhukovsky, Russia. The model has been tested in TsAGI's T-128 wind tunnel, and was sent to AEDC with the balance and sting support hardware for the 16T test. The AEDC PSP and the Russian PSP were applied to separate wings of the model. Conventional pressure, PSP, and force data were acquired simultaneously at Mach numbers 0.60, 0.85, and 0.95 while angle of attack was varied from -10 to 10 deg. The stagnation pressure and temperature were also varied to permit evaluations of the pressure and temperature sensitivity of each paint. Comparisons of the conventional pressure and PSP measurements are presented.				
14. SUBJECT TERMS Pressure Sensitive Paint, transonic flow, wind tunnel test, force and moment data, surface pressure distribution			15. NUMBER OF PAGES 102	
			16. PRICE CODE	
17. SECURITY CLASSIFICATION OF REPORT UNCLASSIFIED	18. SECURITY CLASSIFICATION OF THIS PAGE UNCLASSIFIED	19. SECURITY CLASSIFICATION OF ABSTRACT UNCLASSIFIED	20. LIMITATION OF ABSTRACT SAME AS REPORT	

PREFACE

The work reported herein was conducted by the Arnold Engineering Development Center (AEDC), Air Force Materiel Command (AFMC), under Program Element 65130D, at the request of AEDC/DOT, Arnold AFB, TN 37389-6000. The AEDC project manager was Capt. Jay Cossentine. The results of the tests were obtained by Micro Craft Technology/AEDC Operations, support and technical service contractor for the aerospace flight dynamics test facilities at AEDC, AFMC, Arnold Air Force Base, TN. The analysis was performed during the period from May 1995 through August 1995 under AEDC Job Number 2171. This manuscript was submitted for publication on October 30, 1995.

CONTENTS

	<u>Page</u>
1.0 INTRODUCTION	5
1.1 Background.....	5
2.0 APPARATUS.....	7
2.1 Test Article.....	7
2.2 Pressure Sensitive Paint Application	7
2.3 PSP Data System	8
3.0 PROCEDURES	8
3.1 Test Conditions.....	8
3.2 Data Acquisition.....	9
3.3 PSP Data Reduction	9
4.0 RESULTS AND DISCUSSION	11
5.0 SUMMARY	13
REFERENCES.....	13

ILLUSTRATIONS

<u>Figure</u>	<u>Page</u>
1. Basic Luminescence Process	15
2. Luminescence as Described by the Stern-Volmer Model	16
3. PSP Temperature Sensitivity	17
4. Generic Wall Interference Model Details	18
5. PSP Data Acquisition System	19
6. Spectral Characteristics of AEDC PSP and L2 PSP	20
7. PSP Laboratory Calibration	21
8. AEDC PSP 2nd-Order Fit Coefficient Variation with Temperature	22
9. L2 PSP 2nd-Order Fit Coefficient Variation with Temperature	23
10. Temperature Calculation Comparison for AEDC PSP	24
11. Wing CP Comparison using Two Temperature Methods for AEDC PSP.....	36
12. Fuselage CP Comparison using Two Temperature Methods for AEDC PSP	48
13. AEDC and L2 PSP Comparison.....	60
14. Pressure Coefficient Distribution Comparison.....	79

TABLES

<u>Table</u>	<u>Page</u>
1. Pressure Orifice Designation and Location	93
2. Nominal Test Conditions	94
3. PSP Calibration Coefficients	94
4. Registration Mark Designation and Location	95
 NOMENCLATURE.....	 97

1.0 INTRODUCTION

Pressure sensitive paint (PSP) is a surface coating whose luminosity varies with local surface pressure when it is excited by light of an appropriate wavelength. The major advantages of using PSP are in its ability to provide a complete surface pressure distribution and to obtain information in areas where it is not possible to install pressure orifices. Unfortunately, the paints currently available also respond to changes in surface temperature, to varying magnitudes, which affects the accuracy of pressure determination. To make PSP a viable alternative to replacing conventional pressure instrumentation, the temperature sensitivity must be eliminated, or a way of simultaneously measuring the global surface temperature must be found.

The objective of this project was to conduct a comparative evaluation of pressure sensitive paints developed at the Arnold Engineering Development Center (AEDC) and by OPTROD Ltd. in Zhukovsky, Russia. Consequently, a test was performed in the AEDC Propulsion Wind Tunnel 16T to obtain pressure data with each paint and with standard pressure orifice instrumentation. A generic wall interference model, balance, and sting support equipment (designed and fabricated in Russia) were used during the test. The OPTROD and AEDC paints were applied to separate wings of the model. Data were acquired at Mach numbers 0.60, 0.85, and 0.95 while angle of attack was varied from -10 to 10 deg. The stagnation pressure (1,000 and 2,000 psfa) and temperature (90° and 120°F) were also varied to permit comparisons of PSP pressure and temperature sensitivity.

1.1 BACKGROUND

Employees at the Central Aerohydrodynamic Institute (TsAGI) in Zhukovsky, who formed the OPTROD company, developed several paints for use in wind tunnels in the early 1980's. OPTROD has two proprietary PSP formulations that they claim have little sensitivity to changes in temperature and do not require pressure orifice instrumentation for determination of surface pressure. One is used for shock tunnels (very fast response to change in pressure but not very durable) and the other for continuous-flow wind tunnels (adequate pressure response and very durable). The paint used for continuous-flow wind tunnels, designated L2, was chosen for comparison with the AEDC-developed paint to evaluate the relative performance characteristics in Tunnel 16T.

The paint developed at AEDC uses platinum octaethylporphyrin (PtOEP) for the pressure sensitive luminescent molecule and is very sensitive to changes in temperature, which results in surface pressure determination errors. Gross temperature changes from wind-off to wind-on conditions have been accounted for by using pressure orifice instrumentation to determine the relationship between the paint luminescence and surface pressure. However, this *in-situ* method of paint calibration does not account for temperature variations across the surface at the wind-on condition.

As described in Refs. 1 and 2, when the luminescent molecule (PtOEP or other) absorbs a photon of appropriate energy, the molecule enters an excited state. From this state, the molecule decays to the ground state through a series of transitions, with at least one resulting in the emission of a photon. Fluorescence is the emission of a photon with a lifetime on the order of 10^{-8} sec and arises from a singlet transition. In contrast, phosphorescence is a delayed emission with a lifetime on the order of 10^{-3} to 100 sec and arises from a triplet-singlet transition. Most luminescent molecules emit very little fluorescence and strong phosphorescence (which is measured). A schematic of the lowest energy level transitions is shown in Fig. 1. Since the energy decay resulting in the photon emission is never complete, the emitted photon will have less energy and, therefore, a longer wavelength than the original exciting photon. The shift in emission wavelength from the absorption wavelength permits the measurement of emission intensity, or luminescence, with the use of appropriate filters. An alternate transition to the ground state is provided by collision with an oxygen molecule. Rather than emitting a photon, the excess energy of the luminescent molecule is absorbed by the oxygen molecule during a collisional deactivation. Increasing amounts of oxygen increase the collisional deactivations, resulting in decreased luminescence. Since the number of oxygen molecules is directly proportional to the local pressure, low-pressure regions on the surface of a model will be brighter than those of high pressure. The process can be modeled using a simplified form of the Stern-Volmer relation:

$$\frac{I_0}{I} = 1 + K_q P_{O_2} \quad (1)$$

where I_0 is the PSP luminescence in the absence of oxygen, I and P_{O_2} are the PSP luminescence and partial pressure of oxygen at some pressure, respectively, and K_q is the Stern-Volmer constant. Presented in Fig. 2 is a graphic representation of the inverse of Eq. (1) for several Stern-Volmer constants, along with the characteristics of the AEDC PSP and L2 PSP. The AEDC PSP has a large K_q (approximately 0.9 at room temperature), which performs well at pressures near and below 0.5 atm, but does not have enough sensitivity to permit accurate measurement of pressures near or above 1 atm. The L2 PSP has a small K_q , which permits measuring pressures from vacuum to above 1 atm, but with lower pressure resolution at the lower pressure levels.

The PSP paint formulations have different sensitivities to changes in temperature which are not accounted for in Eq. (1). The temperature sensitivity of the AEDC PSP and L2 PSP is illustrated in Fig. 3. The curves have been normalized by the reference luminescence (I_{ref}) value measured at 1 atm and approximately 70°F. The paint sensitivity to pressure typically increases with increasing temperature. However, the AEDC and L2 luminescent molecules are destroyed at temperatures above 150° and 300°F, respectively. The AEDC PSP is considerably more sensitive to temperature than the L2 PSP.

2.0 APPARATUS

2.1 TEST ARTICLE

Details of the generic wall interference model (GWIM) are presented in Fig. 4. The GWIM is a scaled-up version of a model tested at AEDC in the late 70's to investigate an adaptive wall technique for removing wall interference effects. The model has a cylindrical body diameter of 8.661 in. with an elliptical nose. The wing and horizontal tail are symmetrical NACA 0012 airfoils with 30-deg swept-back leading and trailing edges. The model has a span of 51.964 in. and is 73.622 in. long. The fuselage, wing, and horizontal tail each have one row of pressure orifices. The surface pressures were measured using two 48-port electronically scanned pressure (ESP) modules mounted inside the model. The pressure orifice designations and locations are listed in Table 1. The model was mounted on a six-component balance to measure vehicle aerodynamic loads. An accelerometer (developed by TsAGI) was mounted inside the model to provide a secondary measurement of the model pitch attitude. The top surface of the starboard wing (with pressure orifices) was painted with the AEDC PSP, and the bottom surface of the port wing was painted with the L2 PSP.

2.2 PRESSURE SENSITIVE PAINT APPLICATION

Two layers of paint typically are applied to the model surface. The first is a white substrate that helps reflect the luminescent light away from the model surface. The second, the PSP layer, contains the luminescent molecule and is applied over the substrate. The OPTROD application uses a white epoxy paint for the substrate. The luminescent molecule in the L2 PSP is mixed with a polymer binder that is highly permeable to oxygen and is sprayed onto the epoxy paint. In this application, the PSP layer does not interact with the substrate. At least 48 hours is required for completion of the polymerization process in the PSP layer. The AEDC application uses Very High Temperature (VHT®) white paint as the substrate. The AEDC luminescent molecule is not suspended in a binder and is not oxygen sensitive until it bonds with the VHT. The AEDC PSP is sprayed onto the VHT and dries almost instantaneously.

2.3 PSP DATA SYSTEM

A schematic of the PSP data acquisition and processing system used during the test is shown in Fig. 5. The upper surface of the starboard wing was painted with the AEDC PSP and illuminated with xenon-arc lamps. Ninety percent or more of the light between 350 and 550 nm was reflected by two cold mirrors, each set at 67.5-deg incidence to the incoming light, through a short wave pass (SWP) dichroic filter designed to pass wavelengths below 550 nm. The filtered light from the xenon-arc lamps passed through optics which spread the light to a diameter of approximately 4 ft at the tunnel centerline. A shutter placed in front of each lamp was opened to pass light while images were being acquired. The luminescent light emitted by the paint passed to the camera through a hot mirror designed to reflect light above 700 nm, and a long wave pass (LWP) dichroic filter designed to pass light above 600 nm. A scientific grade CCD camera was used to obtain black-and-white images of the luminescent surface. The CCD array had $1,024 \times 1,024$ pixel spatial resolution and was digitized at 16-bit grey level resolution.

The lower surface of the port wing was painted with the L2 PSP. The model was rolled 180 deg to permit illumination of the PSP with similar xenon-arc lamps with additional output below 325 nm. Ninety percent or more of the light between 300 and 380 nm was reflected by a single cold mirror set at 45-deg incidence to the incoming light, through an absorption glass filter designed to pass wavelengths below 400 nm. The filtered light from the xenon-arc lamps passed through optics which spread the light to a diameter of approximately 4 ft at the tunnel centerline. A shutter placed in front of each lamp was opened to pass light while images were being acquired. The luminescent light emitted by the paint passed to the camera through a sandwich filter designed to pass light between 420 and 550 nm.

The AEDC and L2 PSP excitation and emission spectral characteristics, with each spectrum normalized by its peak output, are presented in Fig. 6, along with the filtered light source spectrum.

3.0 PROCEDURES

3.1 TEST CONDITIONS

The test was conducted at nominal Mach numbers of 0.60, 0.85, and 0.95 at total pressures of 1,000 and 2,000 psfa and total temperatures of approximately 90° and 120°F. The nominal test conditions established during the test are given in Table 2. The angle of attack was varied from -10 to 10 deg.

3.2 DATA ACQUISITION

Model aerodynamic loads data, conventional pressure data, and PSP images were acquired automatically under the control of the facility computer. The facility computer set the requested model attitude and signaled a personal computer (PC) to acquire a PSP image while the facility computer acquired the loads and conventional pressure data. The PC commanded the power supplies for the xenon-arc lamps to increase to full power and opened the shutter in front of each lamp. An image was acquired and stored on the workstation (see Fig. 5) hard drive via ethernet. The camera shutter exposure times varied from 0.3 to 0.9 sec, depending on the tunnel conditions and paint being tested. After the image was acquired, the lamp shutters were closed and the lamps were reduced to half power. The PC returned a signal, indicating the image had been stored, which allowed the facility computer to move the model to the next attitude. A file containing tunnel conditions and conventional pressure data was transferred from the facility computer to the workstation via ethernet. The data acquisition process took approximately 35 sec per point, with the majority of the time required for storing the image on the workstation hard disk.

3.3 PSP DATA REDUCTION

Determining I_0 in Eq. (1) is not practical in the wind tunnel environment. As described in Ref. 1, ratioing the intensities of an image at a known reference (wind-off) condition to an operating (wind-on) condition eliminates the need to determine I_0 . Also, the effects of nonuniformities in illumination and paint thickness on the amount of luminescence are eliminated. Equation (1) does not include any terms to account for the temperature sensitivity of the paints. To account for the paint temperature sensitivity, the AEDC PSP was modeled by the following equation to determine pressure:

$$P = (a_{00} + a_{01} \cdot T + a_{02} \cdot T^2 + a_{03} \cdot T^3) + (a_{10} + a_{11} \cdot T + a_{12} \cdot T^2 + a_{13} \cdot T^3) \cdot \frac{I_{ref}}{I} + (a_{20} + a_{21} \cdot T + a_{22} \cdot T^2 + a_{23} \cdot T^3) \cdot \left(\frac{I_{ref}}{I}\right)^2 \quad (2)$$

where I_{ref} is the PSP luminescence at the reference condition (typically 1 atm and ambient temperature), and I and P are the PSP luminescence and surface pressure at temperature T . The curves of pressure as a function of intensity ratio (I_{ref}/I) at each temperature, determined from a laboratory calibration of the AEDC PSP and presented in Fig. 7a, were fit to the second order. The variations of the curve fit coefficients with temperature are presented in Fig. 8, and the a_{ij} coefficients in Eq. (2) are third-order fits of these curves. In Eq. (2), it is assumed that the wind-off I_{ref} is taken at the same pressure and temperature as that during the laboratory PSP calibration. This

is usually not the case; therefore, I_{ref} (or I_{ref}/I) must be corrected for any deviation of pressure and temperature from the calibration reference condition. The correction factor is calculated by solving for intensity ratio in Eq. (2) at the wind-off condition using the wind-off P and T . The measured I_{ref}/I at each pixel is then multiplied by this factor, and the product of that result is used in Eq. (2) to solve for P at each pixel.

The L2 PSP was modeled by the following equation to determine pressure:

$$P = (a_{00} + a_{01} \cdot T + a_{02} \cdot T^2) + (a_{10} + a_{11} \cdot T + a_{12} \cdot T^2) \cdot \frac{I_{ref}}{I} + (a_{20} + a_{21} \cdot T + a_{22} \cdot T^2) \cdot \left(\frac{I_{ref}}{I}\right)^2 \quad (3)$$

Again, the curves of pressure as a function of intensity ratio at each temperature, determined from a laboratory calibration of the L2 PSP and presented in Fig. 7b, were fit to the second order. The variations of the curve fit coefficients with temperature are presented in Fig. 9, and the a_{ij} coefficients in Eq. (3) are second-order fits of these curves. As for the AEDC PSP, the same type of correction factor for deviation of the wind-off condition from the calibration reference condition was applied to the L2 PSP. The calibration coefficients used in the data reduction for both paints are listed in Table 3.

Taking the ratio of wind-off to wind-on intensities assumes the model position and shape in the image remain constant. However, at the wind-on condition, the model moved in the field of the camera as a result of deflections from operating loads. Using the image registration technique described by Bell (Ref. 4), small targets were placed on the surface at known coordinates so that the wind-on image could be stretched and shifted (registered) to match the wind-off image. The registration mark numbering and locations are listed in Table 4. The registration marks were also used to relate the 2-D image coordinate system to the 3-D model coordinate system. After the test, the photogrammetry methods described by Bell (Ref. 4) were used to overlay the 2-D images onto a 3-D mesh grid of the model surface. A file was generated with pressure coefficient data at each mesh point to permit display of the pressure coefficient distribution using color pressure maps.

For the AEDC PSP, T was computed by two methods. The first method used the conventional pressure measurements on the upper surface of the wing and fuselage and the corresponding intensity ratio at each pressure orifice (20 locations on the wing and 10 on the fuselage) to solve for T in Eq. (2) at each location. The surface temperatures for the wing (made of steel) and fuselage (made of aluminum) were averaged separately. The appropriate average temperature and the computed intensity ratio at each pixel were then used to calculate the surface pressure over the entire

painted surface (wing or fuselage). This *in-situ* calculation of T does not permit an independent comparison to the conventional pressure data because this method uses the directly measured pressures to determine the temperature. The second method of computing surface temperature used the recovery factor values given by Schlichting (Ref. 5) of $r_l = 0.84$ for a laminar boundary layer and $r_t = 0.896$ for a turbulent boundary layer and the following equation:

$$T_{surface} = r \cdot (TT - T_{\infty}) + T_{\infty} \quad (4)$$

where T_{∞} is the free-stream temperature, TT is the stagnation temperature, and r is the appropriate recovery factor. The laminar and turbulent values were used to compute surface temperature for the wing and fuselage, respectively. The wing was assumed to have laminar flow, since boundary-layer trips were not used. This calculation is an approximation; however, it permits a totally independent verification of the PSP data with the conventional pressure measurements. It was not possible to calculate an accurate surface temperature for L2 PSP using the *in-situ* method because of the low sensitivity to changes in temperature. Therefore, Eq. (4) was always used to calculate surface temperature for the L2 PSP.

4.0 RESULTS AND DISCUSSION

The computed chordwise temperature distribution using PSP, the average of these temperatures, and the calculated recovery temperature are presented in Fig. 10 at several angles of attack. Figure 10 shows that the temperature deviation from the average was greater at the 1,000 psfa total pressure than at 2,000 psfa. Figure 3 shows that the intensity ratio has a higher temperature sensitivity at the higher pressure, thus permitting more accurate determination of temperature using the measured pressures and intensity ratios.

A comparison of wing pressure coefficient (CP) data from conventional pressure measurements and from the AEDC PSP using the two temperature methods is presented in Fig. 11. The agreement of the PSP data using the *in-situ* temperature determination method with the conventional pressure data is very good, except at Mach 0.6. The PSP data disagreement appears to be the result of local temperature deviations from the average, as shown in Fig. 10. The PSP data yielded a lower CP when the surface temperature was lower than the average, and higher when the temperature was higher. However, the true surface temperature is not known and can only be approximated using Eq. (4). As expected, when the recovery temperature was close to the *in-situ* determination method temperature, the CP data for both methods agree. The PSP data at Mach number 0.85 and 2,000 psfa are in better agreement because the paint temperature sensitivity is higher at the higher total pressure, as noted above.

A comparison of fuselage pressure coefficients is presented in Fig. 12, and the results are very similar to that on the wing. Although the recovery temperatures were computed differently for the wing and fuselage, they result in good agreement with the conventional pressure measurements on both surfaces, illustrating the importance of knowing the global variation of surface temperature.

A comparison of wing pressure coefficients from conventional pressure measurements and from the AEDC and L2 PSP is presented in Fig. 13. PSP data are also presented at two non-instrumented sections on the wing, one inboard and one outboard of the pressure orifices. The recovery method for computing temperature was used with both paints to compute pressure. The agreement of the L2 PSP data with the conventional pressure data was not consistent, with the best agreement occurring at Mach number 0.85 and total pressure of 2,000 psfa. In the cases where the agreement between data at the instrumented section from the two paints was good, the outboard section data also agreed, but not the inboard section. The AEDC PSP data are most likely in error near the wing root because of the paint temperature sensitivity. The fuselage temperature, as computed from the intensity ratio and measured pressures, was approximately 8°F higher than the wing (at the instrumented section). It would be expected that the wing was warmer near the fuselage. As illustrated in Fig. 7, for a given intensity ratio, a higher pressure would be computed by using a lower than actual temperature. The AEDC PSP data from the inboard section always yielded a higher pressure than the L2 PSP, which is consistent with the AEDC paint temperature characteristics.

The different paint surface characteristics could have had an effect on the shock location as noticed in Figs. 13l and o. The AEDC paint was very hard and smooth while the L2 paint had a "tacky" feel.

Color contours showing the global variation in surface pressure coefficient for the AEDC and L2 PSP are presented in Fig. 14. The streaks in the AEDC pressure distribution are most likely the result of poor paint application procedures or inaccurate model registration and have a varied effect on the data at different conditions. The large, black holes in the L2 pressure distribution are areas that were not painted. The *in-situ* temperature determination method was used for the AEDC PSP (which provided the most accurate results), and the recovery method for the L2 PSP. The surface pressure distributions at Mach 0.6 are very different. This is to be expected, since the CP data at the instrumented section from the L2 PSP were significantly different from the AEDC PSP and conventional pressure data. The data at Mach numbers 0.85 and 0.95 have similar distributions, with some differences seen in shock position, as mentioned above. A higher surface pressure was computed at the wing root for the AEDC PSP than for the L2 PSP, as mentioned above. The discontinuity in the AEDC pressure distribution where the fuselage and wing meet is the result of using different calculated temperatures for the wing and fuselage surfaces. When the fuselage temperature was used to compute the wing surface pressure coefficient distribution, as was done for the data presented in Fig. 15, the agreement between the L2 and

AEDC paint data near the wing root was much better. These results once again demonstrate the sensitivity of the AEDC PSP to the surface temperature.

5.0 SUMMARY

The OPTROD L2 pressure sensitive paint (PSP) did not perform as well as expected at AEDC using the laboratory-derived calibration. However, it is possible that the illumination setup and/or the calibration derived at AEDC is the cause of the errors. TsAGI has reported much better agreement with conventional pressure measurements, and we will continue to investigate why we were unable to match their results. The L2 PSP did exhibit lower temperature sensitivity, but also had lower pressure resolution as compared to the AEDC PSP. It is evident that the L2 PSP would be more suitable to atmospheric or higher pressure conditions than the AEDC PSP. The AEDC PSP would be more accurate if the global temperature distribution of the model was simultaneously determined. For the majority of tests conducted in Tunnel 16T, the AEDC PSP formula, in conjunction with limited pressure orifices or some way to determine surface temperature, appears to be the best choice for global pressure measurement.

Although the AEDC PSP data agreed quite well with the measured pressure data at many test conditions, the error in the PSP data can be more than an order of magnitude greater than conventional measured pressure data if the surface temperature is not known. Thus, continuing work is required to solve this problem before the AEDC PSP can be considered a production tool.

REFERENCES

1. McLachlan, B. G., et al. "Pressure Sensitive Paint Use in the Supersonic High-Sweep Oblique Wing (SHOW) Test." AIAA Paper 92-2686, AIAA 10th Applied Aerodynamics Conference, Palo Alto, California, June 1992.
2. Morris, M. J., et al. "Aerodynamic Applications of Pressure-Sensitive Paint." AIAA Paper 92-0264, 30th AIAA Aerospace Sciences Meeting, Reno, Nevada, January 1992.
3. Uibel, R., Khalil, G., Gouterman, M., Gallery, J., and Callis, J. "Video Luminescent Barometry: The Induction Period." AIAA Paper 93-0179, 31st Aerospace Sciences Meeting, Reno, Nevada, January 1993.
4. Bell, J. H. and McLachlan, B.G. "Image Registration for Luminescent Paint Sensors." AIAA Paper 93-0178, 31st Aerospace Sciences Meeting, Reno, Nevada, January 1993.
5. Schlichting, H. *Boundary Layer Theory*. McGraw-Hill, New York, 1979 (Seventh Edition).

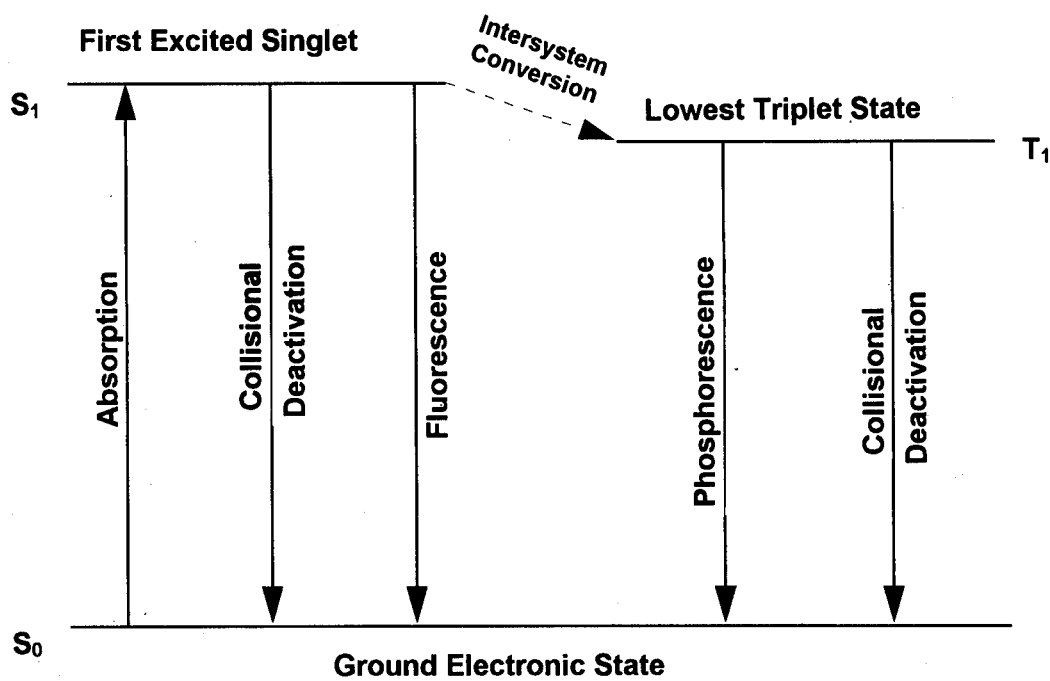


Figure 1. Basic luminescence process.

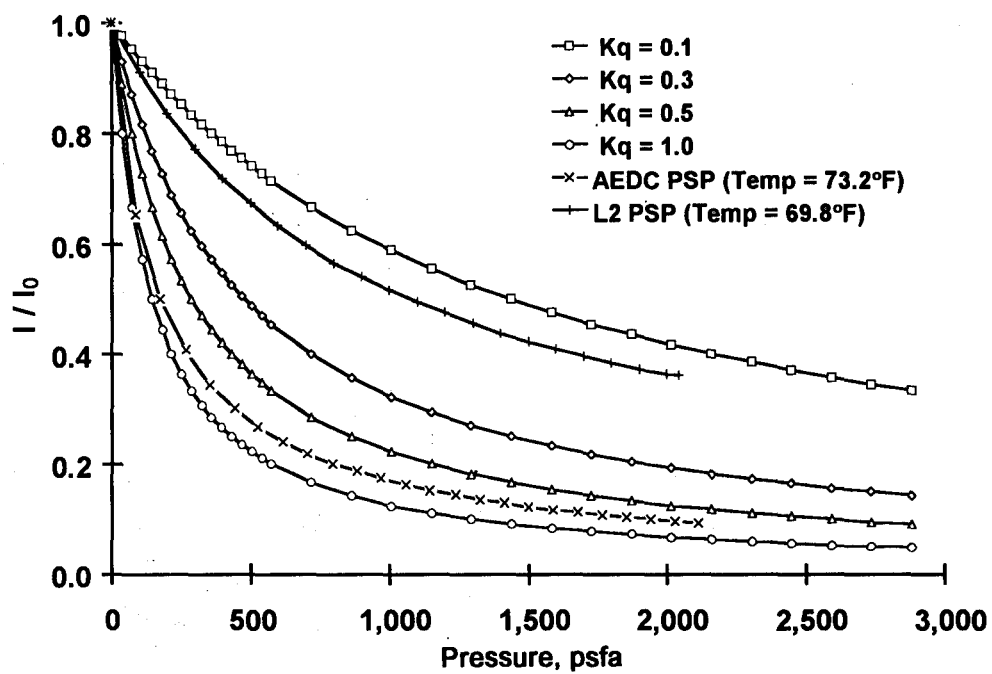
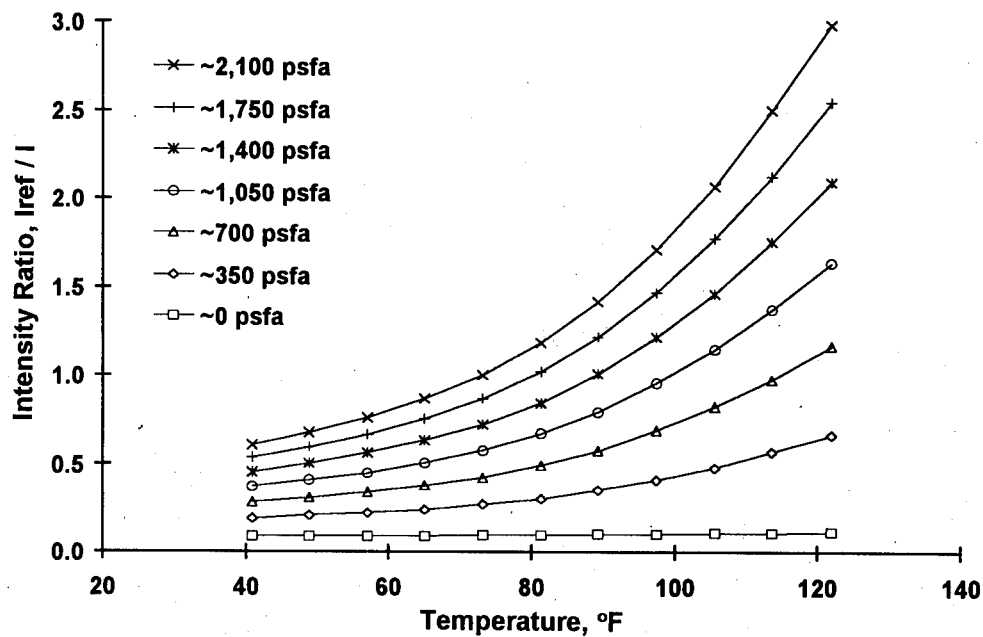
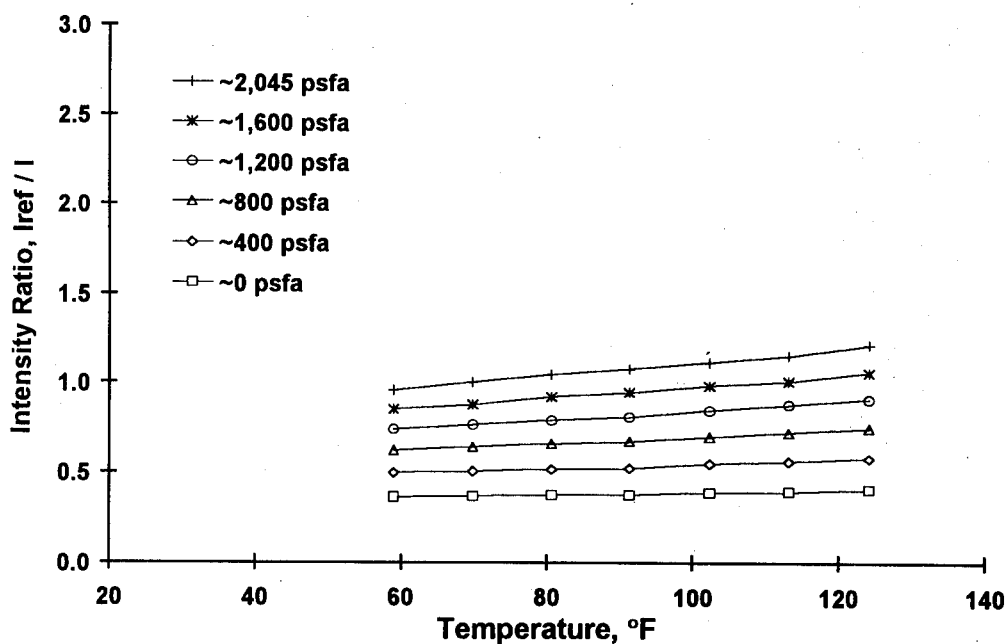


Figure 2. Luminescence as described by the Stern-Volmer model.



a. AEDC PSP



b. L2 PSP

Figure 3. PSP temperature sensitivity.

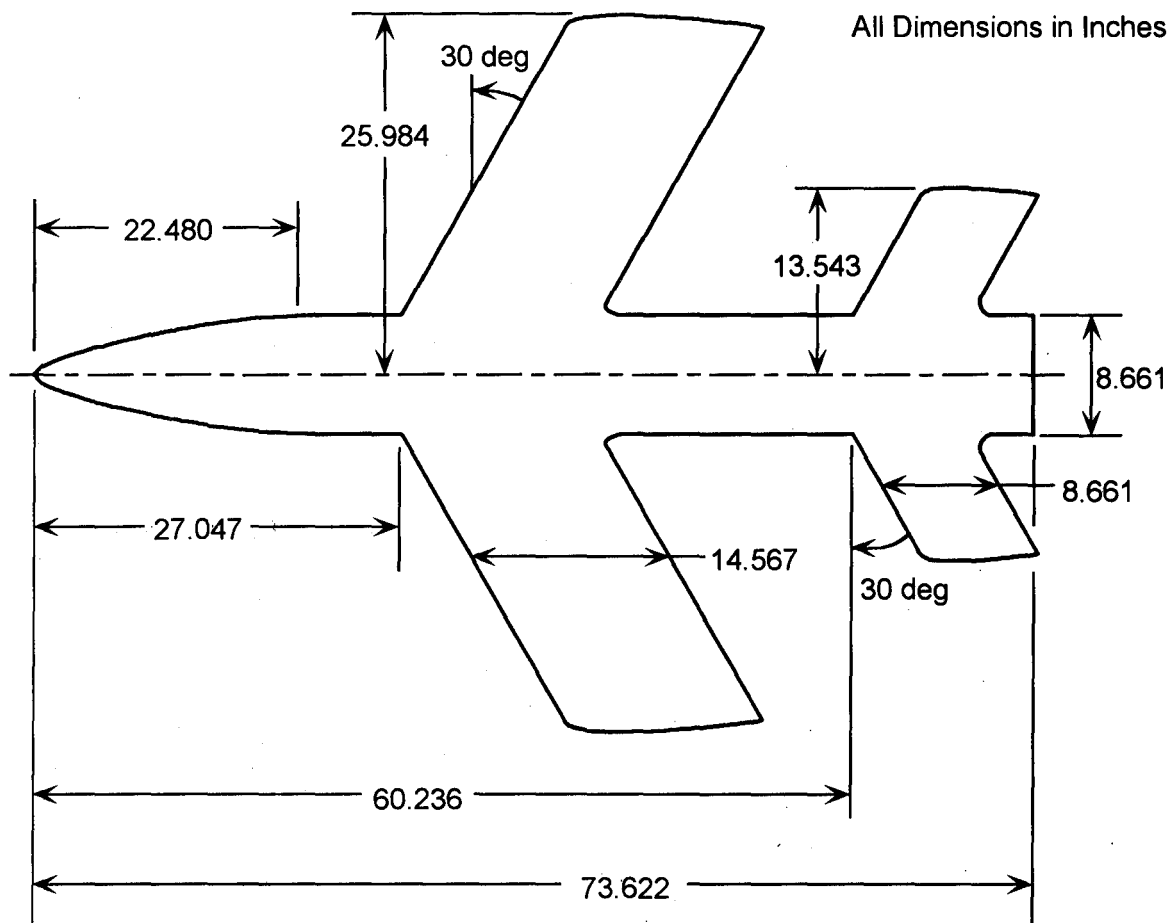


Figure 4. Generic wall interference model details.

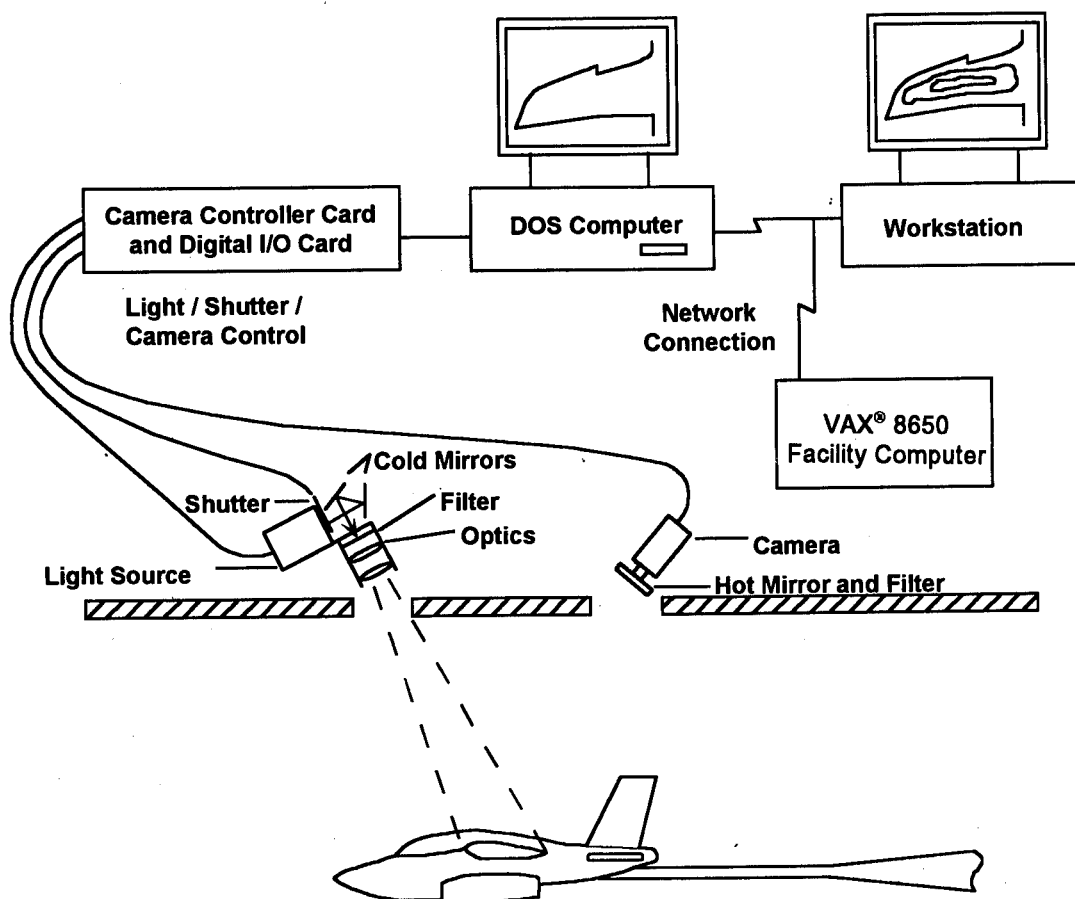
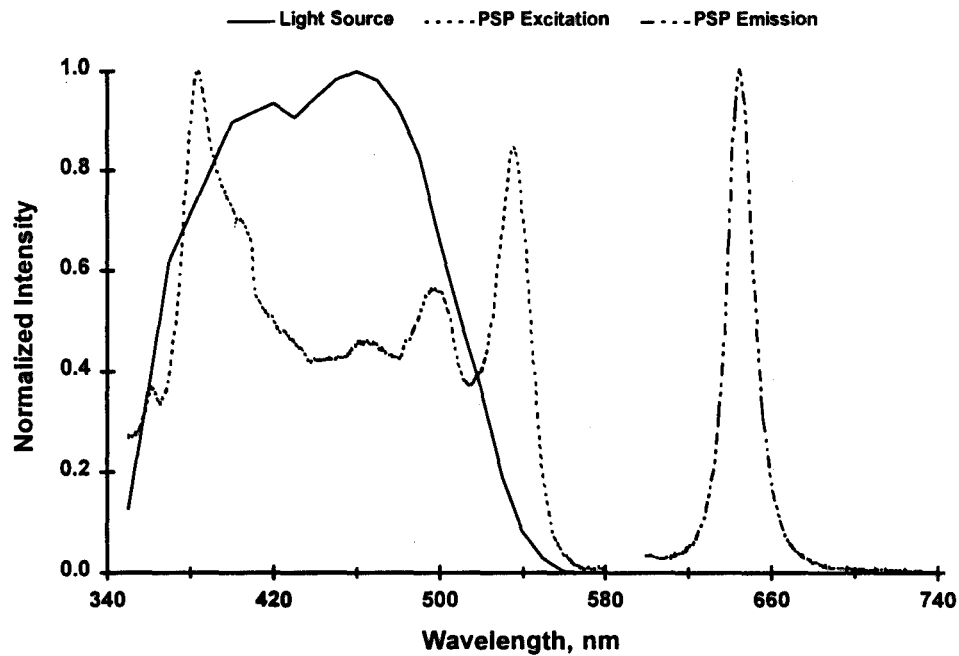
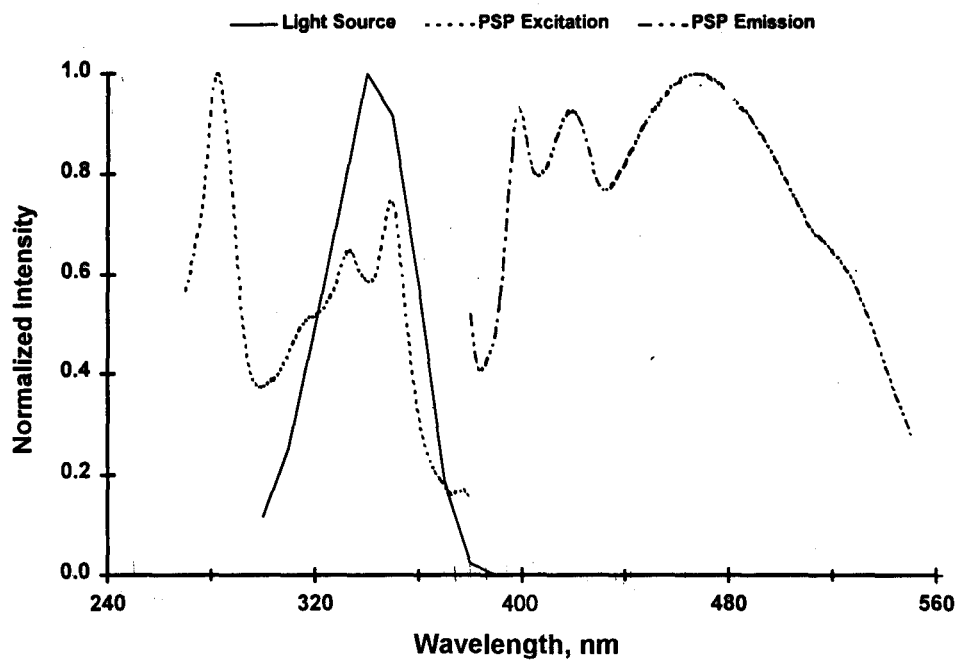


Figure 5. PSP data acquisition system.

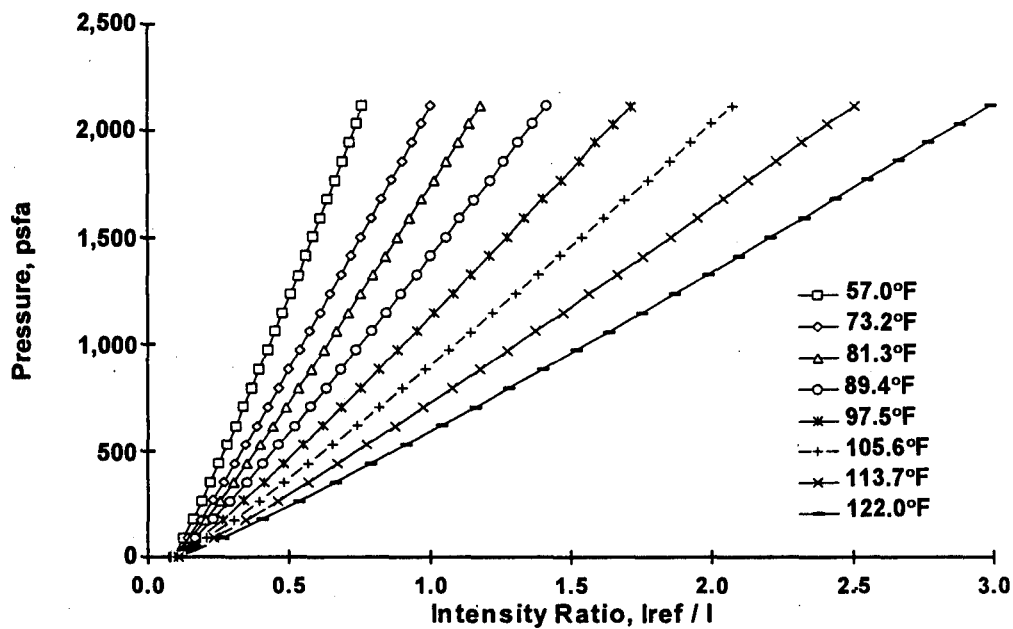


a. AEDC PSP

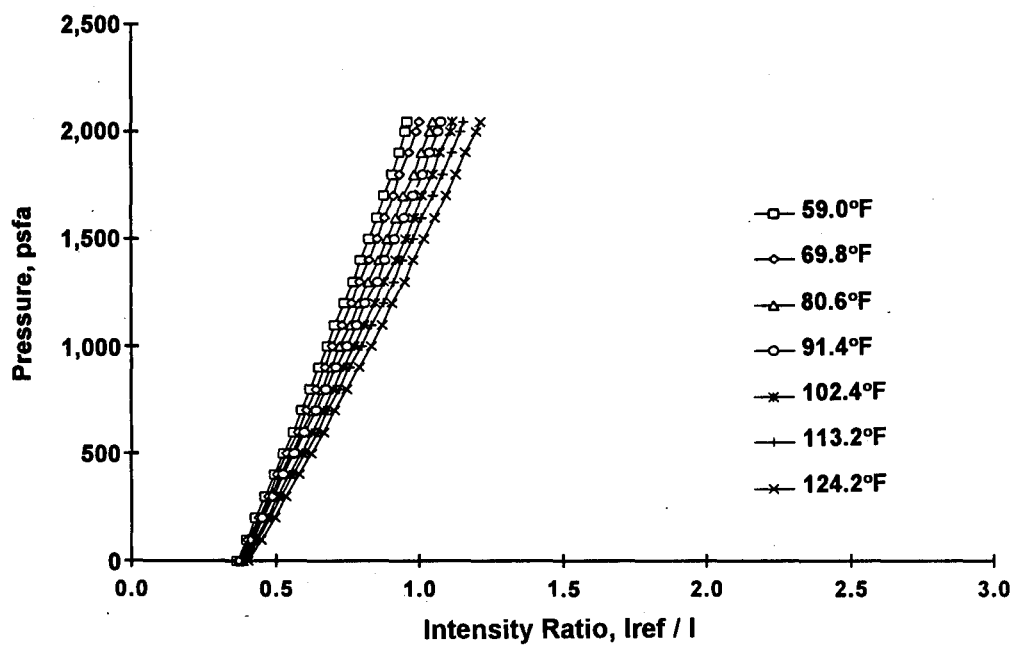


b. L2 PSP

Figure 6. Spectral characteristics of AEDC PSP and L2 PSP.



a. AEDC PSP



b. L2 PSP

Figure 7. PSP laboratory calibration.

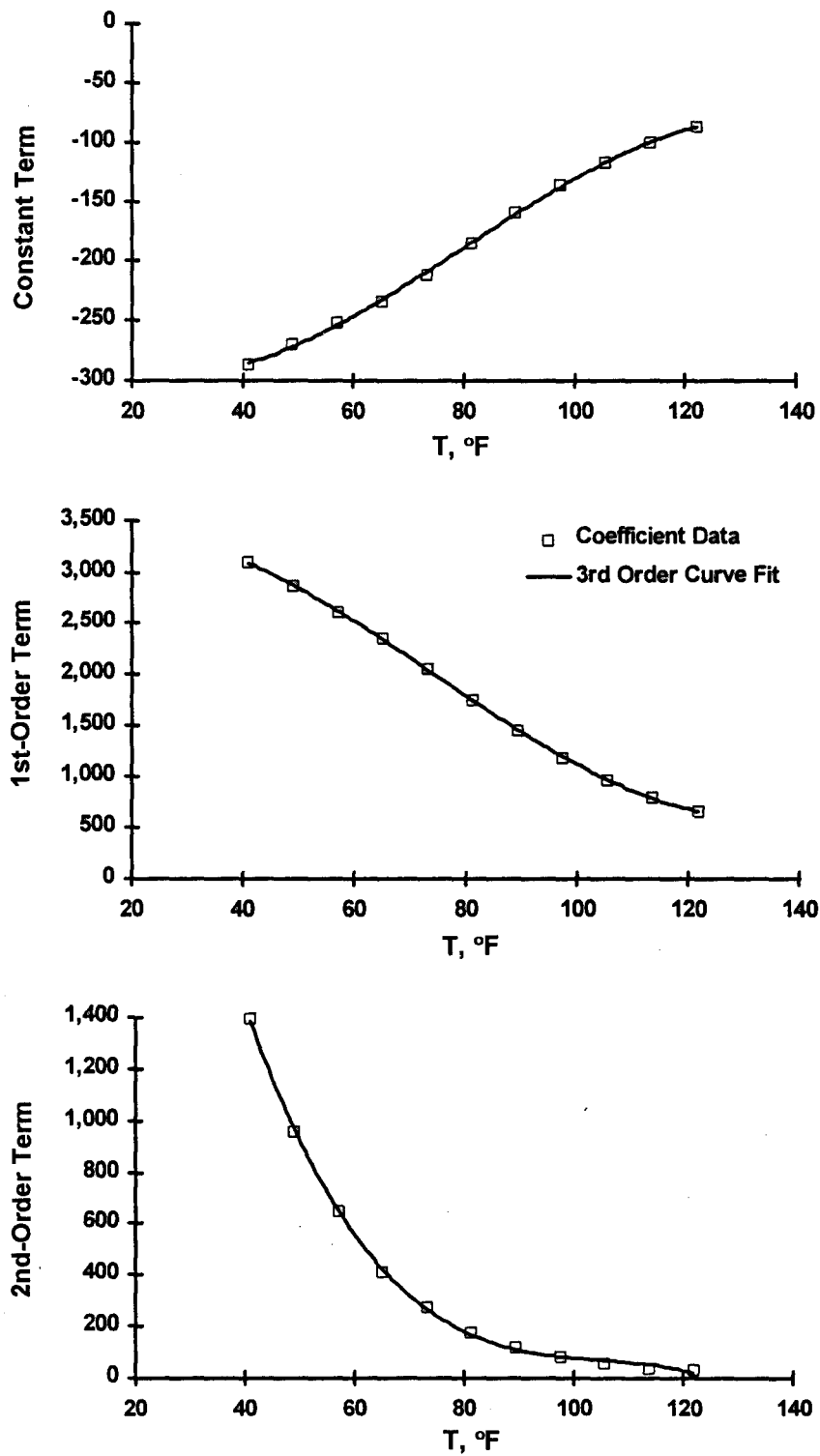


Figure 8. AEDC PSP 2nd-order fit coefficient variation with temperature.

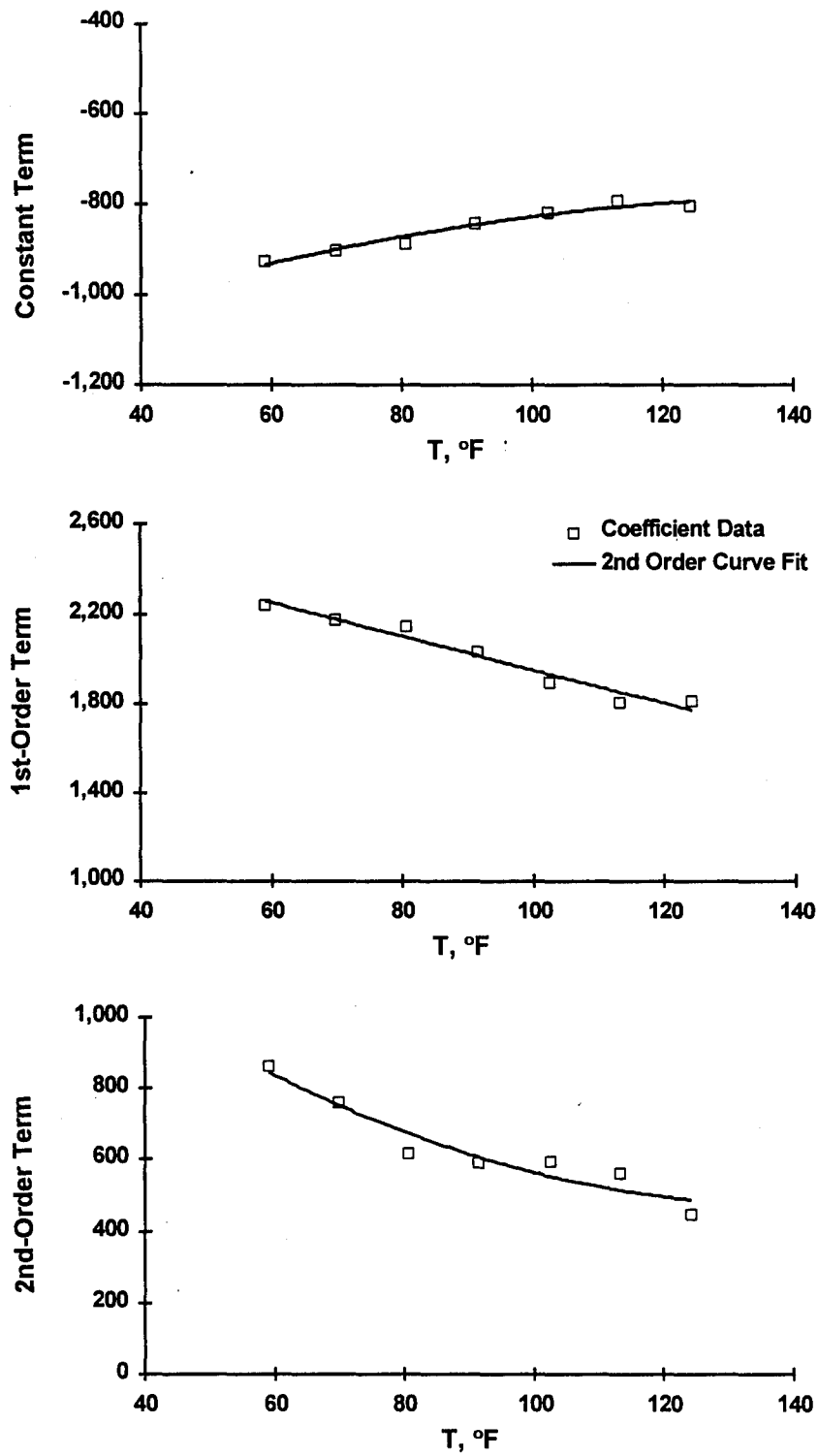
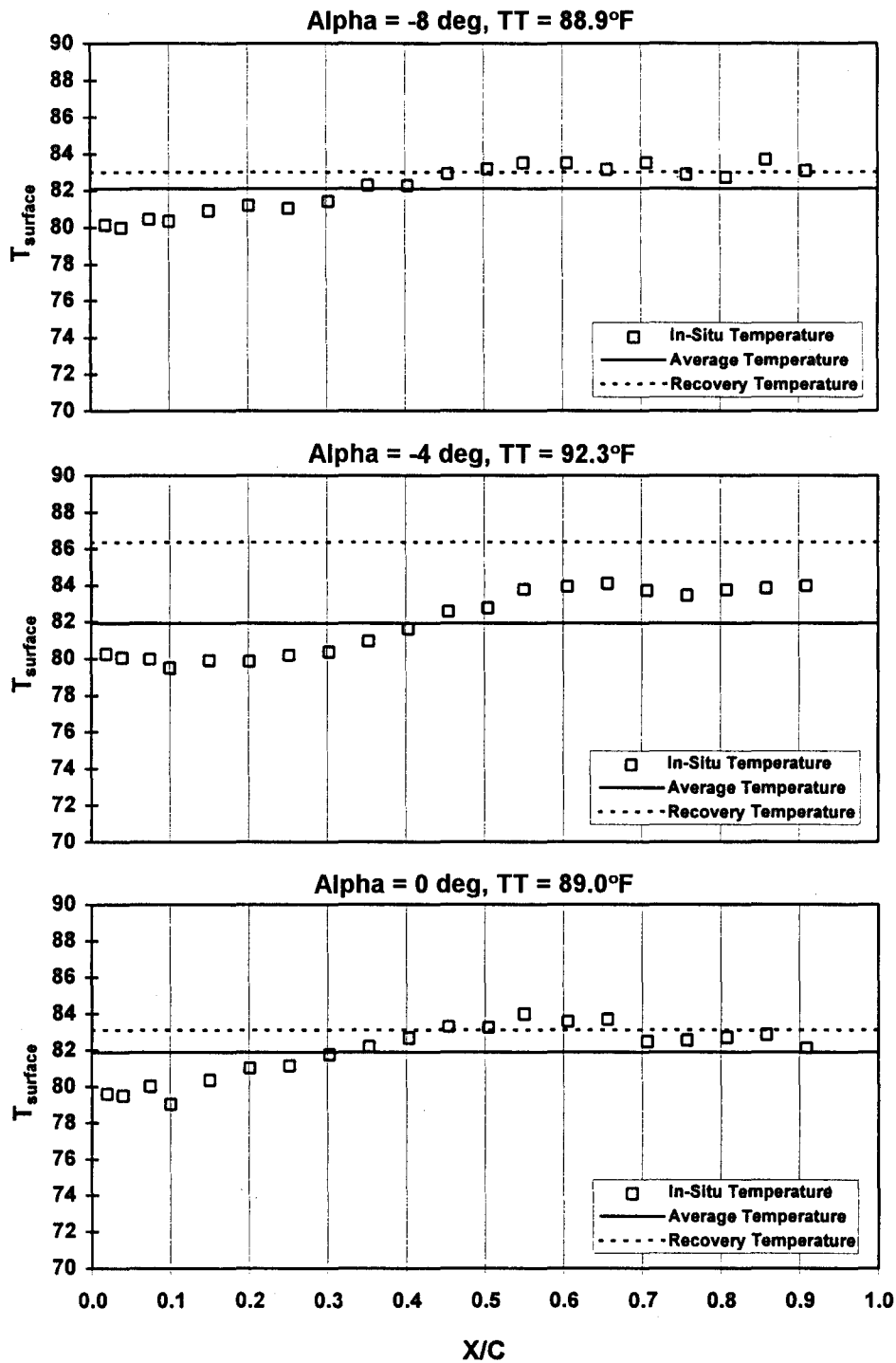
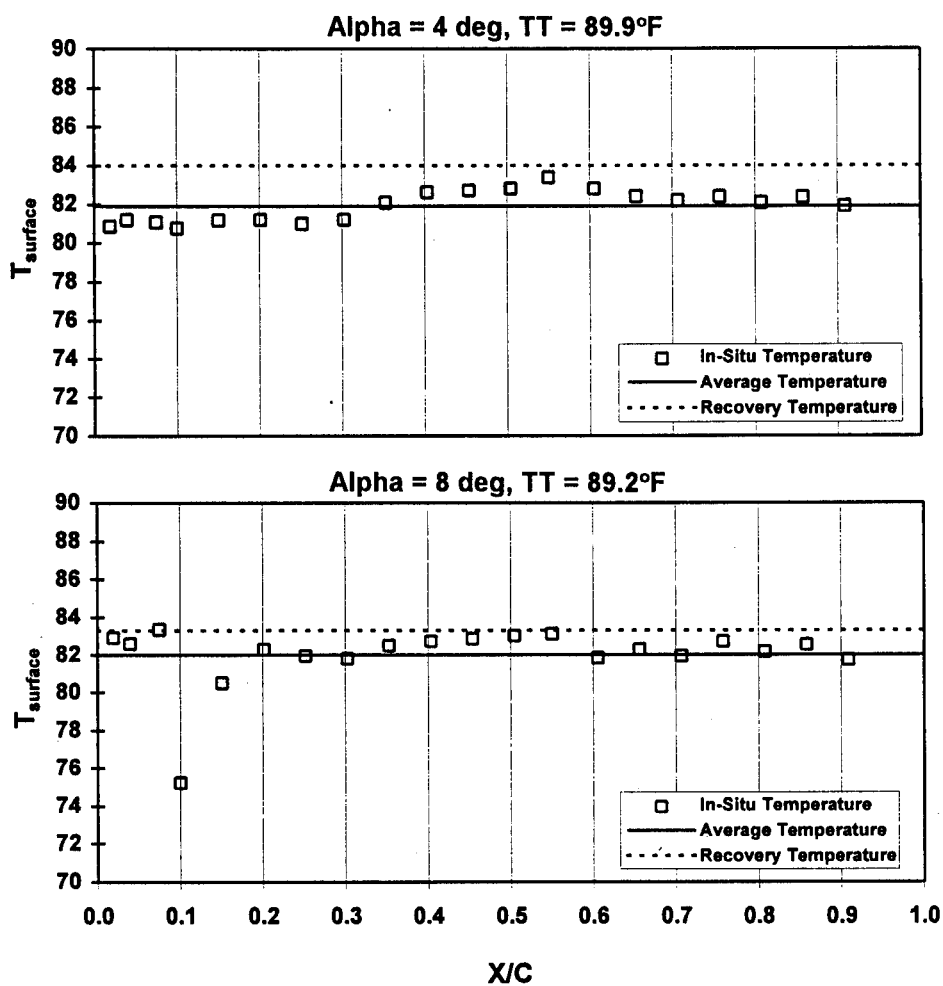


Figure 9. L2 PSP 2nd-order fit coefficient variation with temperature.

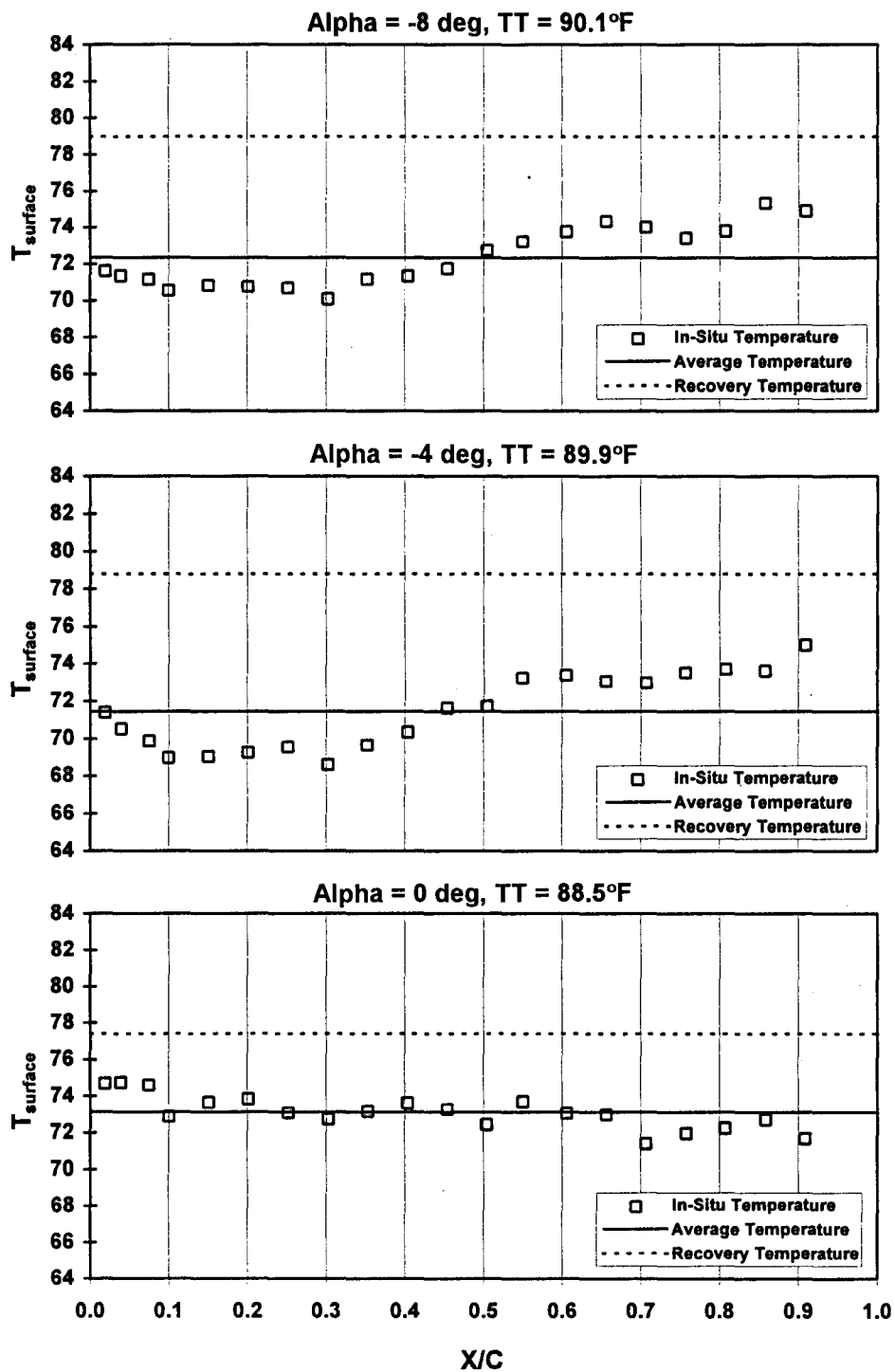


a. Mach = 0.60, PT = 1,000 psfa, TT ≈ 90°F

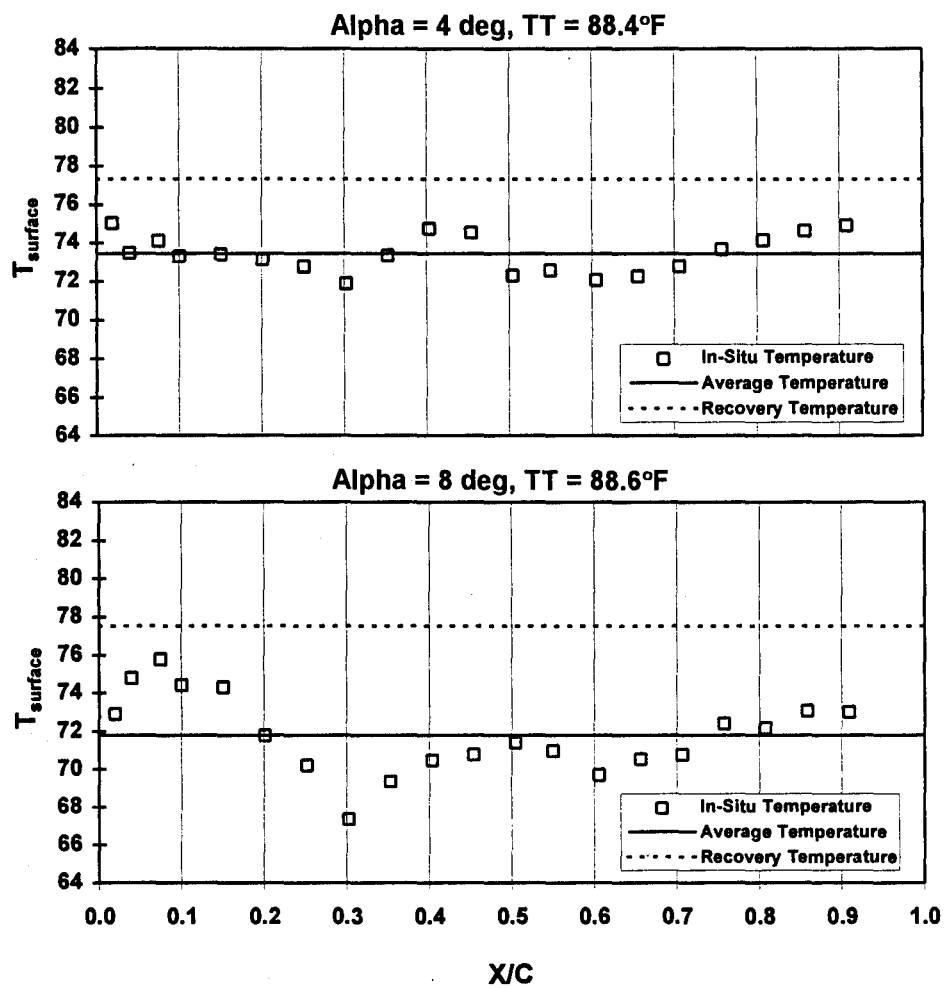
Figure 10. Temperature calculation comparison for AEDC PSP.



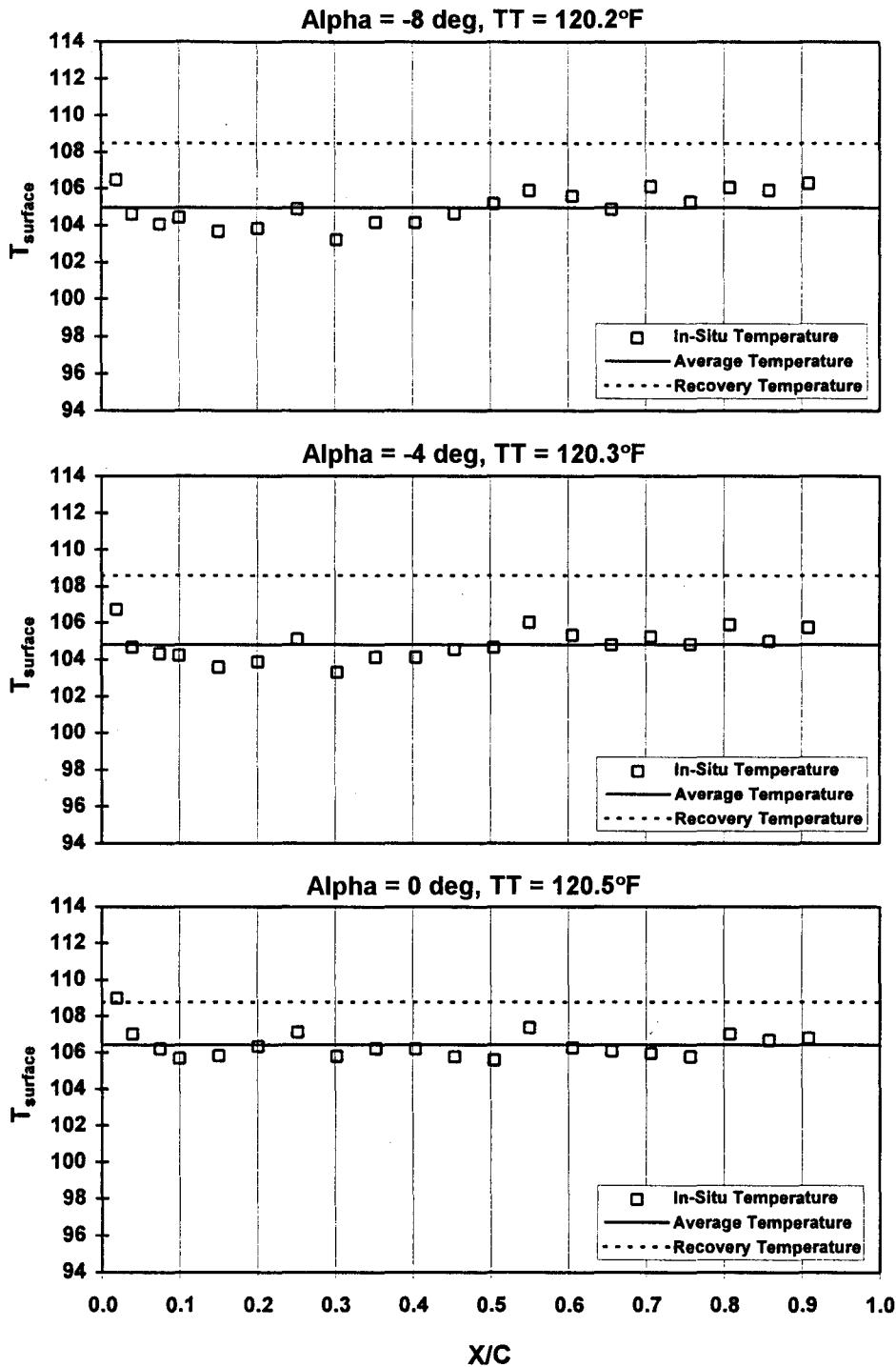
a. Concluded
Figure 10. Continued.



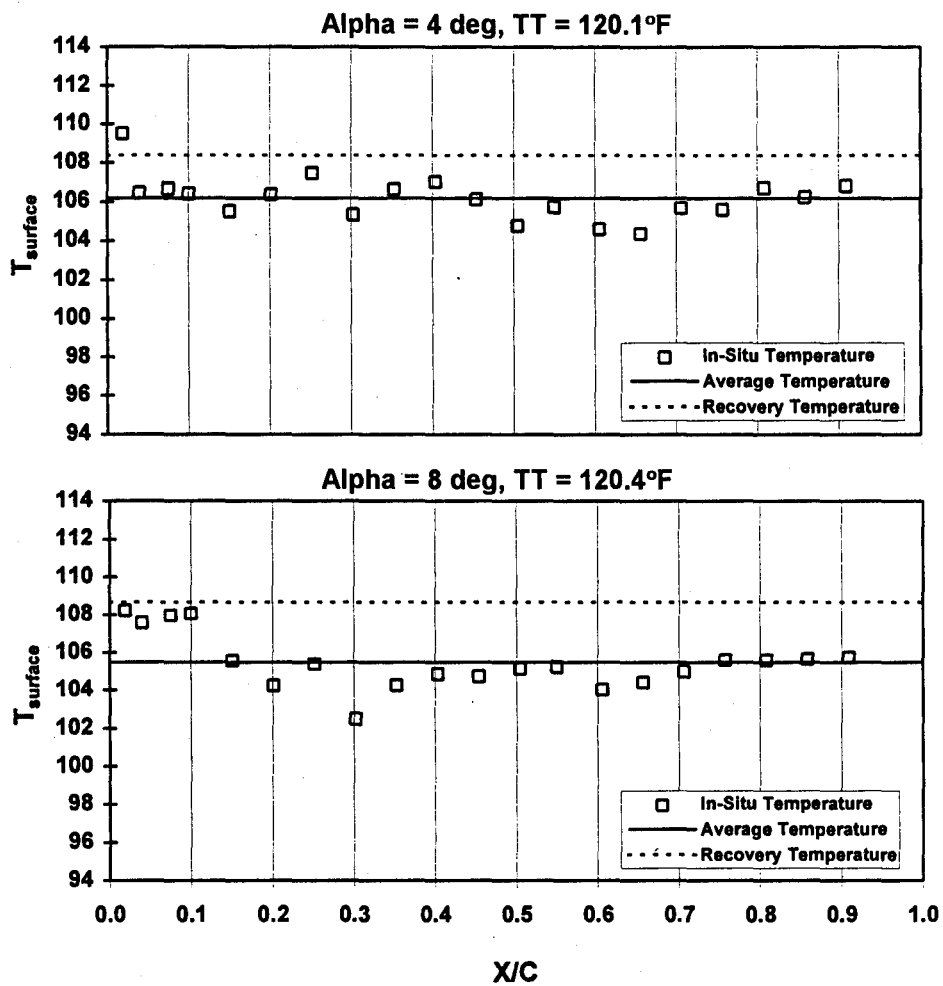
b. Mach = 0.85, PT = 1,000 psfa, TT \approx 90°F
Figure 10. Continued.



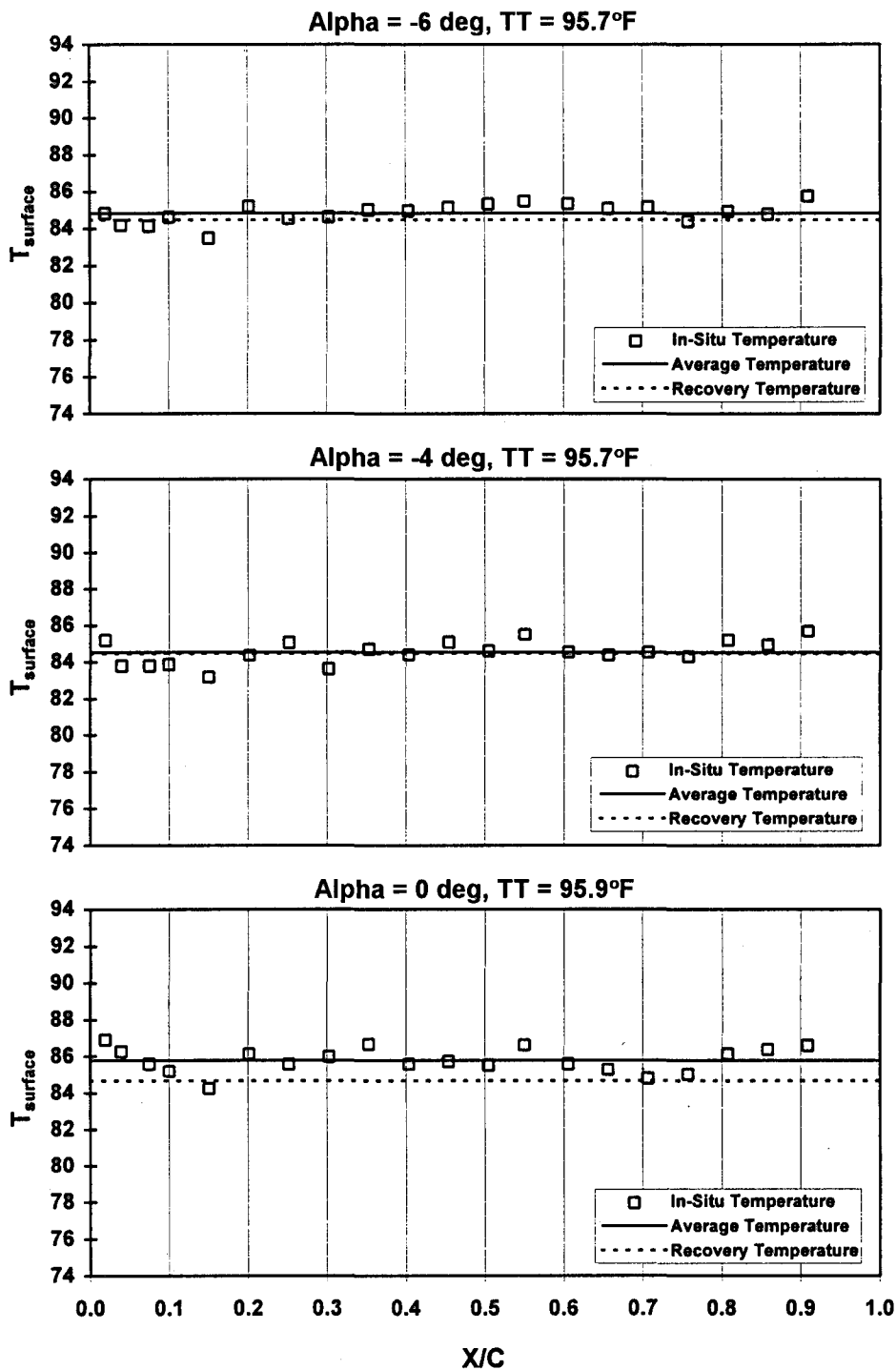
b. Concluded
Figure 10. Continued.



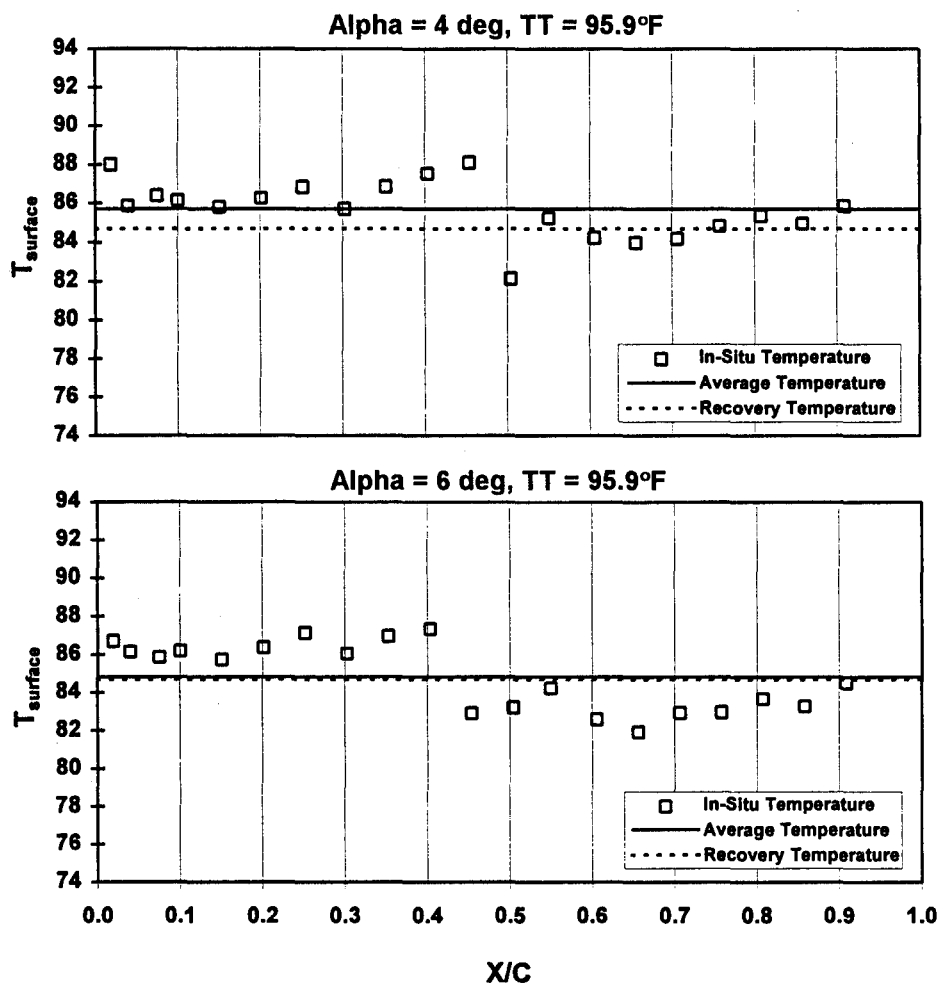
c. Mach = 0.85, PT = 1,000 psfa, TT \approx 120°F
Figure 10. Continued.



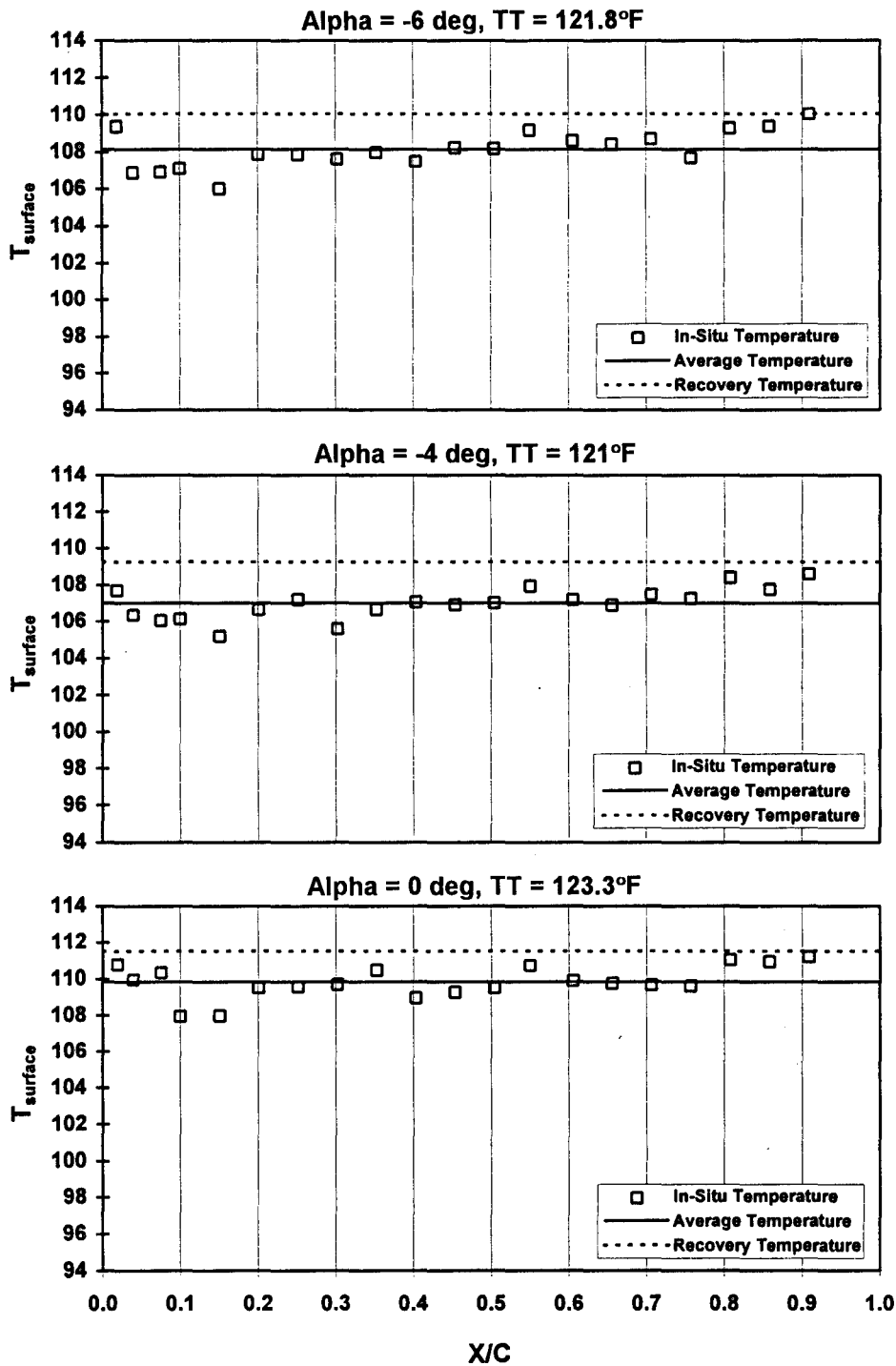
c. Concluded
Figure 10. Continued.



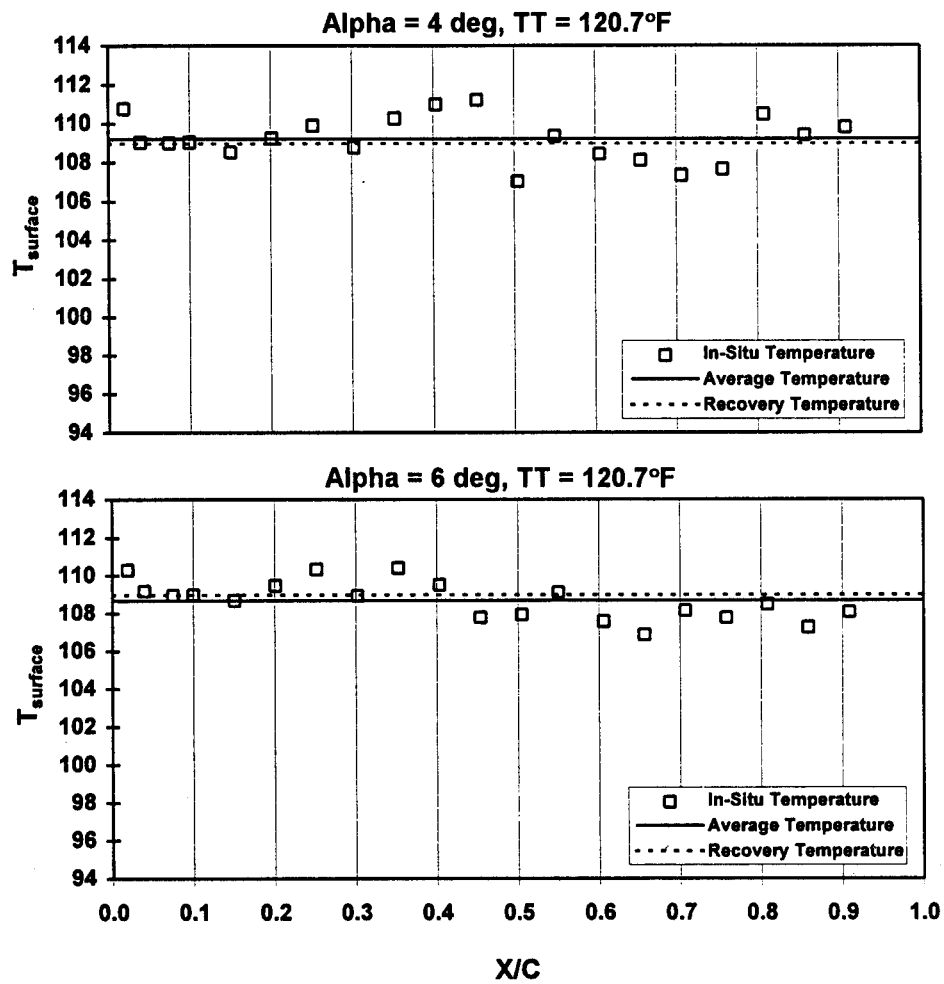
d. Mach = 0.85, PT = 2,000 psfa, TT \approx 95°F
Figure 10. Continued.



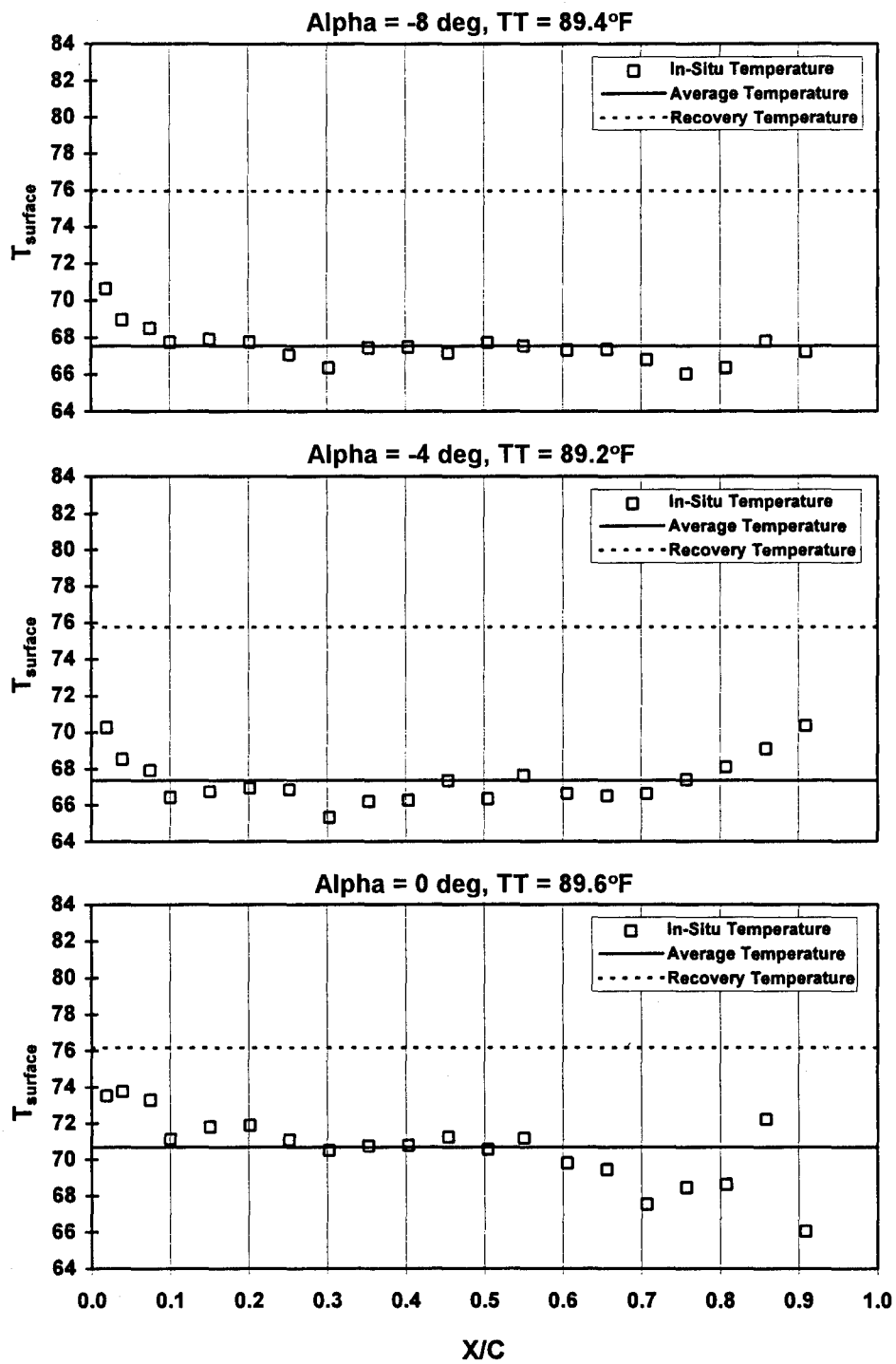
d. Concluded
Figure 10. Continued.



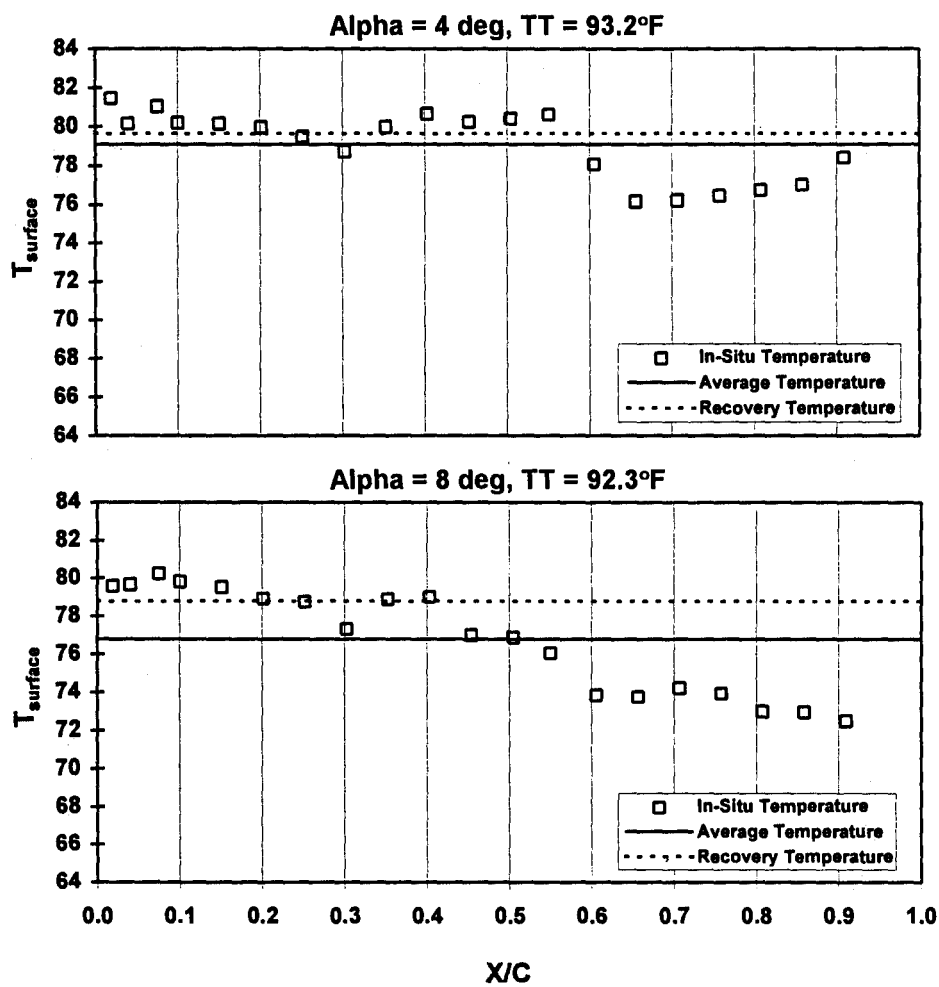
e. Mach = 0.85, PT = 2,000 psfa, TT \approx 120°F
Figure 10. Continued.



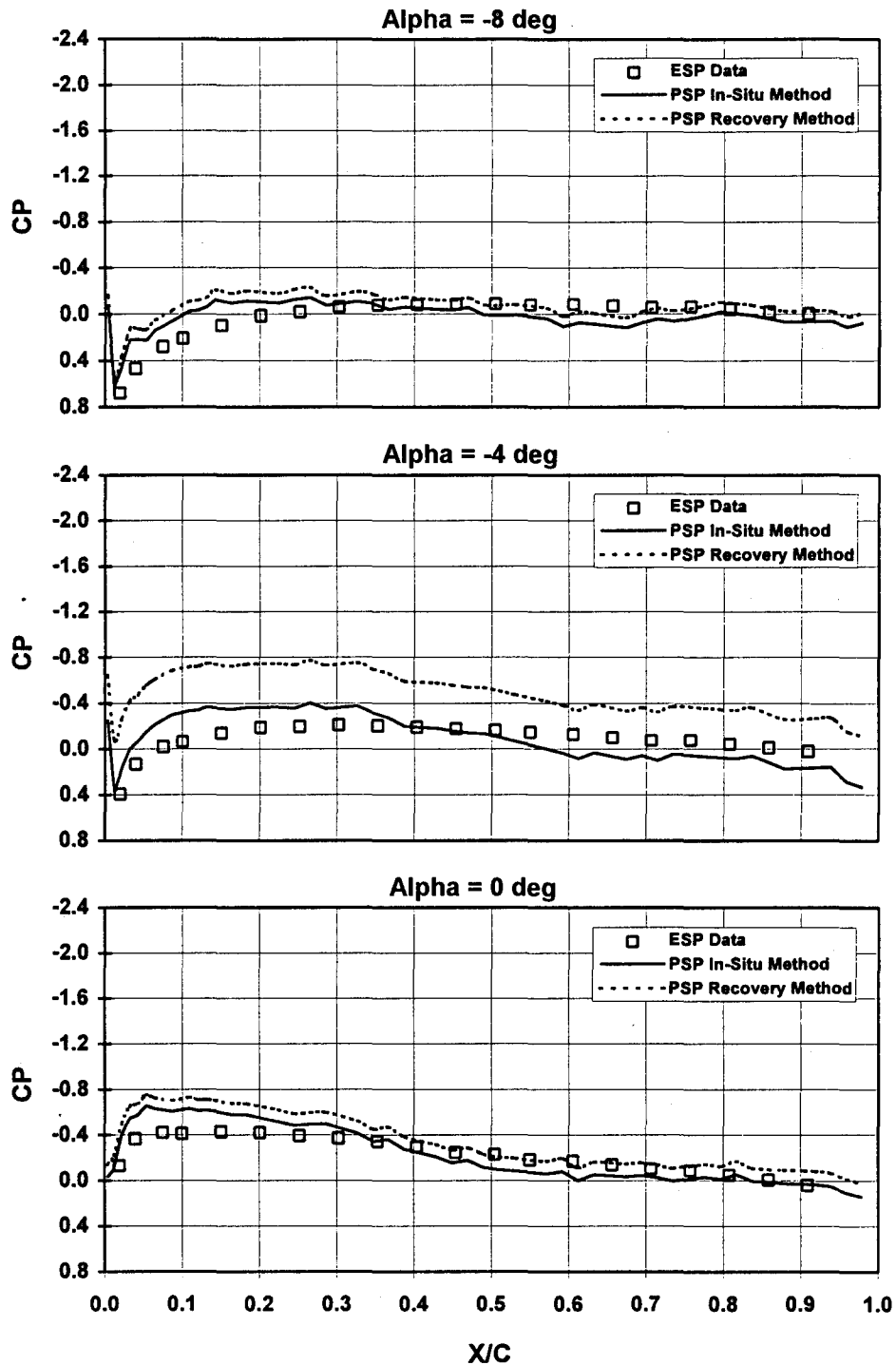
e. Concluded
Figure 10. Continued.



f. Mach = 0.95, PT = 1,000 psfa, $TT \approx 90^\circ\text{F}$
Figure 10. Continued.

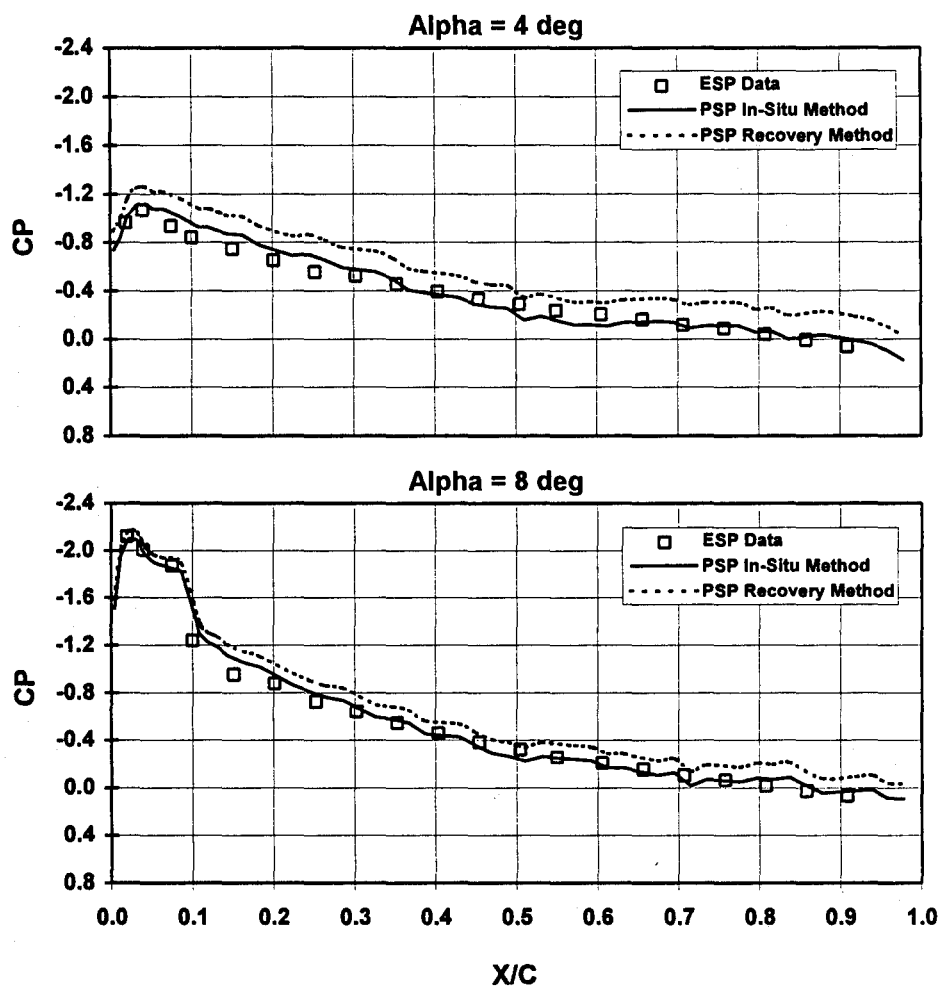


f. Concluded
Figure 10. Concluded.

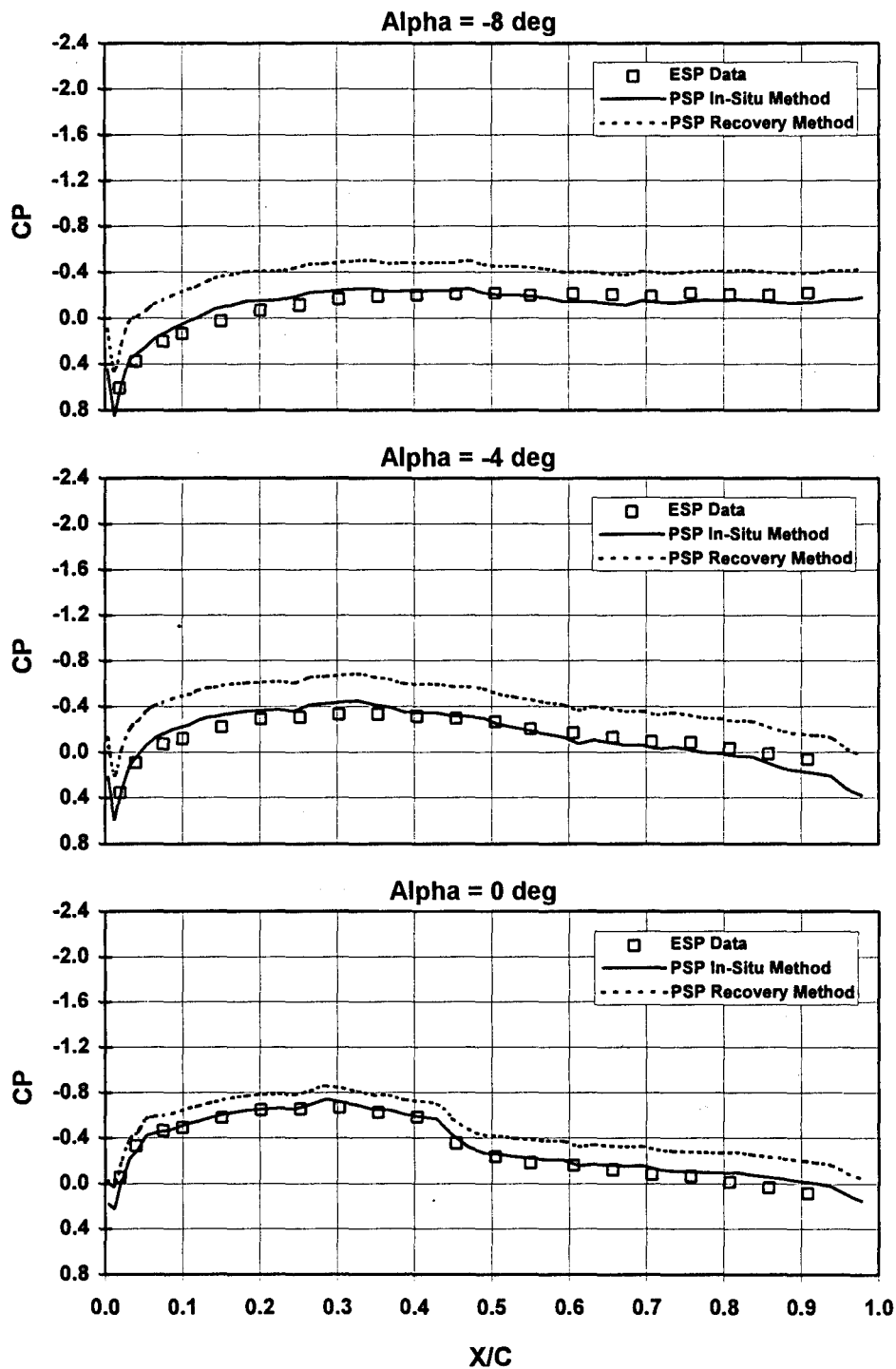


a. Mach = 0.60, PT = 1,000 psfa, TT \approx 90°F

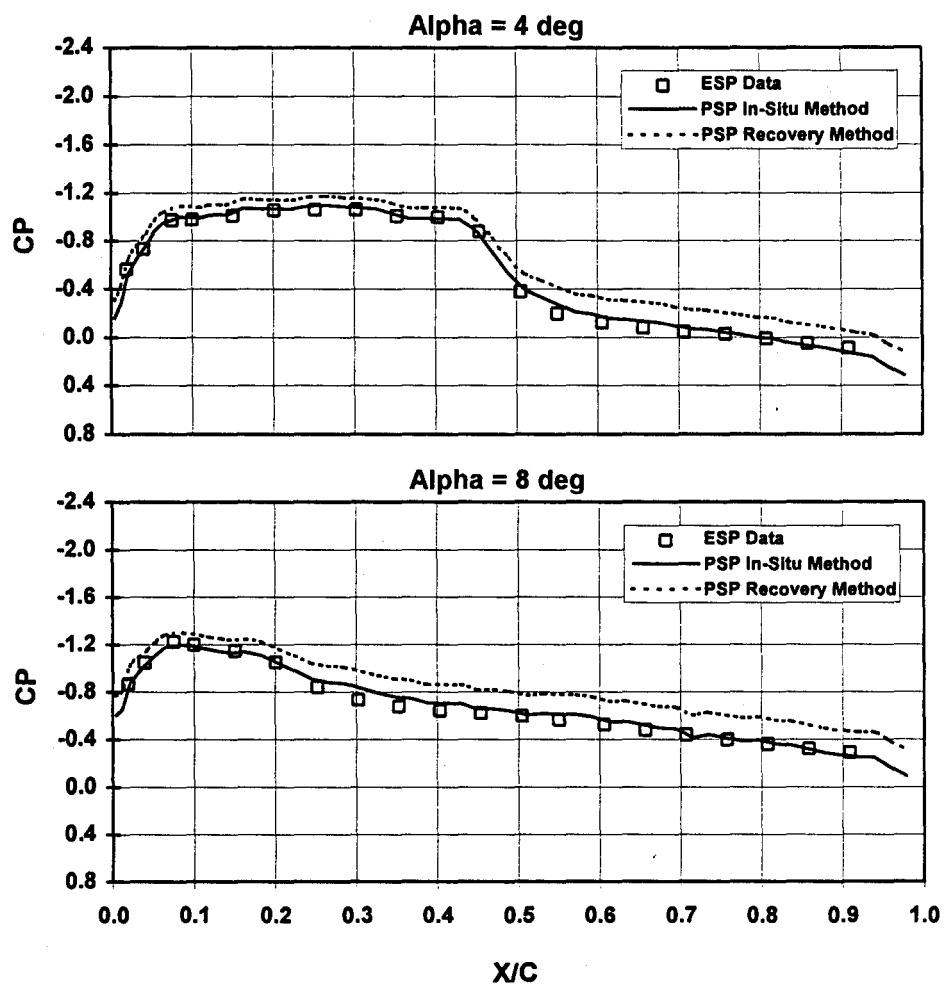
Figure 11. Wing CP comparison using two temperature methods for AEDC PSP.

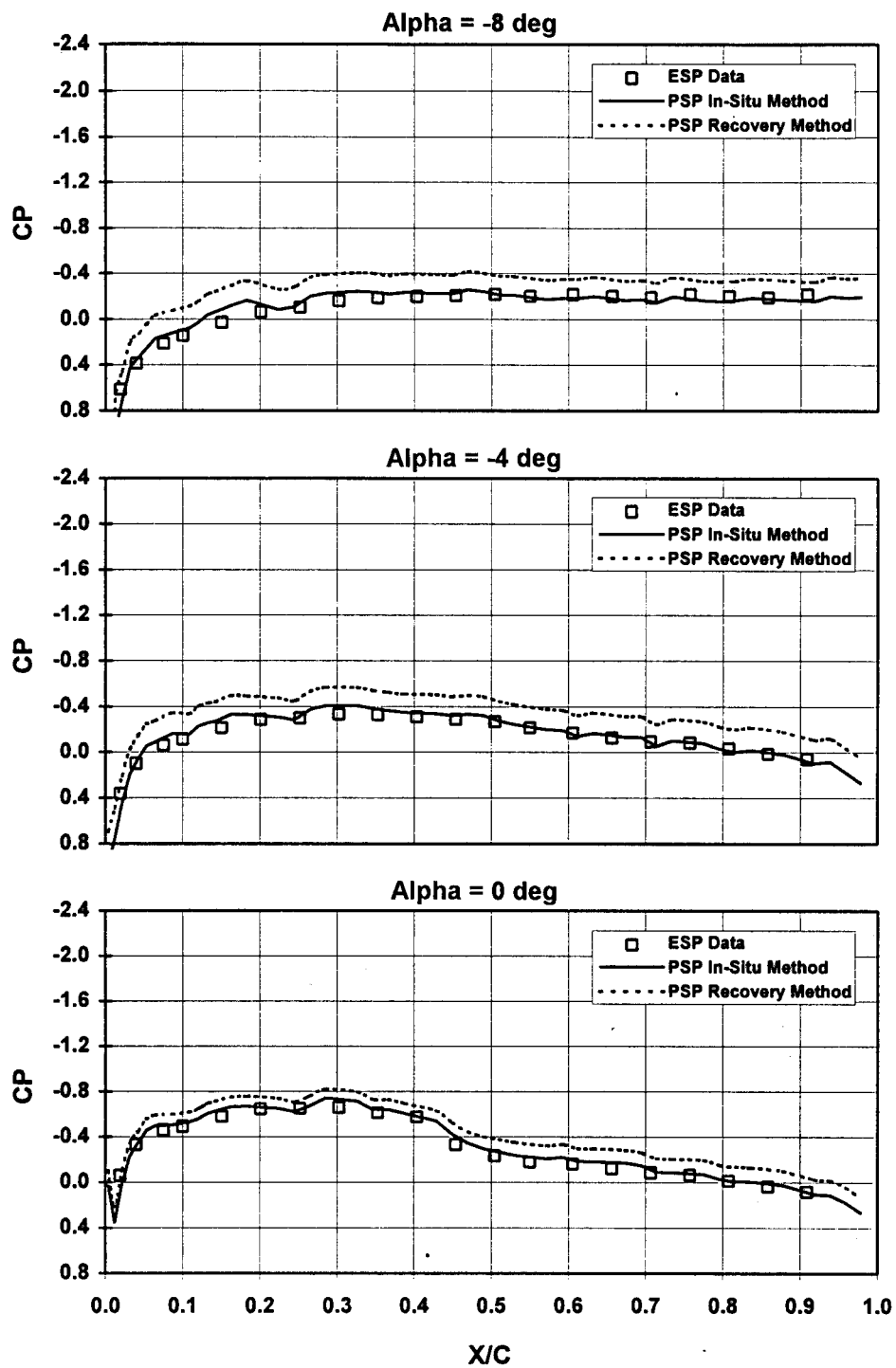


a. Concluded
Figure 11. Continued.



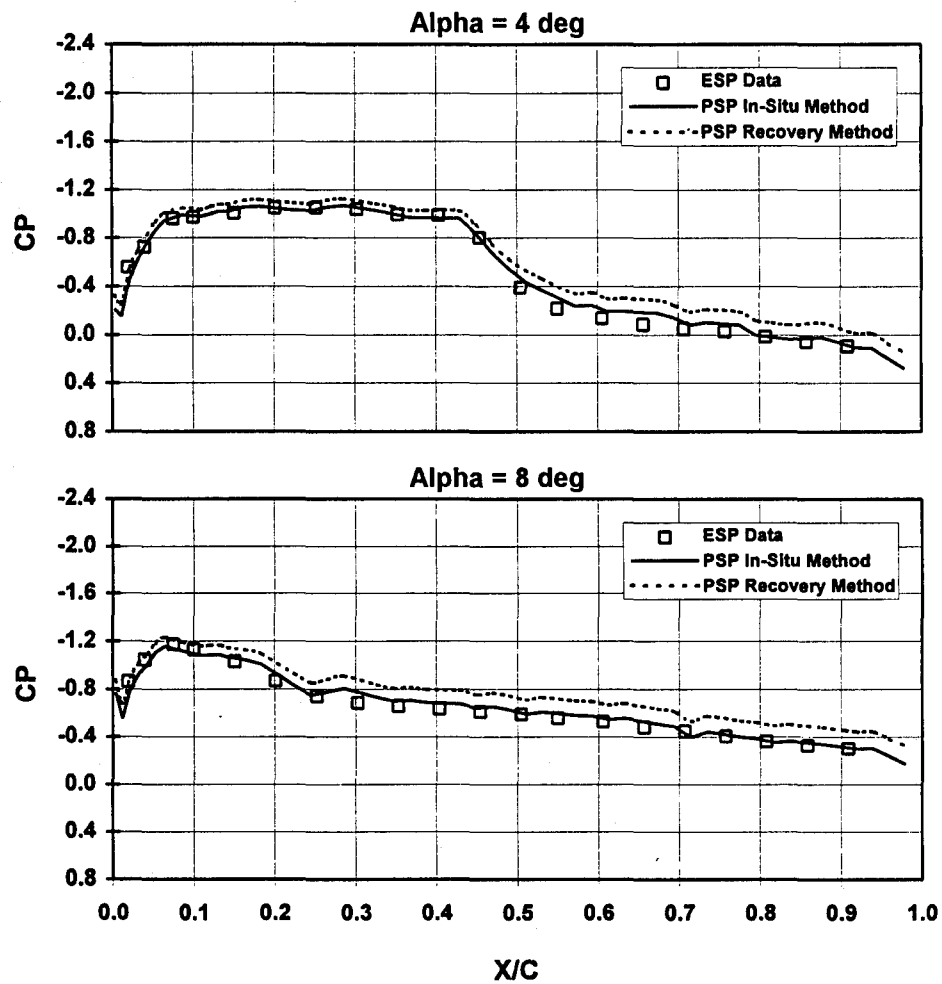
b. Mach = 0.85, PT = 1,000 psfa, TT \approx 90°F
Figure 11. Continued.

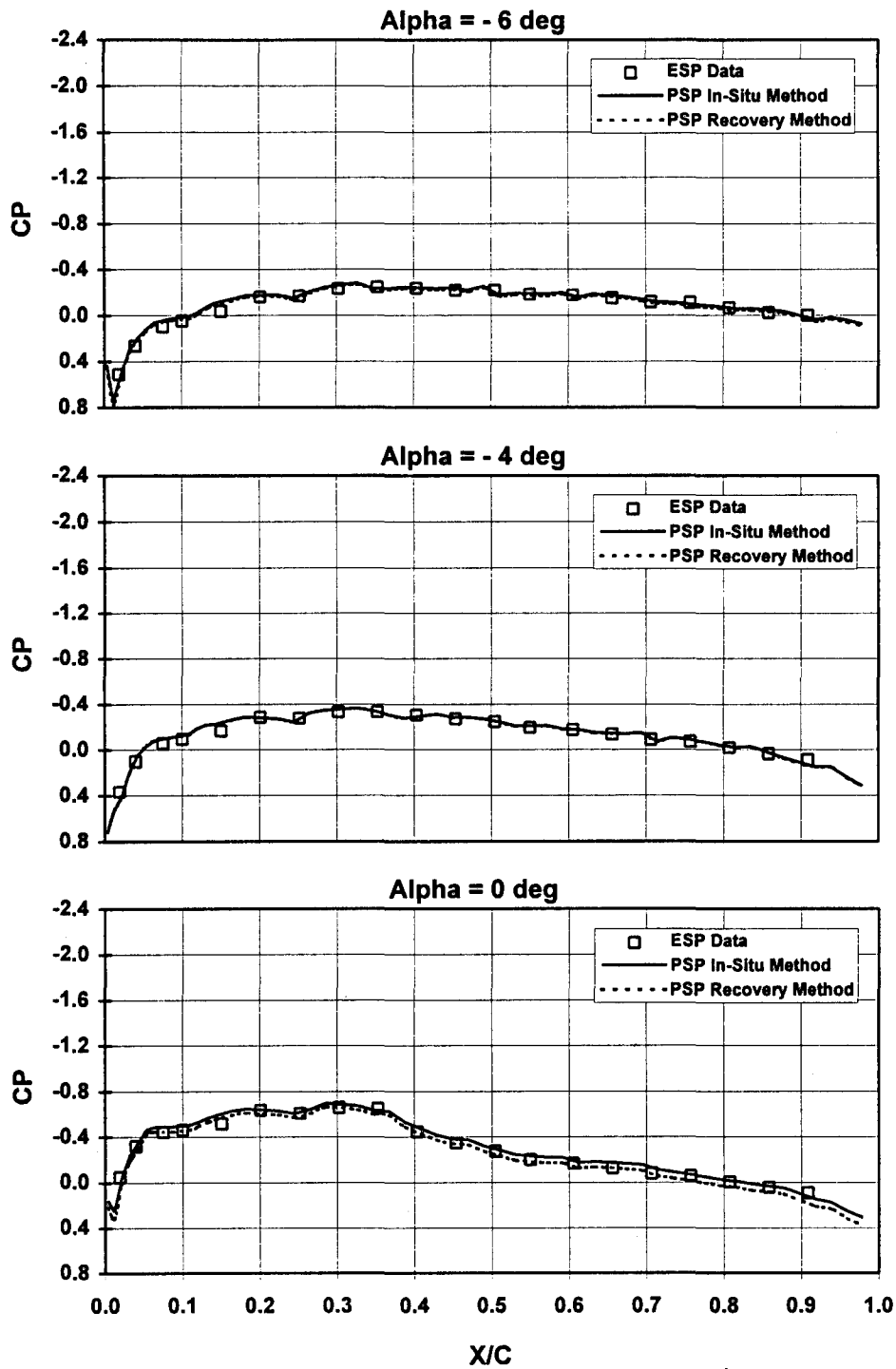




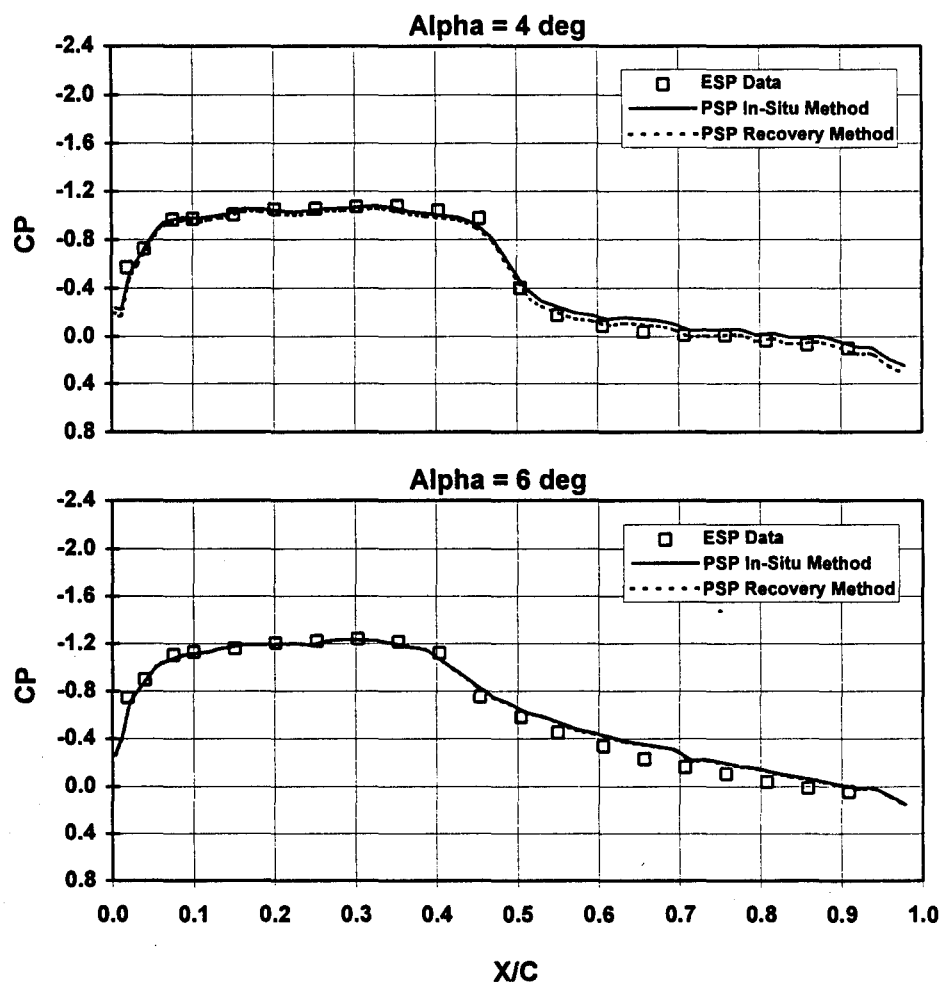
c. Mach = 0.85, PT = 1,000 psfa, TT \approx 120°F

Figure 11. Continued.

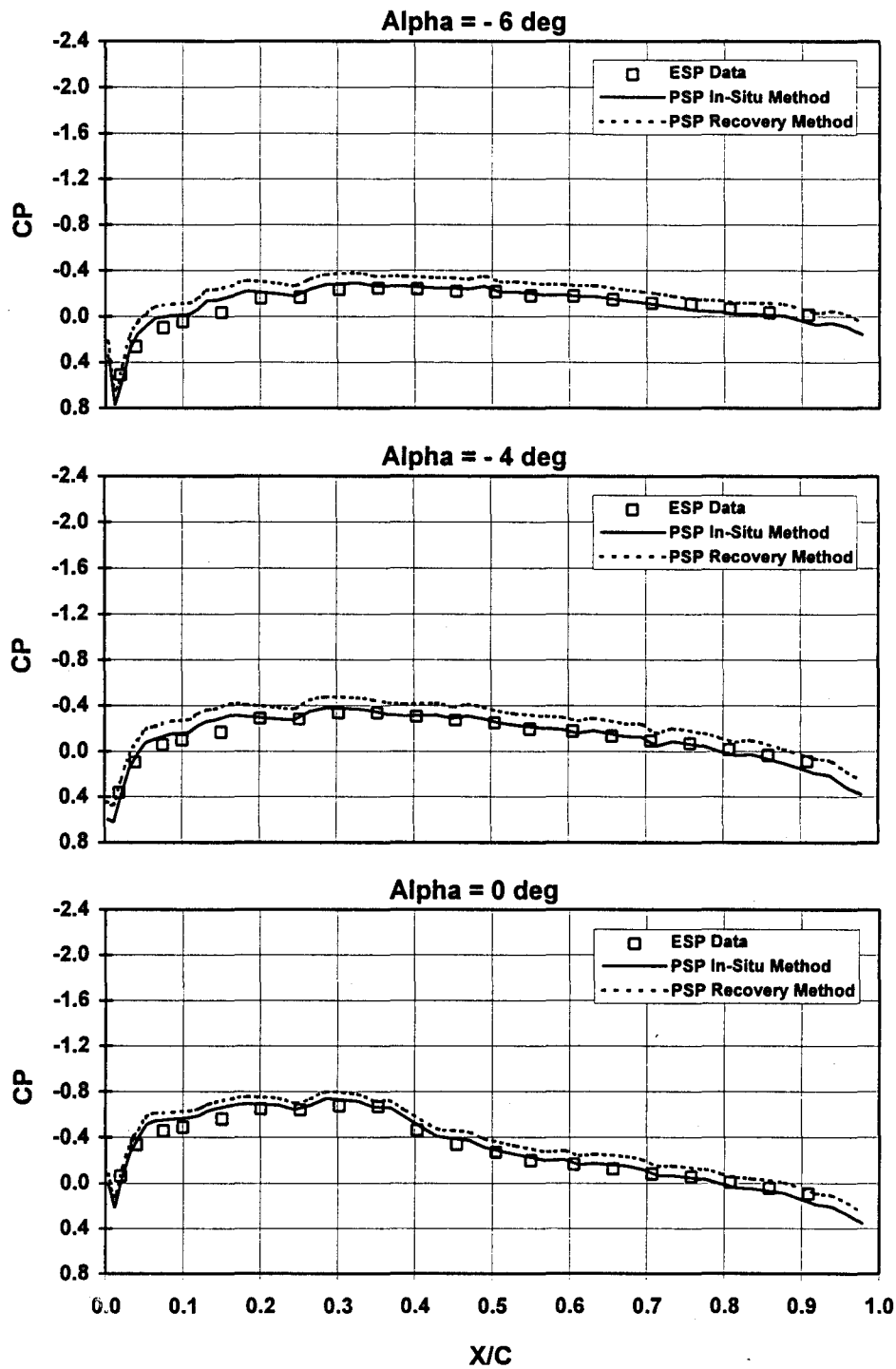




d. Mach = 0.85, PT = 2,000 psfa, TT \approx 95°F
Figure 11. Continued.

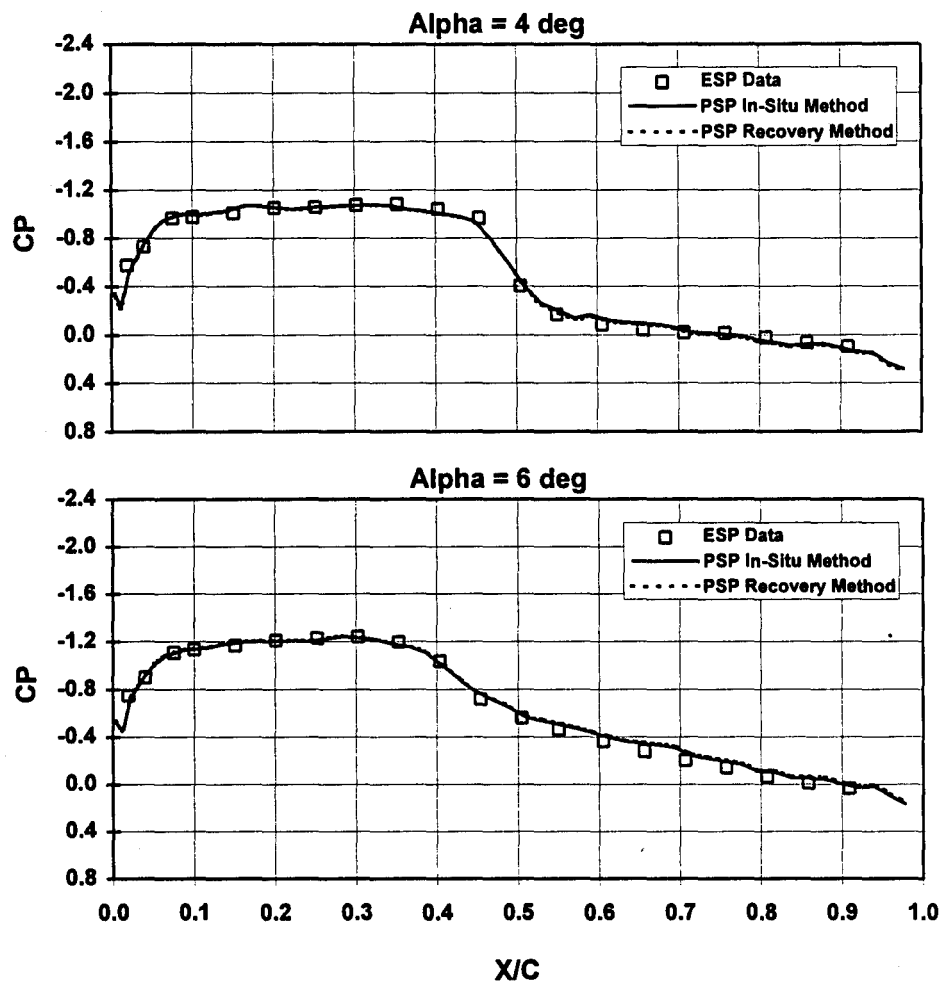


d. Concluded
Figure 11. Continued.

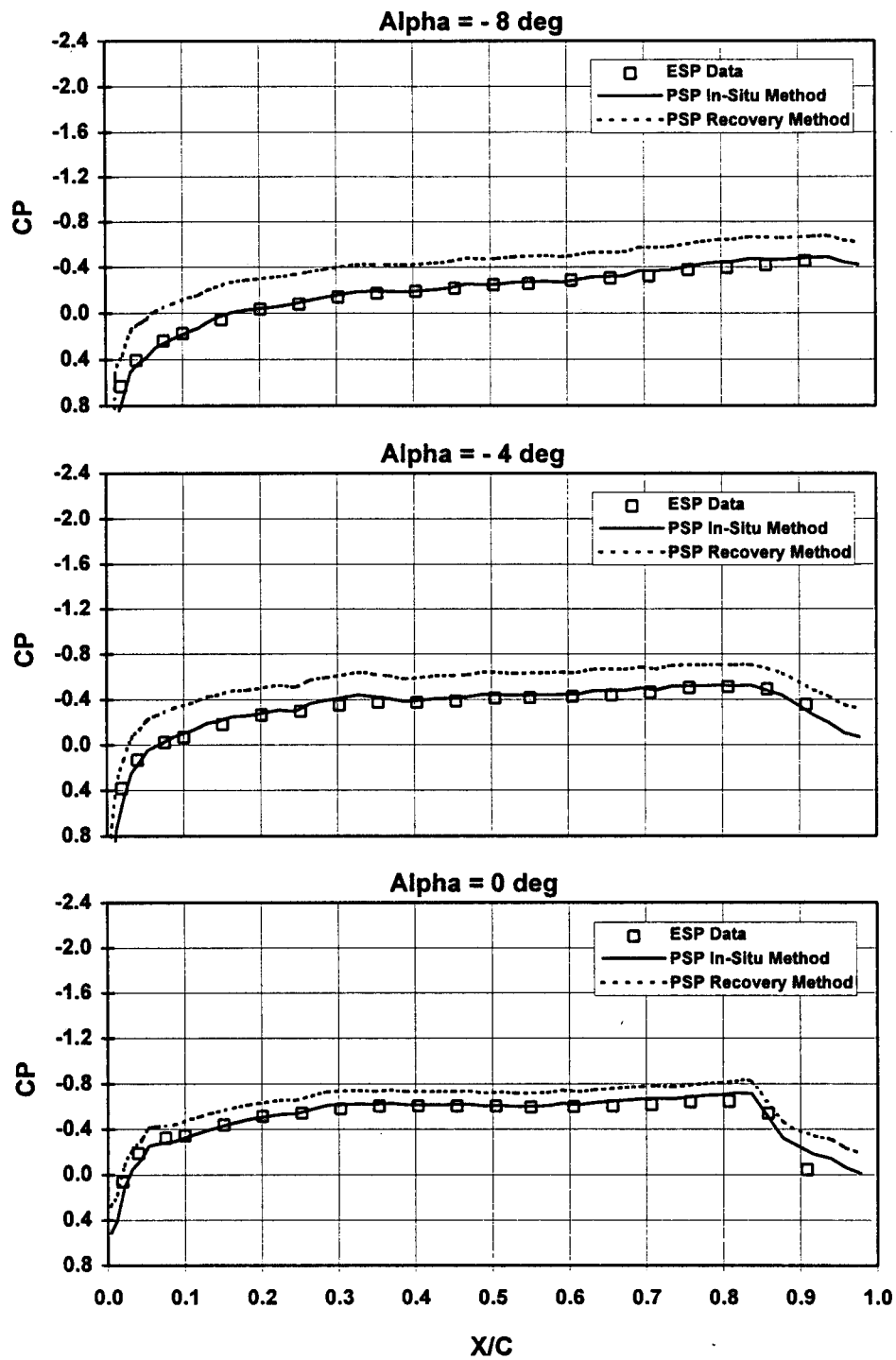


e. Mach = 0.85, $P_T = 2,000$ psfa, $T_T \approx 120^\circ\text{F}$

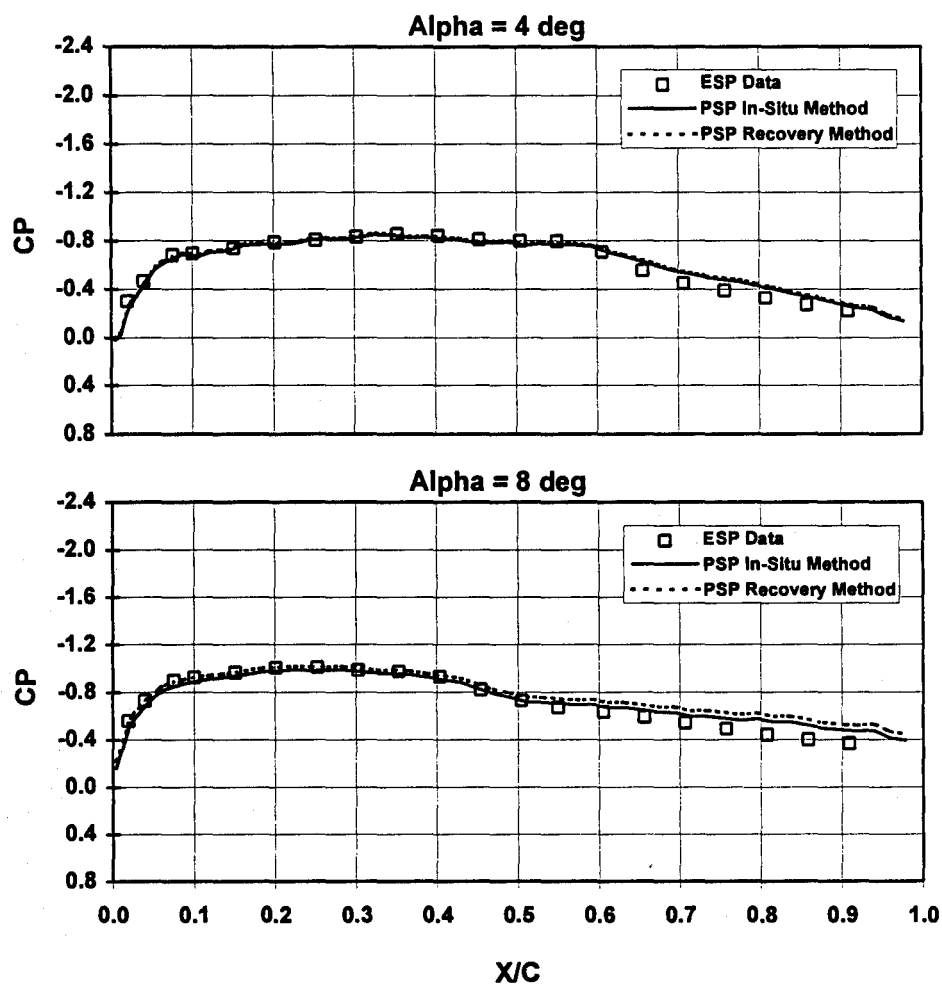
Figure 11. Continued.



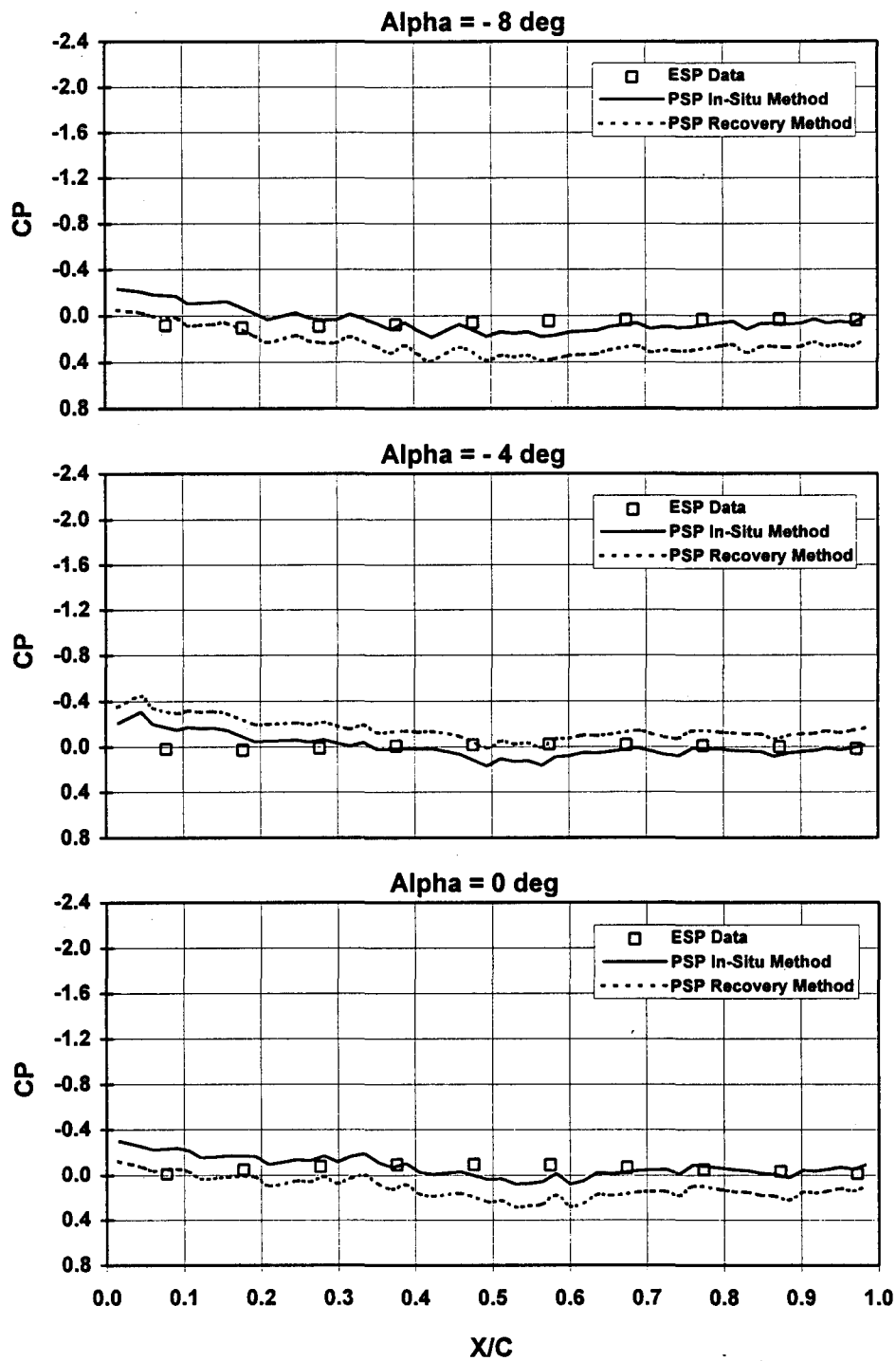
e. Concluded
Figure 11. Continued.



f. Mach = 0.95, $P_T = 1,000$ psfa, $T_T \approx 90^\circ\text{F}$
Figure 11. Continued.

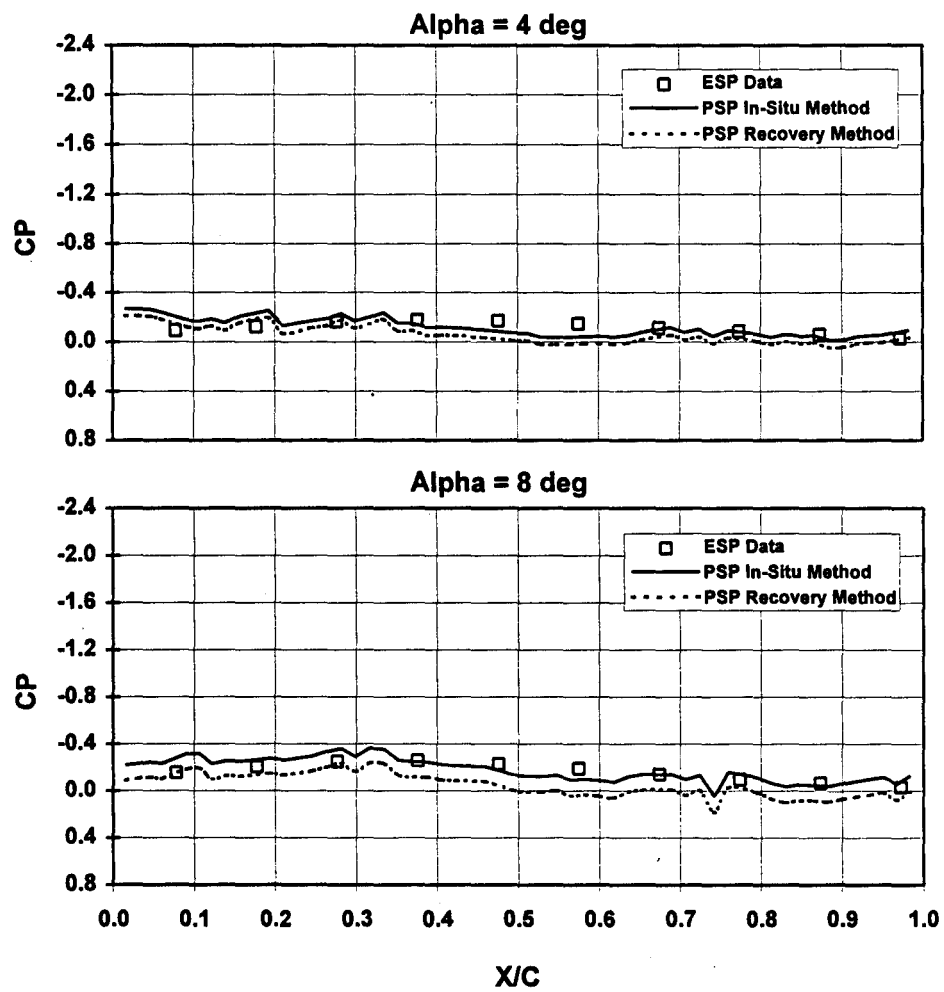


f. Concluded
Figure 11. Concluded.

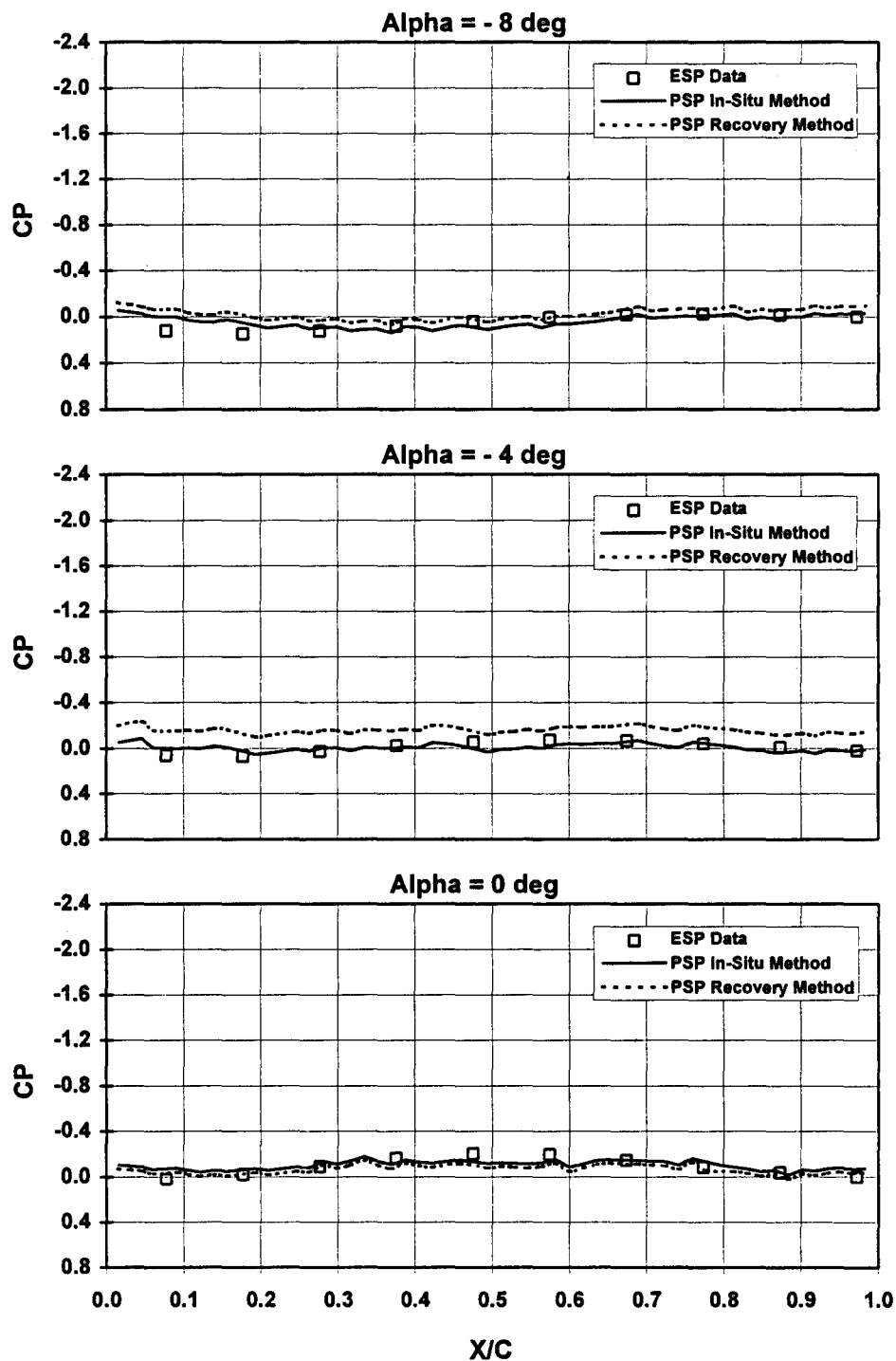


a. Mach = 0.60, PT = 1,000 psfa, TT \approx 90°F

Figure 12. Fuselage CP comparison using two temperature methods for AEDC PSP.

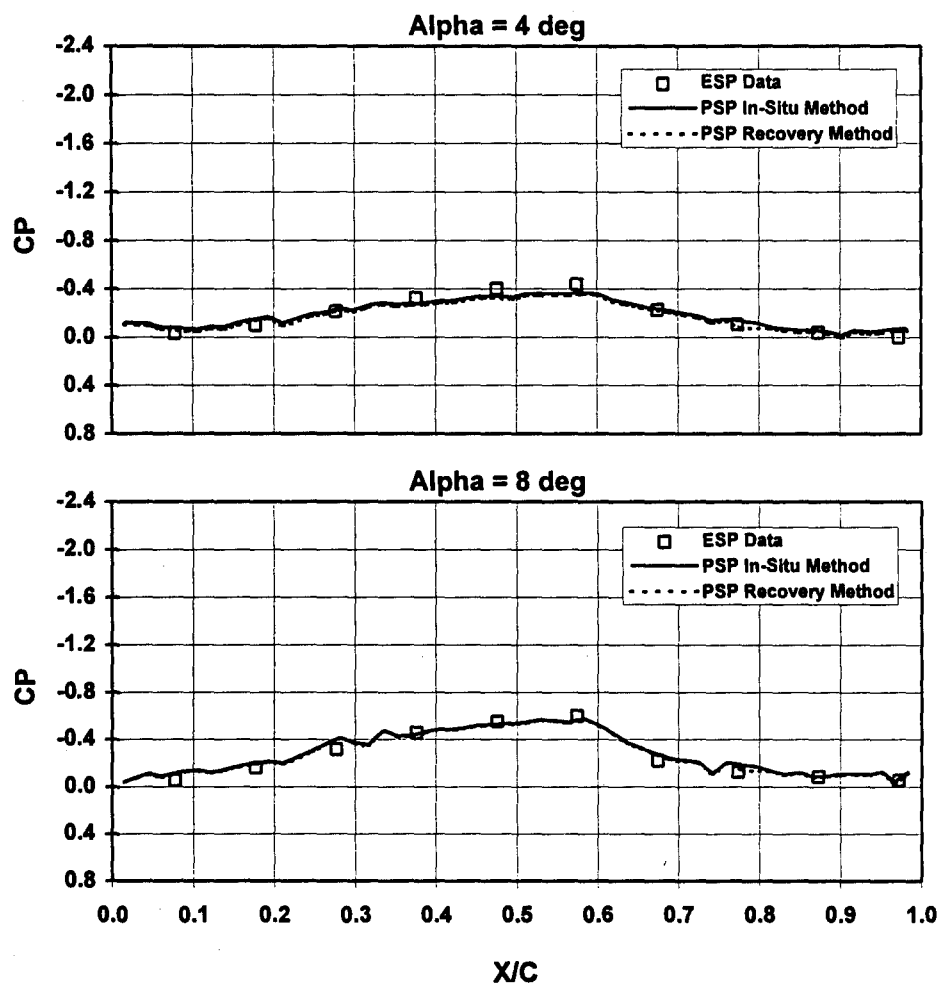


a. Concluded
Figure 12. Continued.

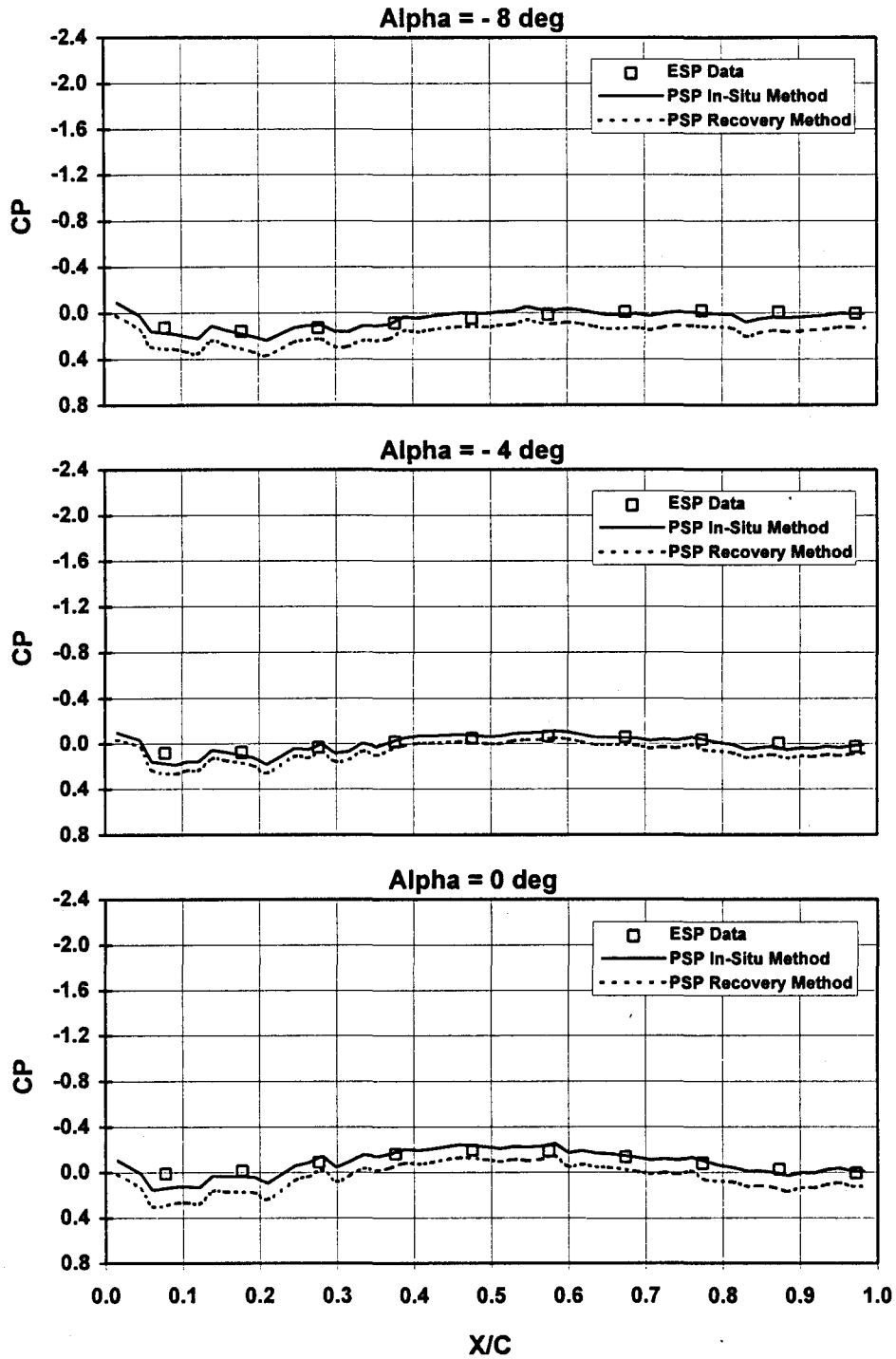


b. Mach = 0.85, $PT = 1,000$ psfa, $TT \approx 90^\circ F$

Figure 12. Continued.

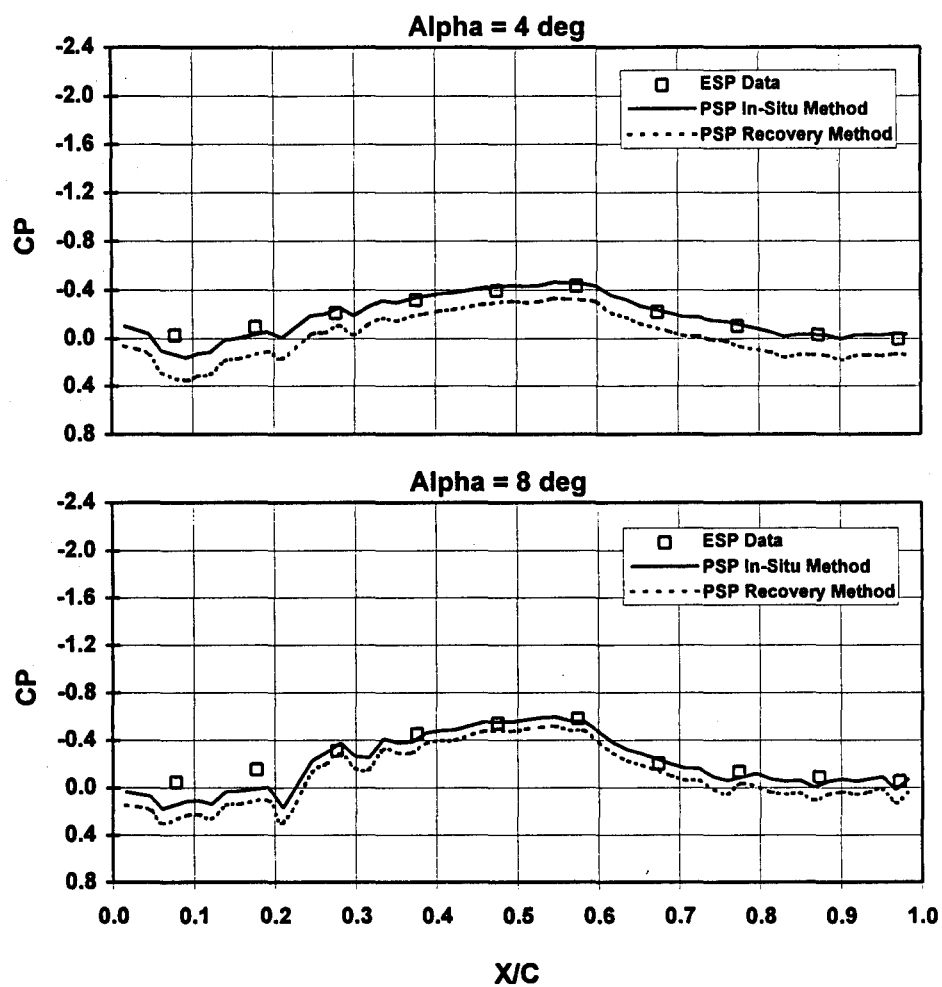


b. Concluded
Figure 12. Continued.

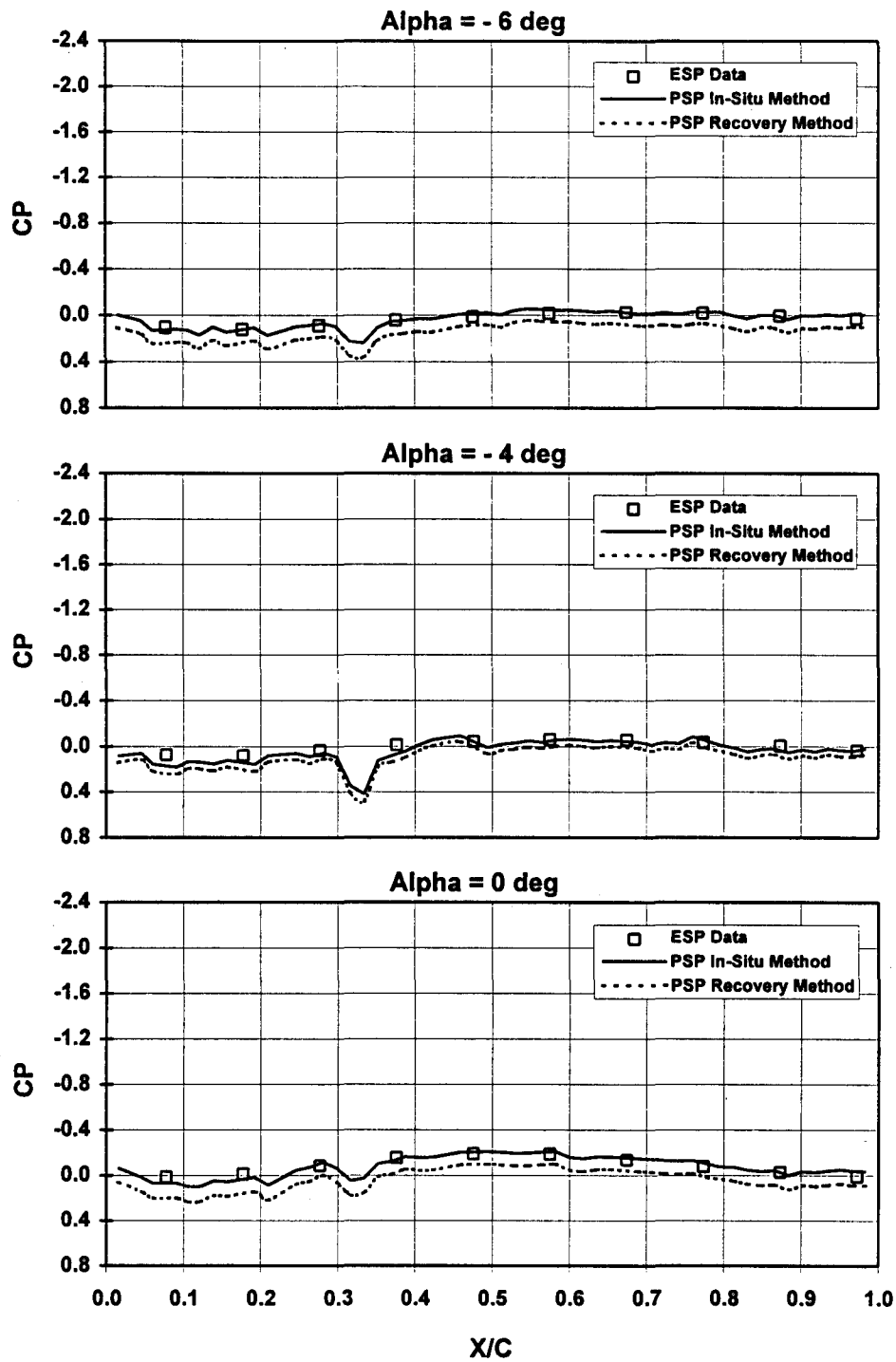


c. Mach = 0.85, $P_T = 1,000$ psfa, $T_T \approx 120^\circ\text{F}$

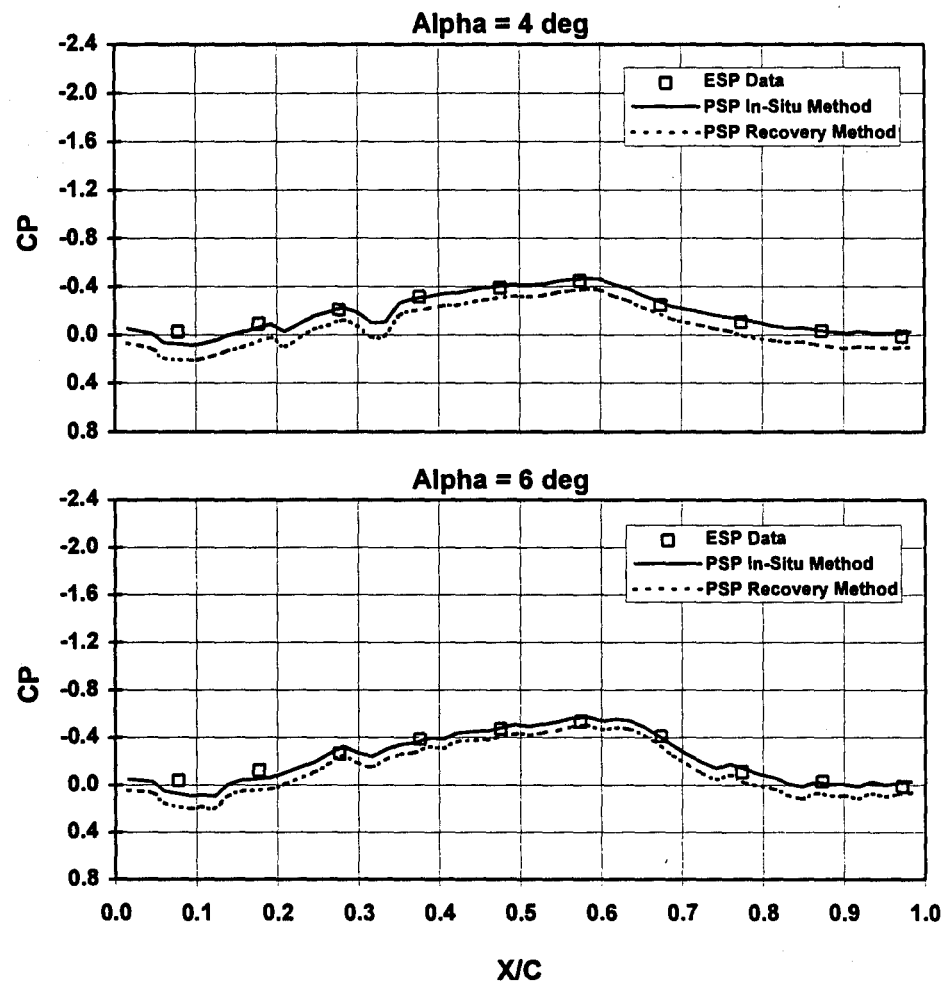
Figure 12. Continued.



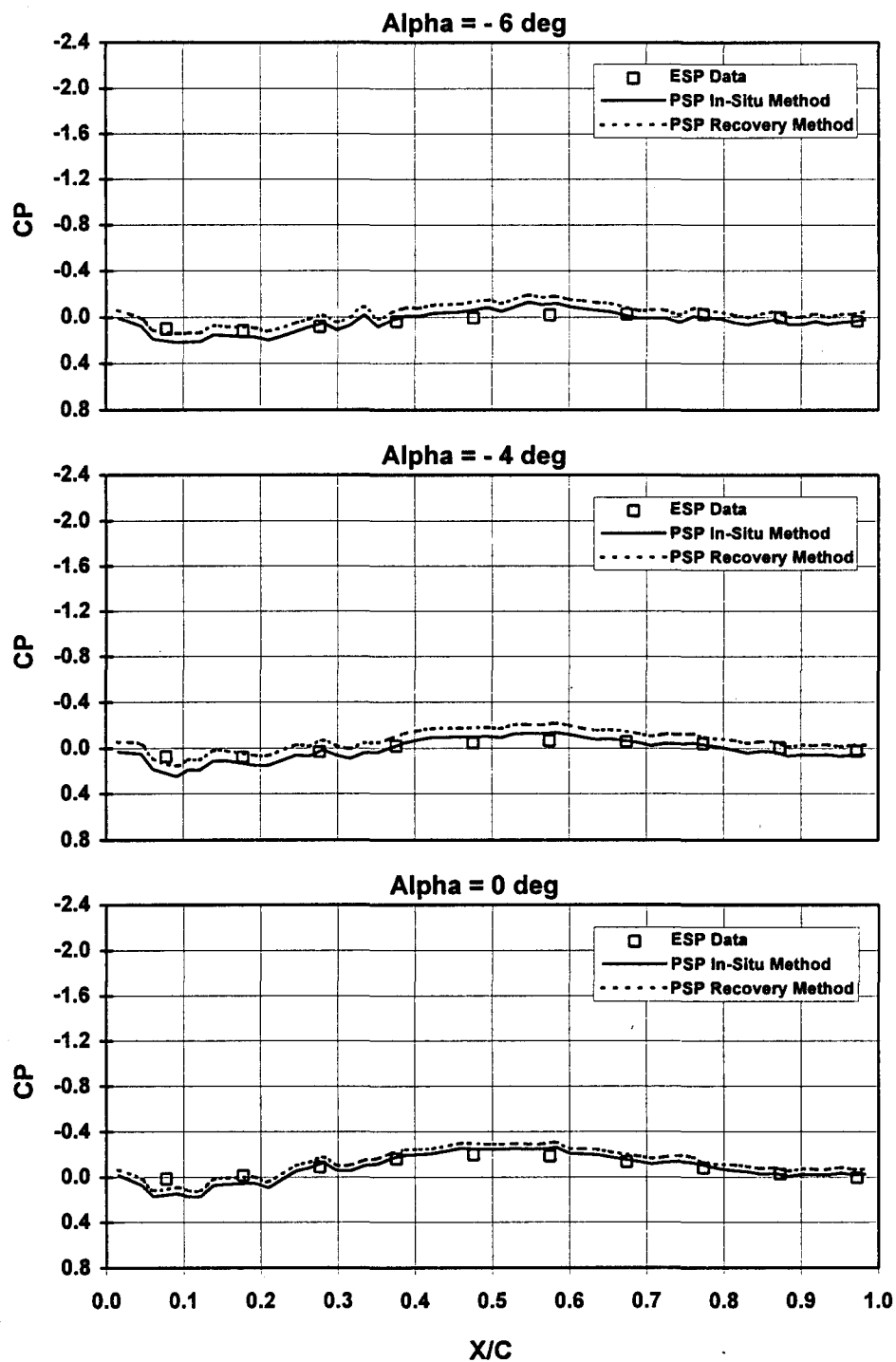
c. Concluded
Figure 12. Continued.



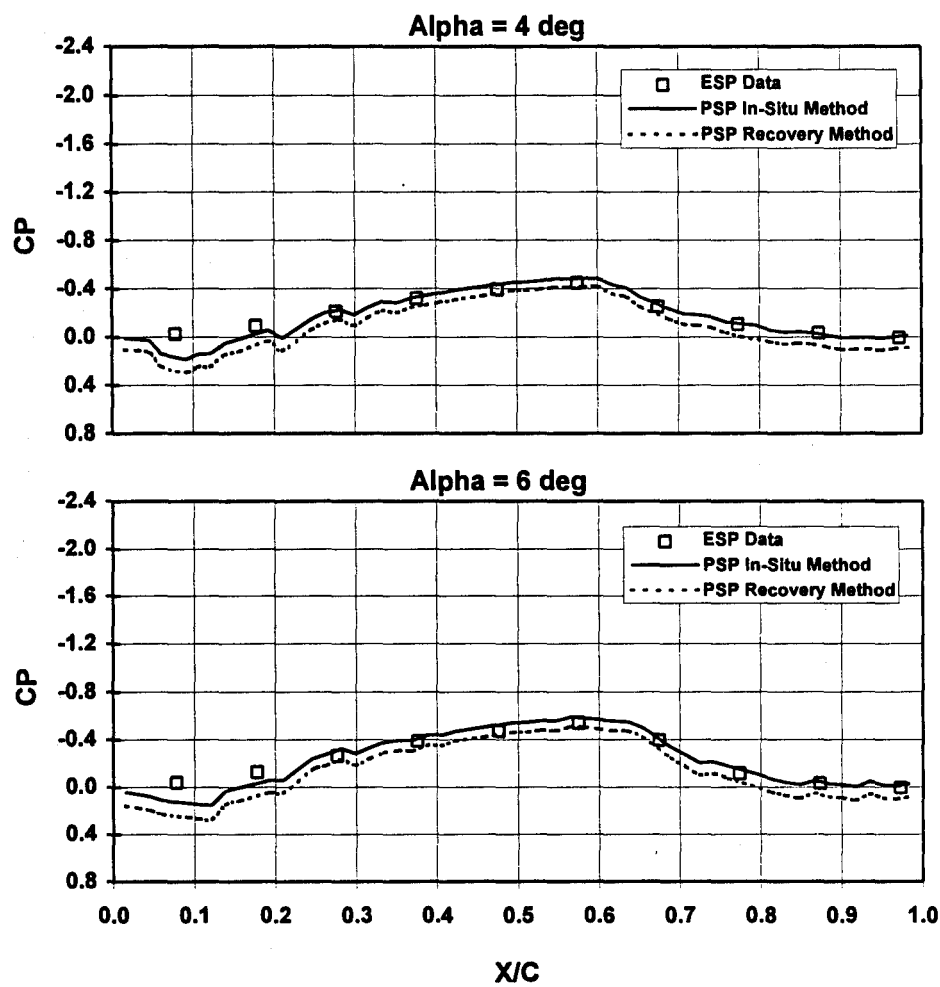
d. Mach = 0.85, PT = 2,000 psfa, TT \approx 95°F
Figure 12. Continued.



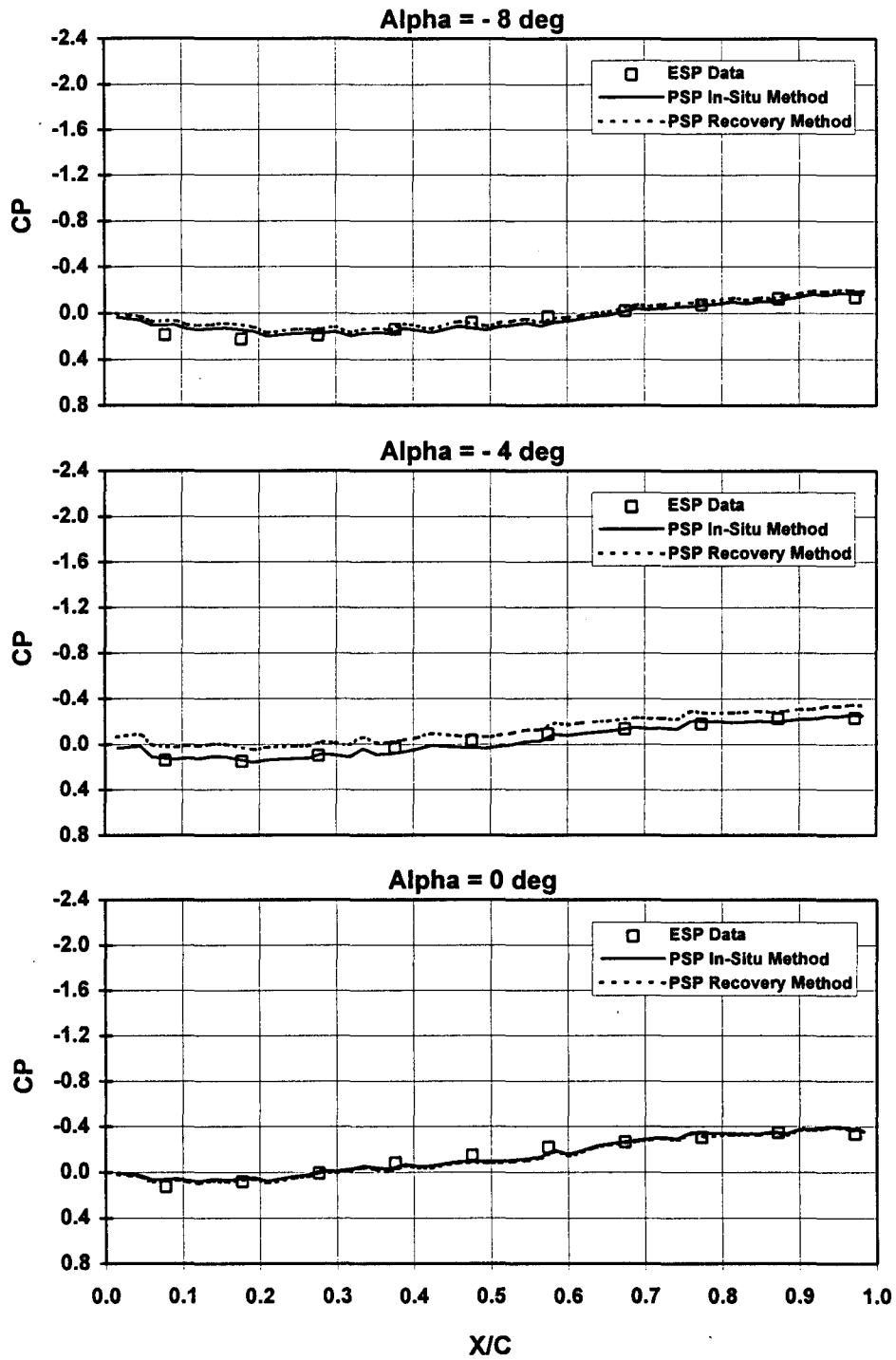
d. Concluded
Figure 12. Continued.



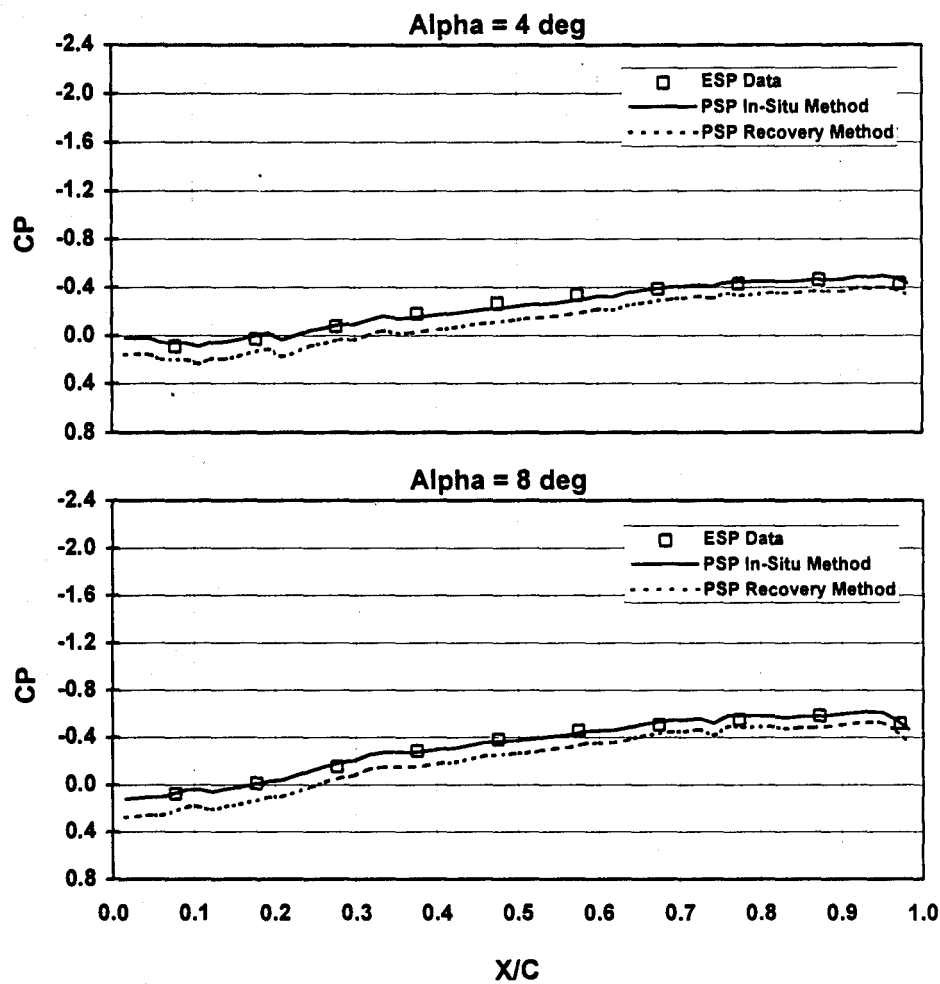
e. Mach = 0.85, PT = 2,000 psfa, TT \approx 120°F
Figure 12. Continued.



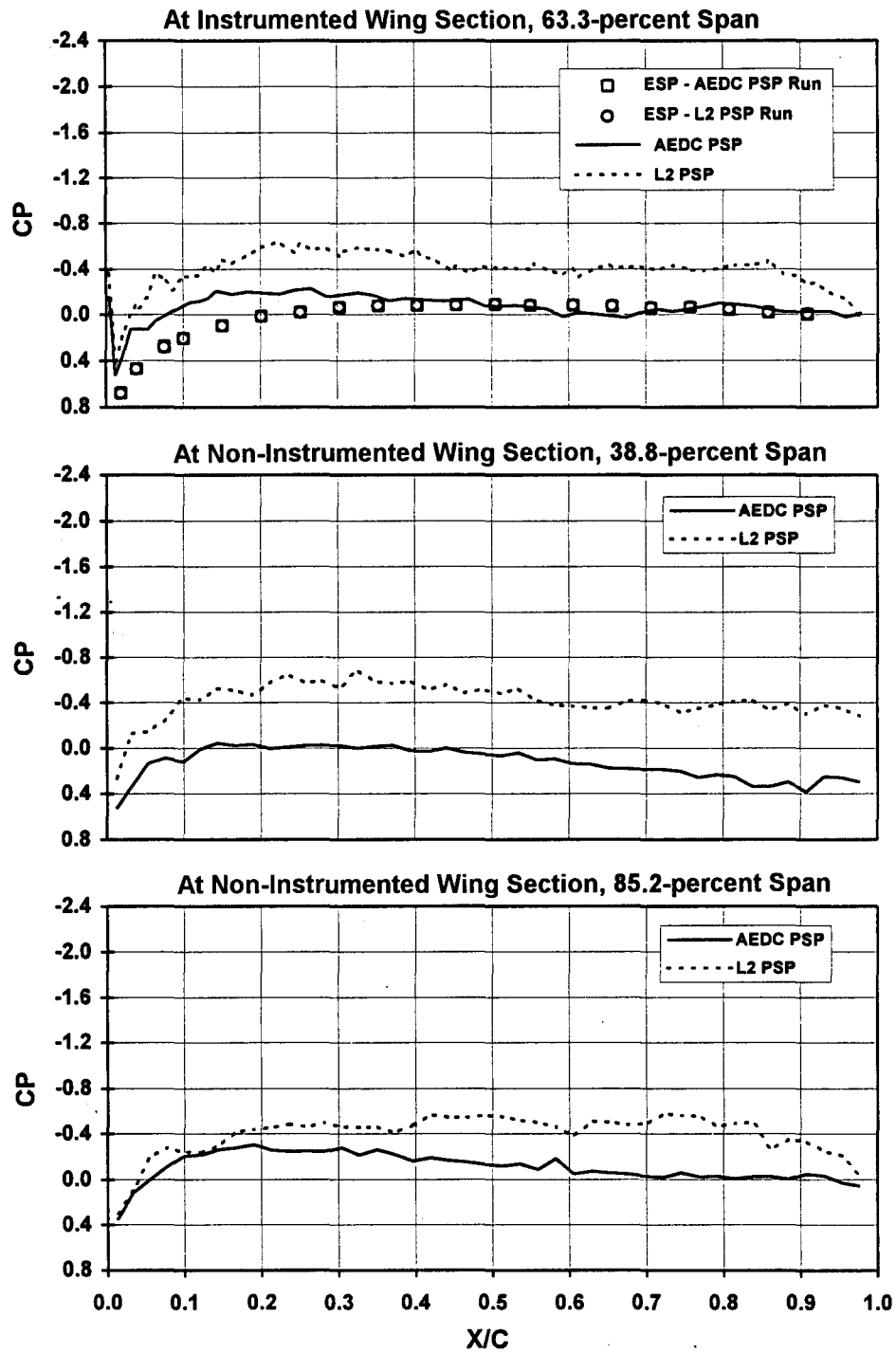
e. Concluded
Figure 12. Continued.



f. Mach = 0.95, PT = 1,000 psfa, TT \approx 90°F
Figure 12. Continued.

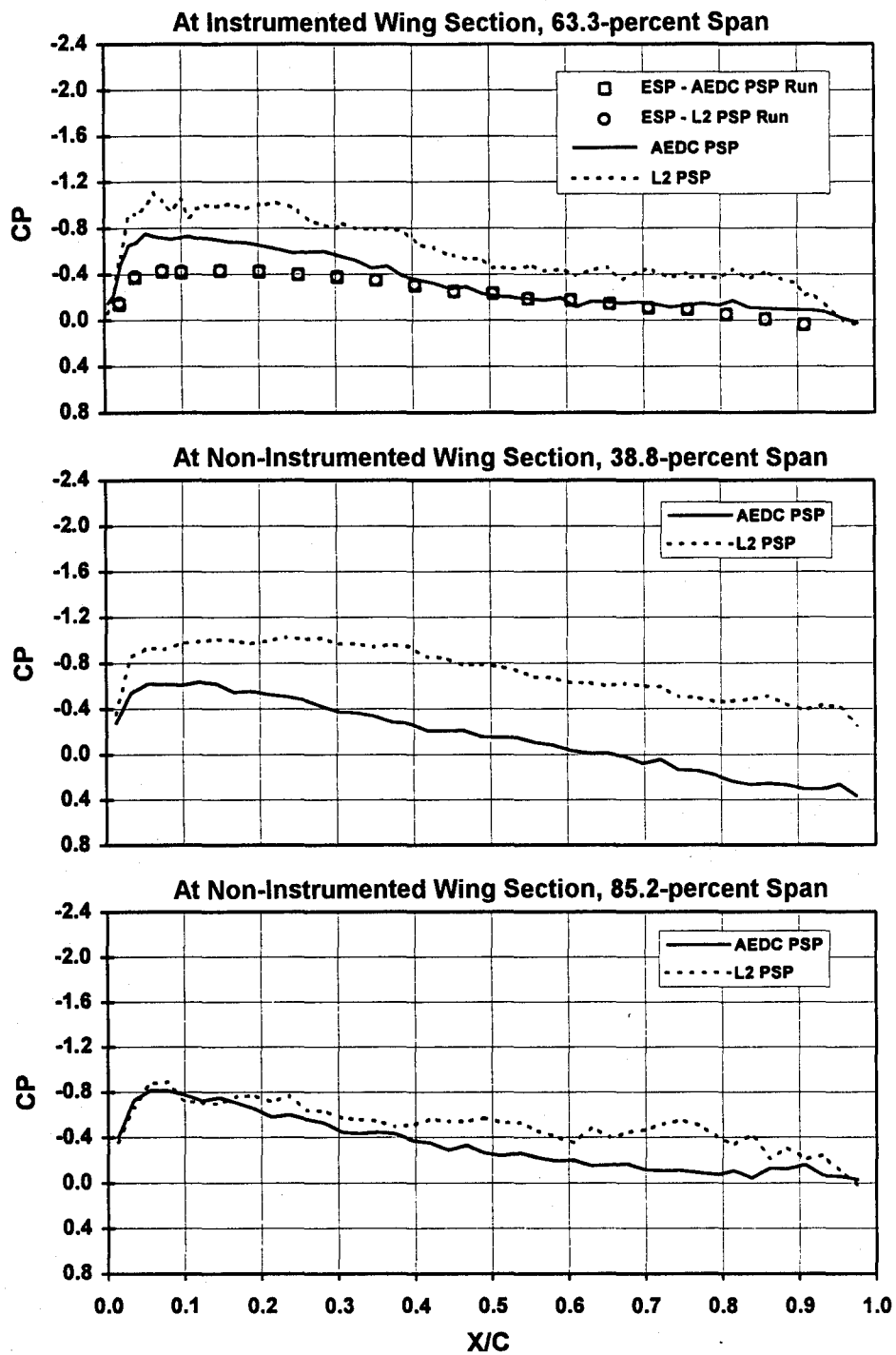


f. Concluded
Figure 12. Concluded.



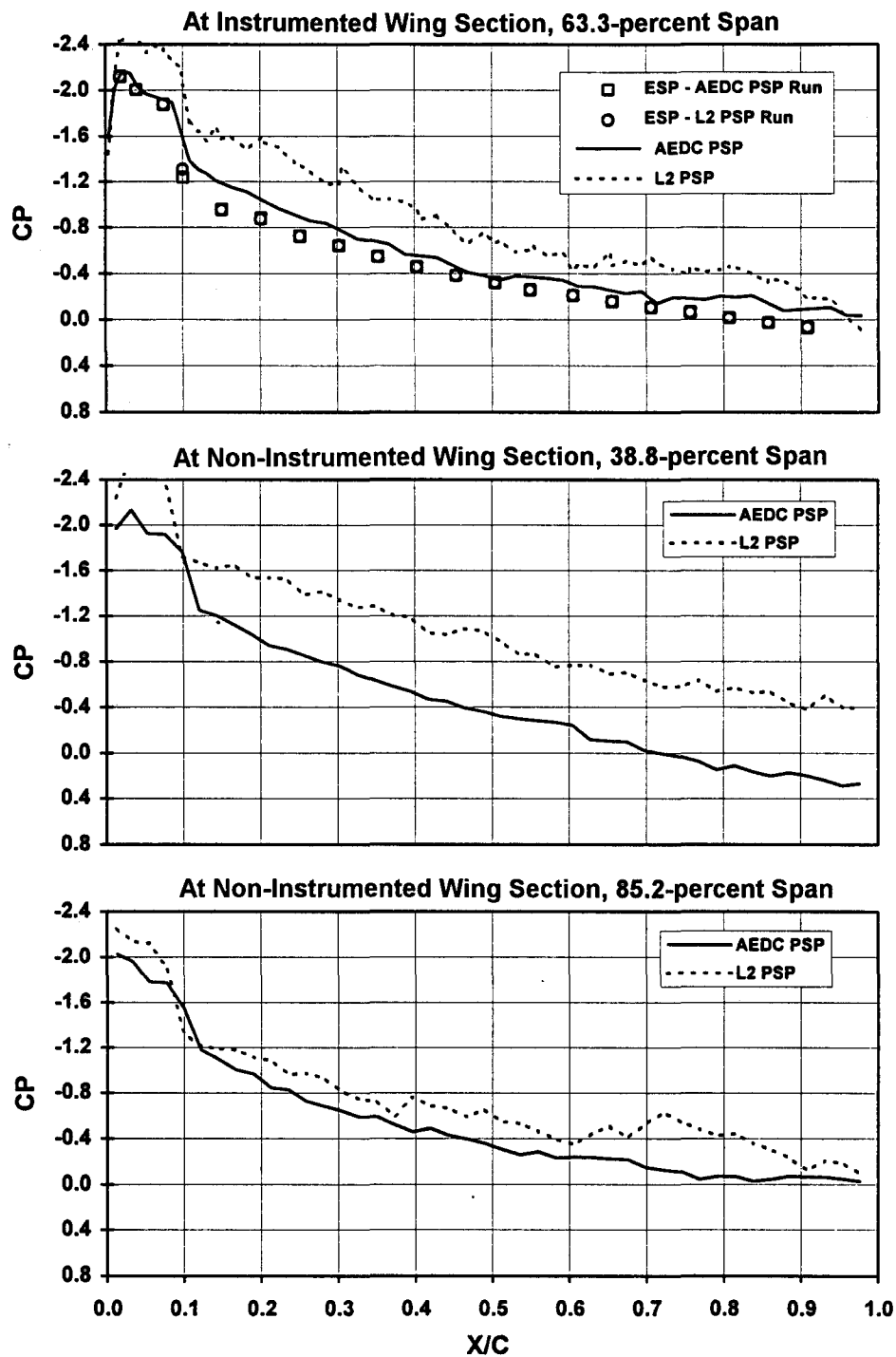
a. Mach = 0.85, Alpha = -8 deg, PT = 1,000 psfa, TT \approx 90°F

Figure 13. AEDC and L2 PSP comparison.

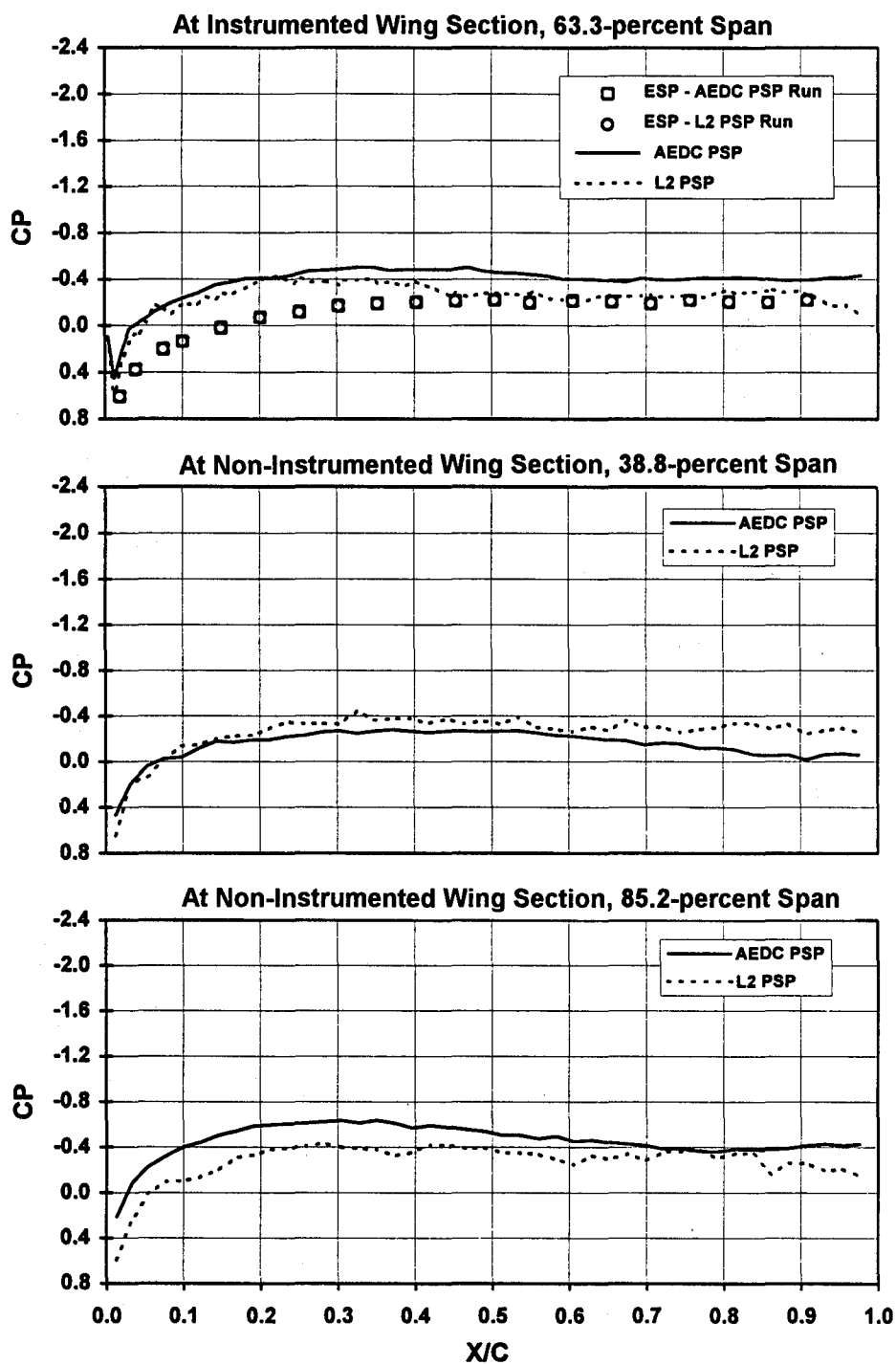


b. Mach = 0.60, Alpha = 0 deg, PT = 1,000 psfa, TT ≈ 90°F

Figure 13. Continued.

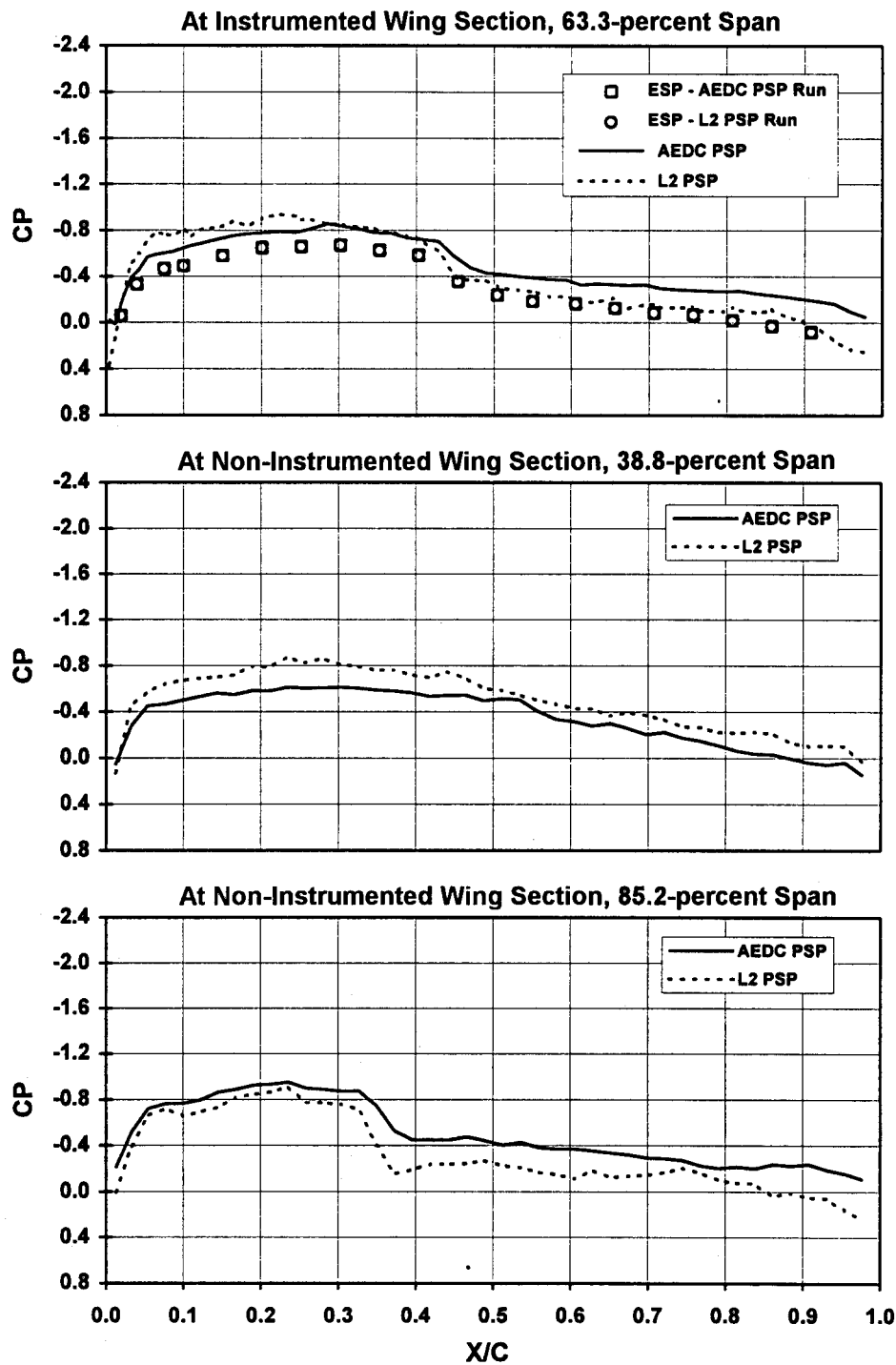


c. Mach = 0.60, Alpha = 8 deg, PT = 1,000 psfa, TT \approx 90°F
Figure 13. Continued.



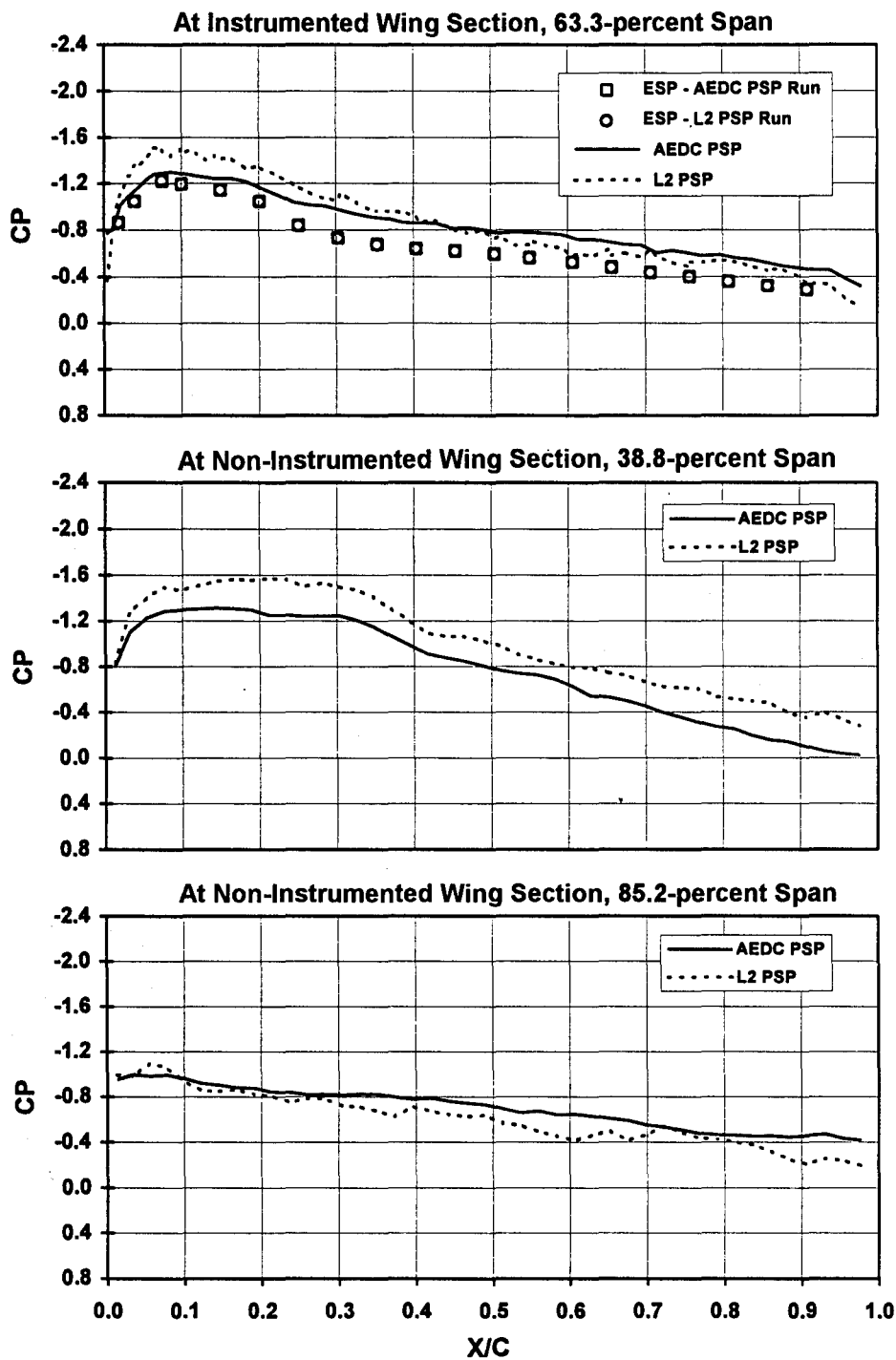
d. Mach = 0.60, Alpha = -8 deg, PT = 1,000 psfa, TT = 90°F

Figure 13. Continued.



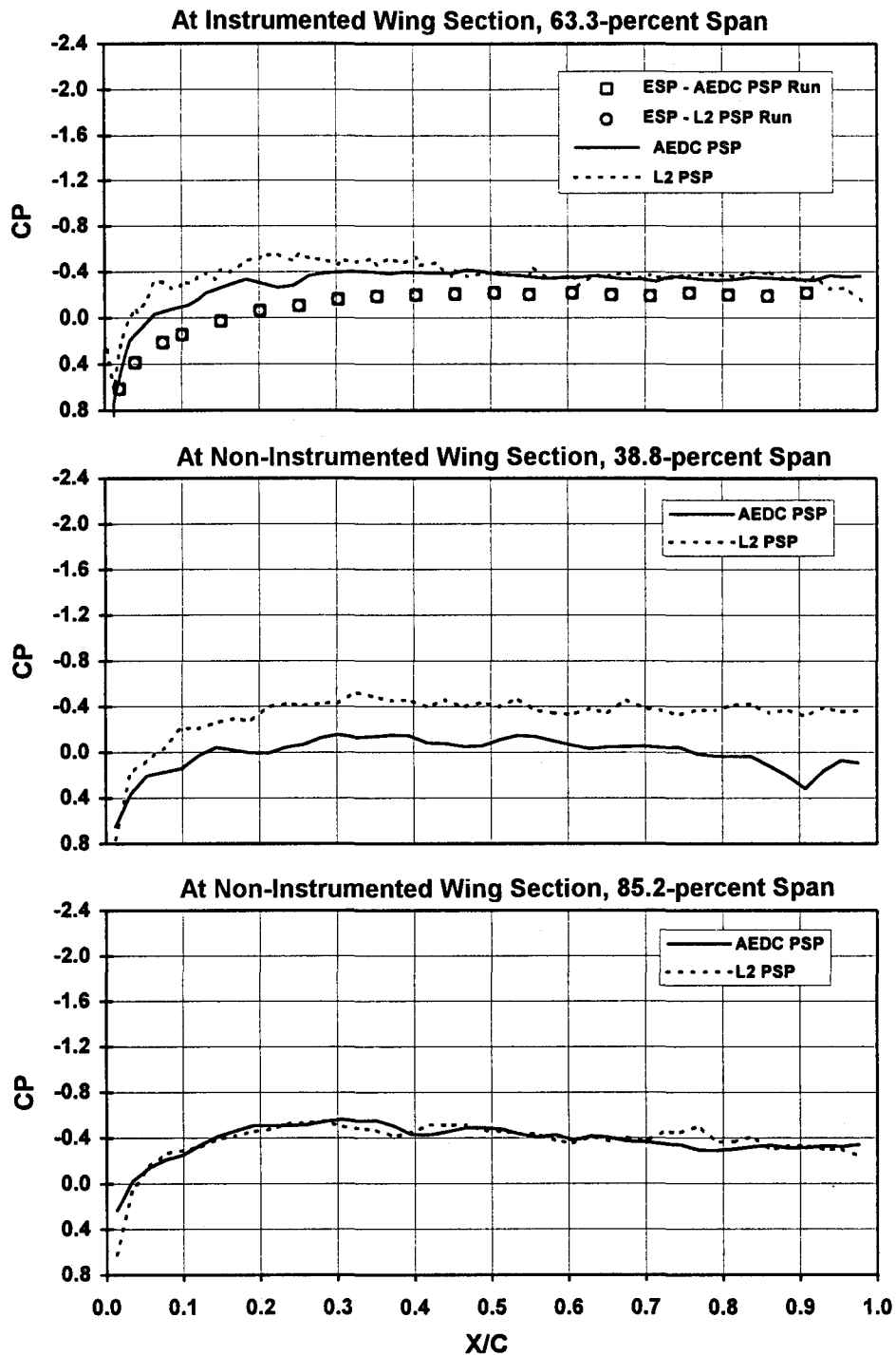
e. Mach = 0.85, Alpha = 0 deg, PT = 1,000 psfa, TT \approx 90°F

Figure 13. Continued.



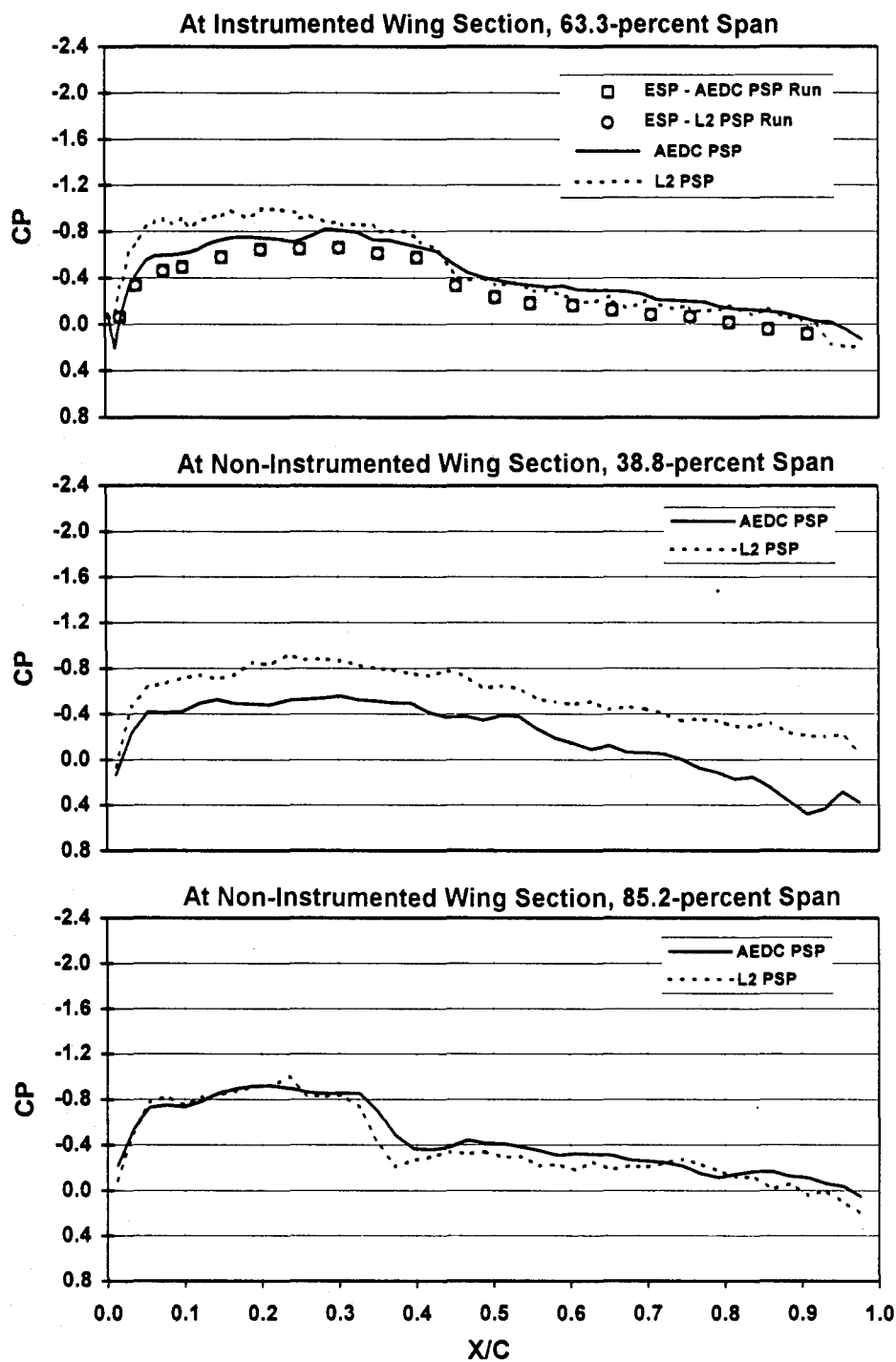
f. Mach = 0.85, Alpha = 8 deg, PT = 1,000 psfa, TT \approx 90°F

Figure 13. Continued.



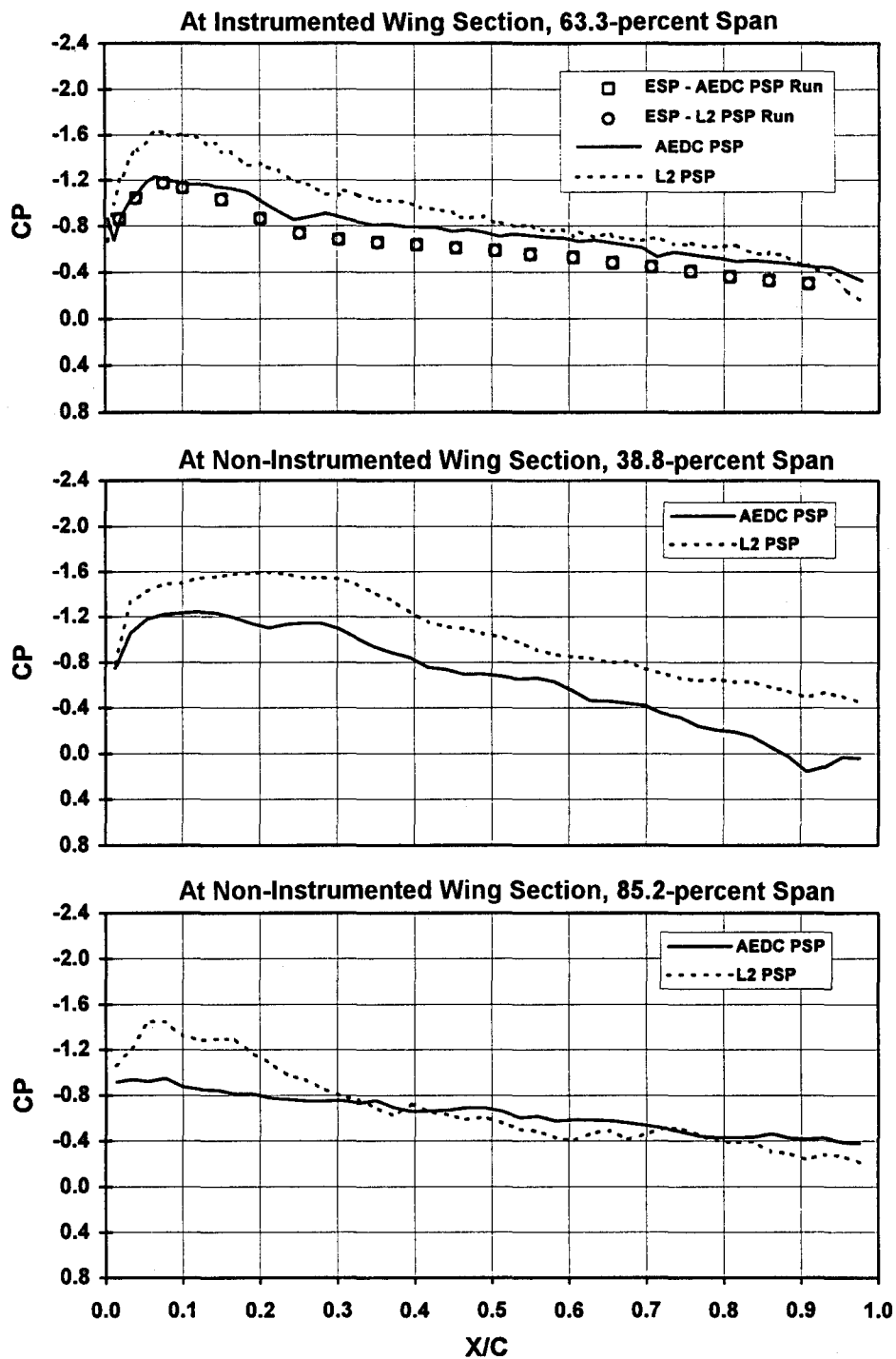
g. Mach = 0.85, Alpha = -8 deg, PT = 1,000 psfa, TT \approx 120°F

Figure 13. Continued.



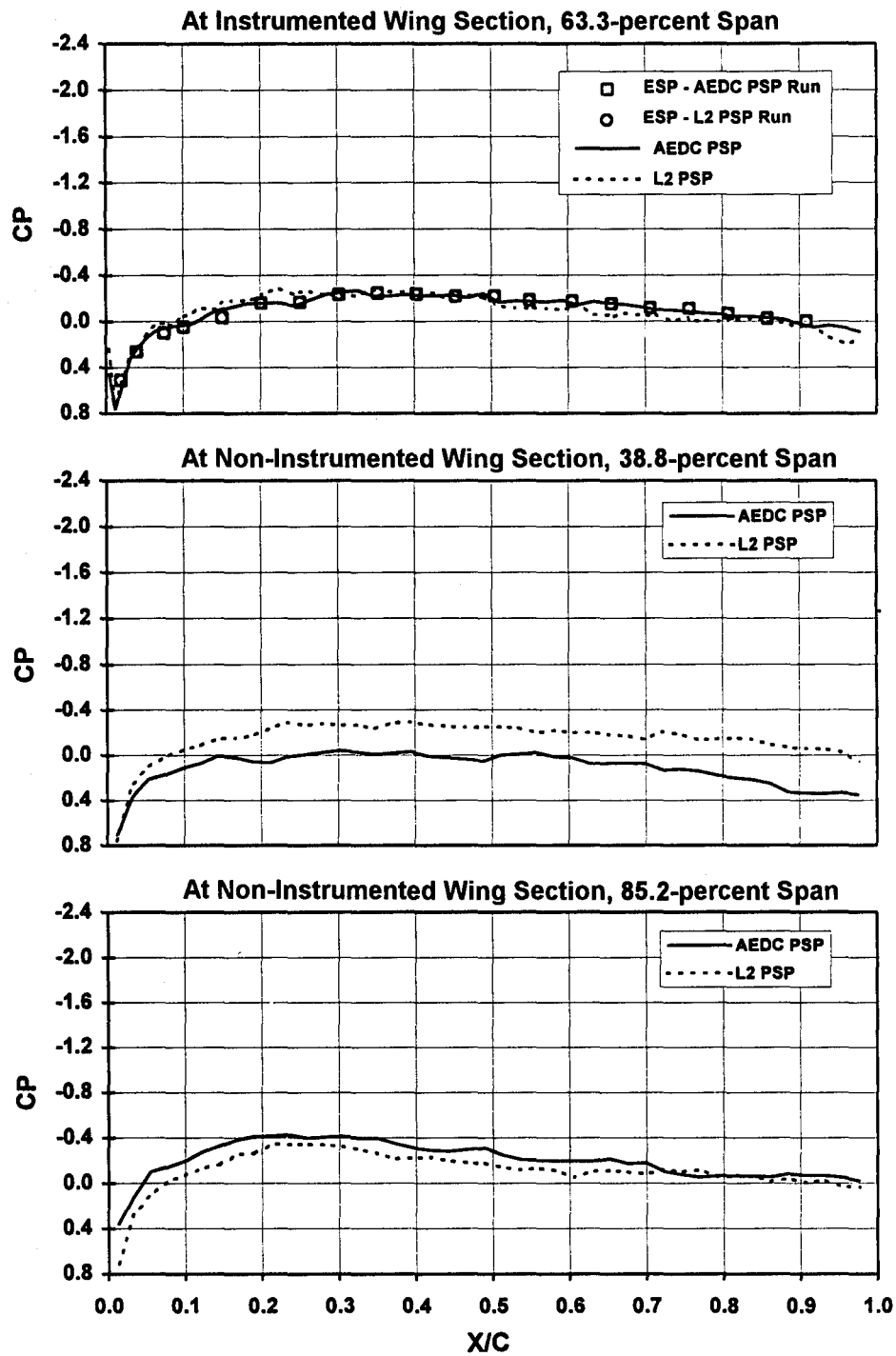
h. Mach = 0.85, Alpha = 0 deg, PT = 1,000 psfa, TT \approx 120°F

Figure 13. Continued.

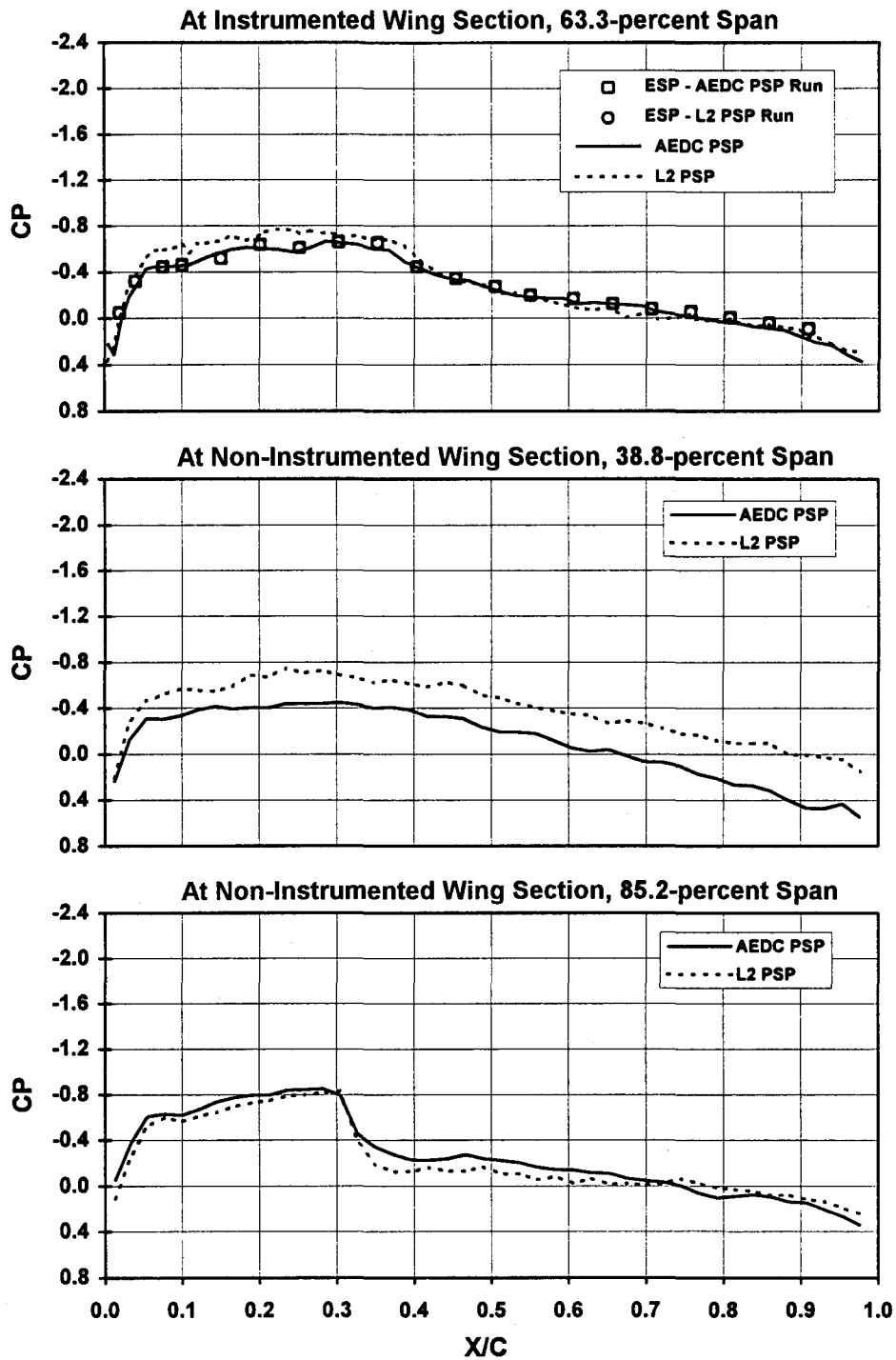


i. Mach = 0.85, Alpha = 8 deg, PT = 1,000 psfa, TT \approx 120°F

Figure 13. Continued.

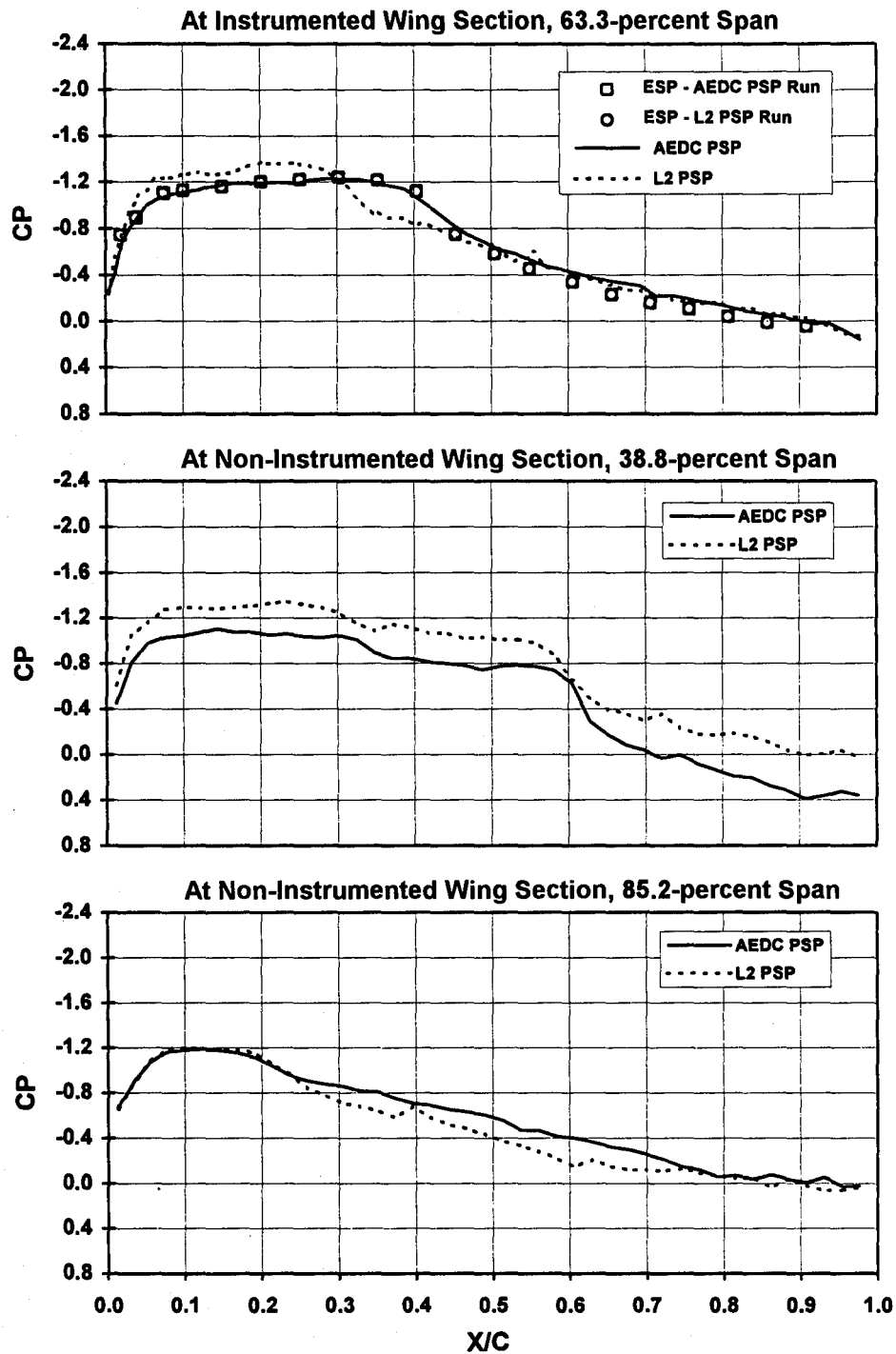


j. Mach = 0.85, Alpha = -6 deg, PT = 2,000 psfa, TT \approx 95°F
Figure 13. Continued.

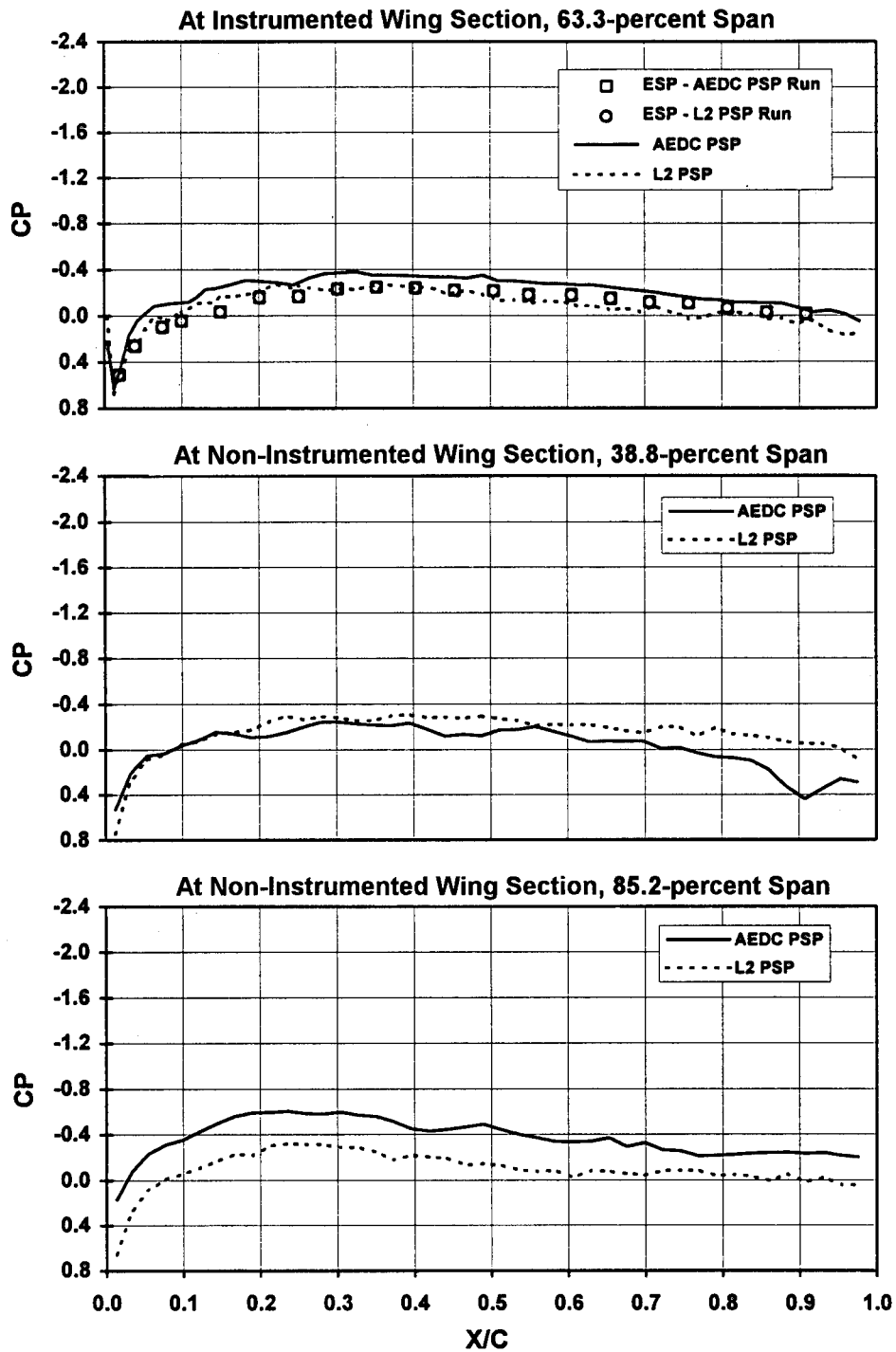


k. Mach = 0.85, Alpha = 0 deg, PT = 2,000 psfa, TT ≈ 95°F

Figure 13. Continued.

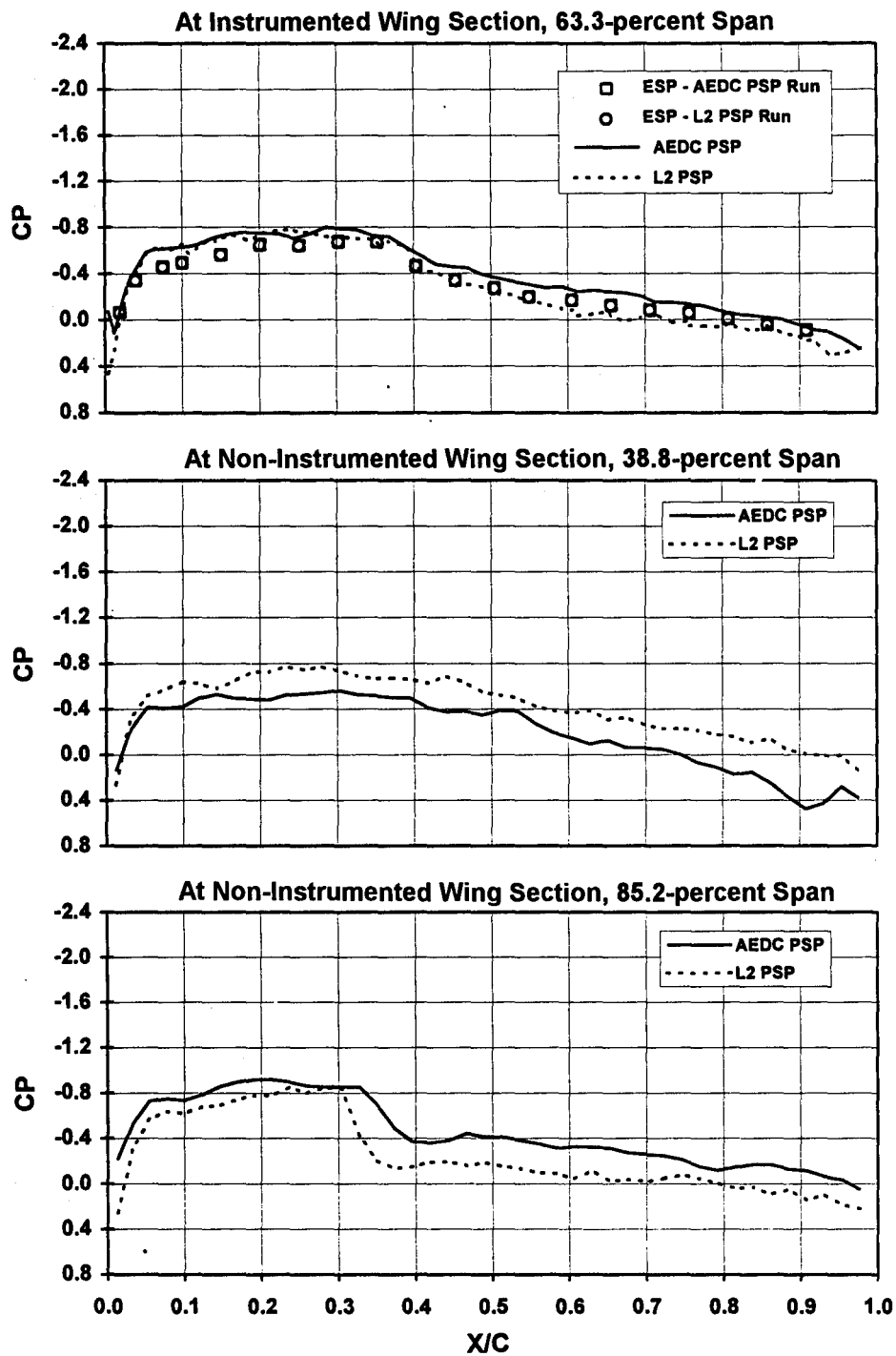


1. Mach = 0.85, Alpha = 6 deg, PT = 2,000 psfa, TT ≈ 95°F
Figure 13. Continued.



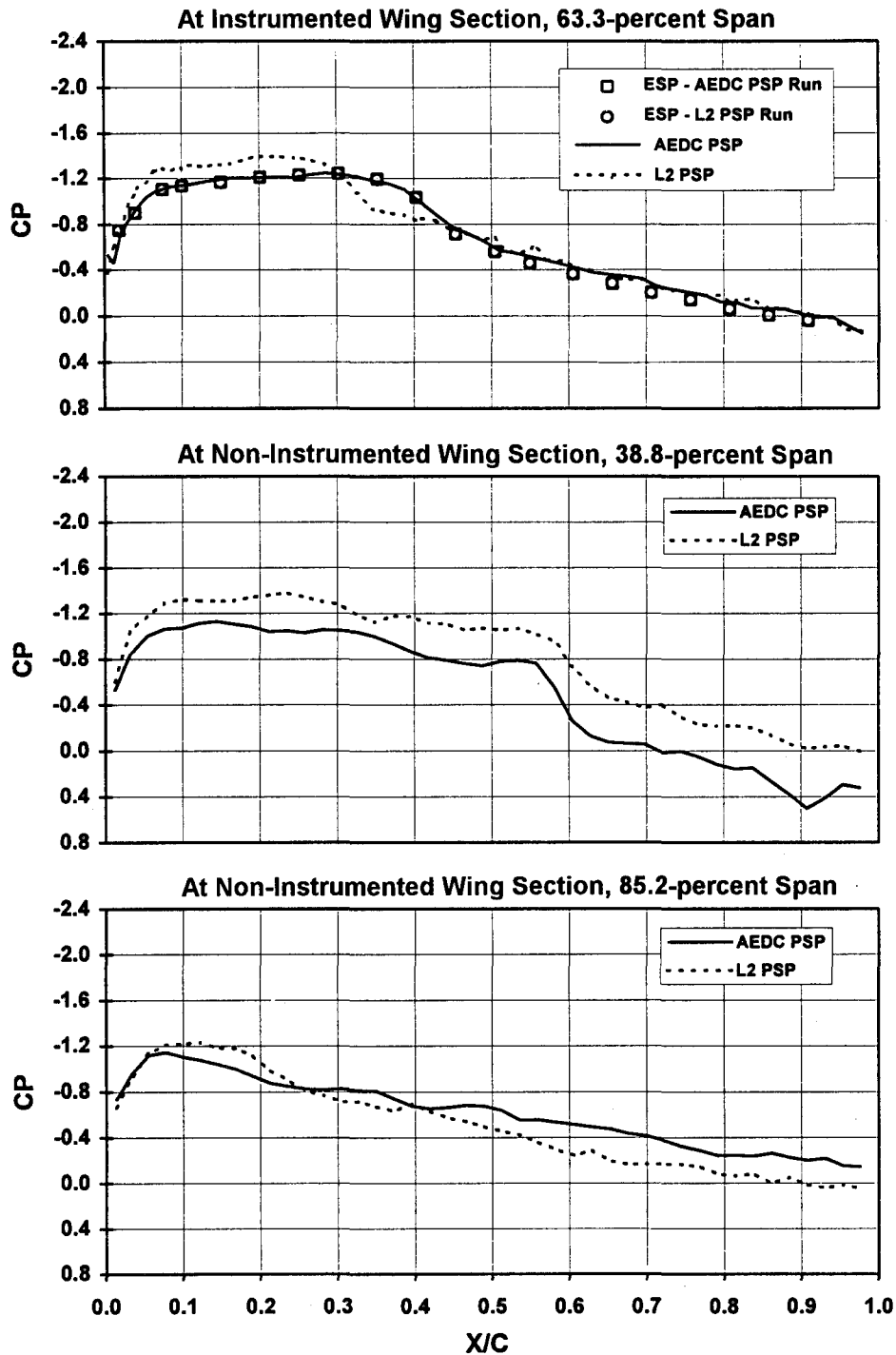
m. Mach = 0.85, Alpha = -6 deg, PT = 2,000 psfa, TT \approx 120°F

Figure 13. Continued.



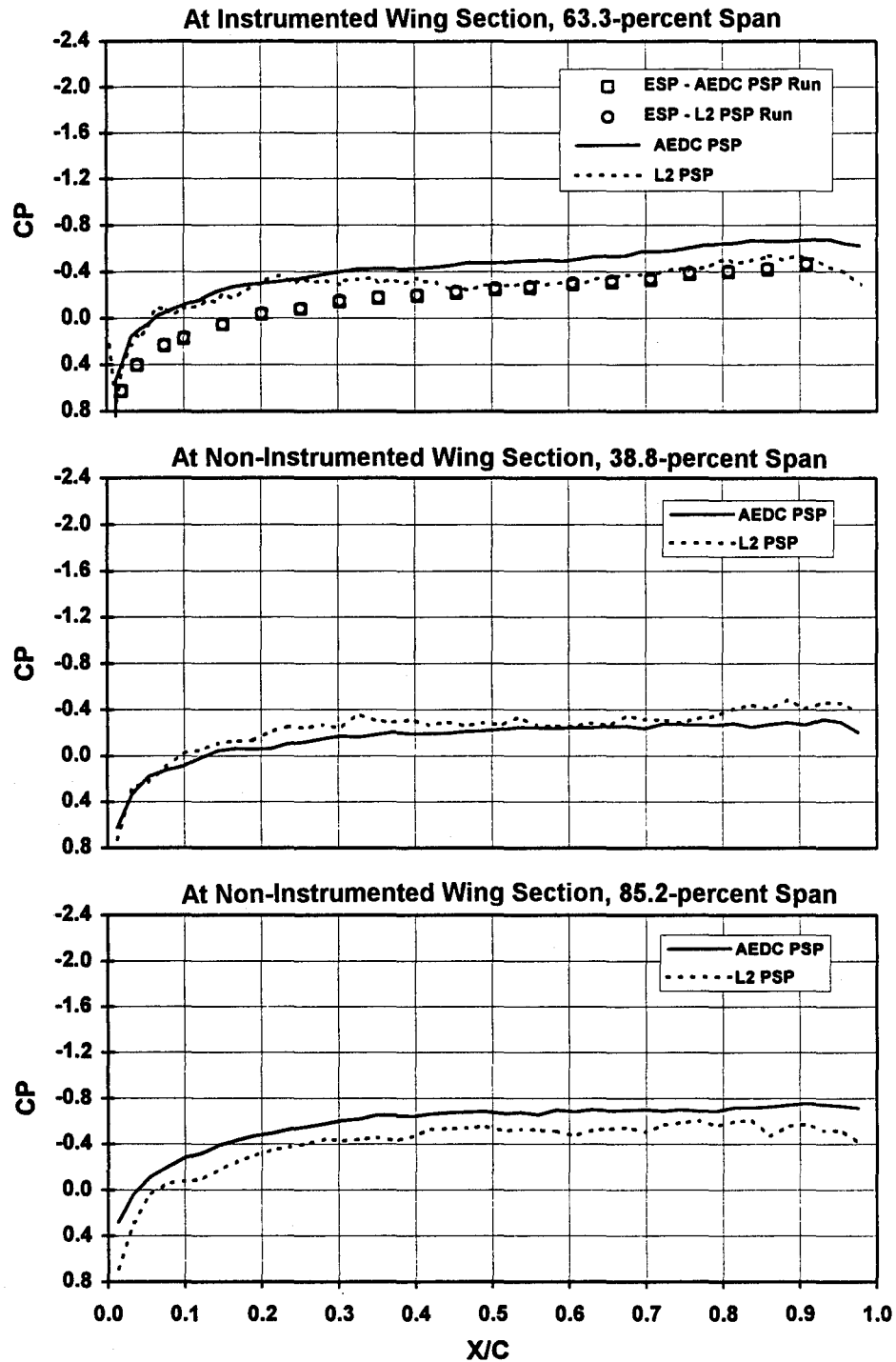
n. Mach = 0.85, Alpha = 0 deg, PT = 2,000 psfa, TT \approx 120°F

Figure 13. Continued.



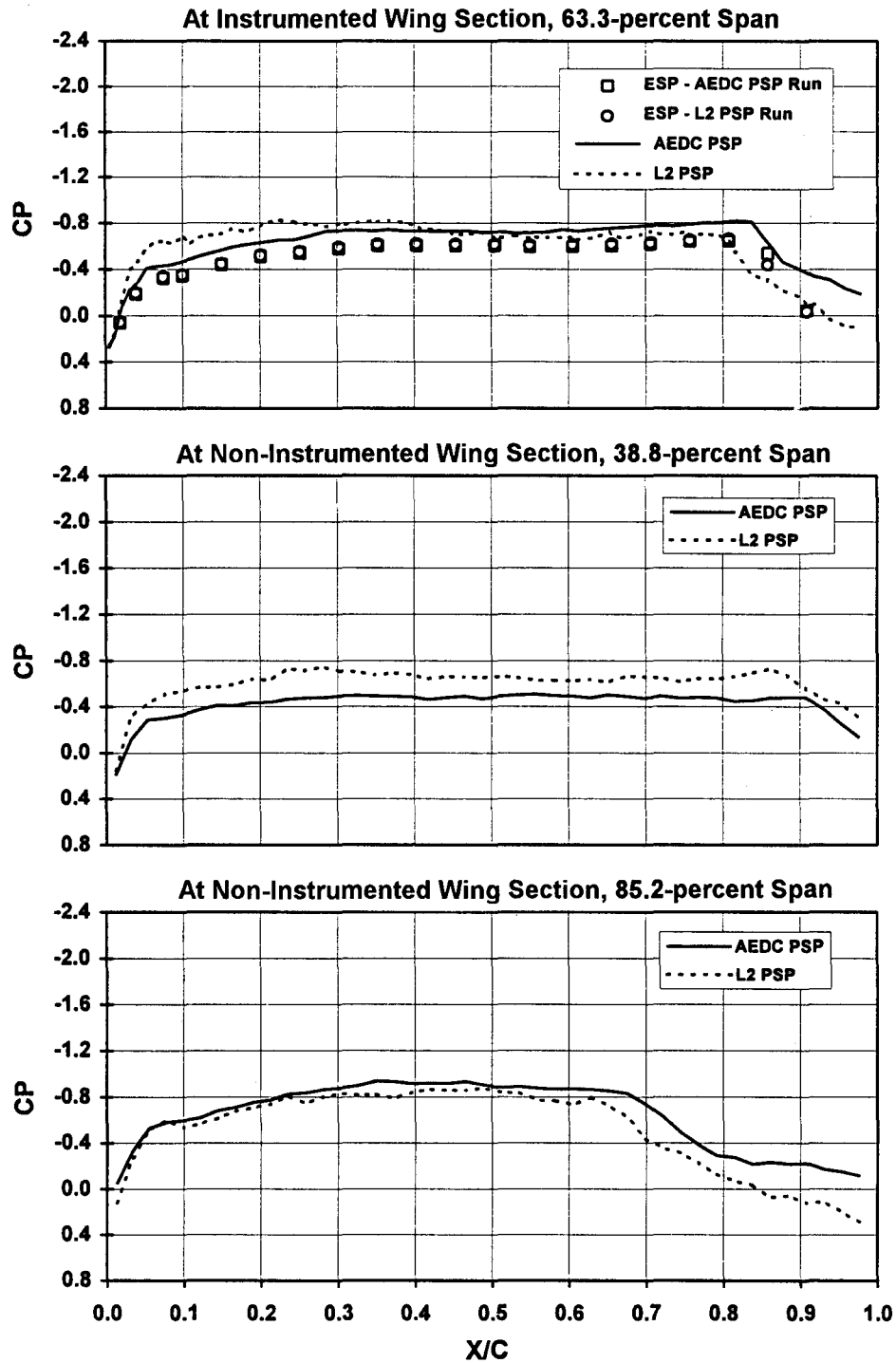
o. Mach = 0.85, Alpha = 6 deg, PT = 2,000 psfa, TT \approx 120°F

Figure 13. Continued.



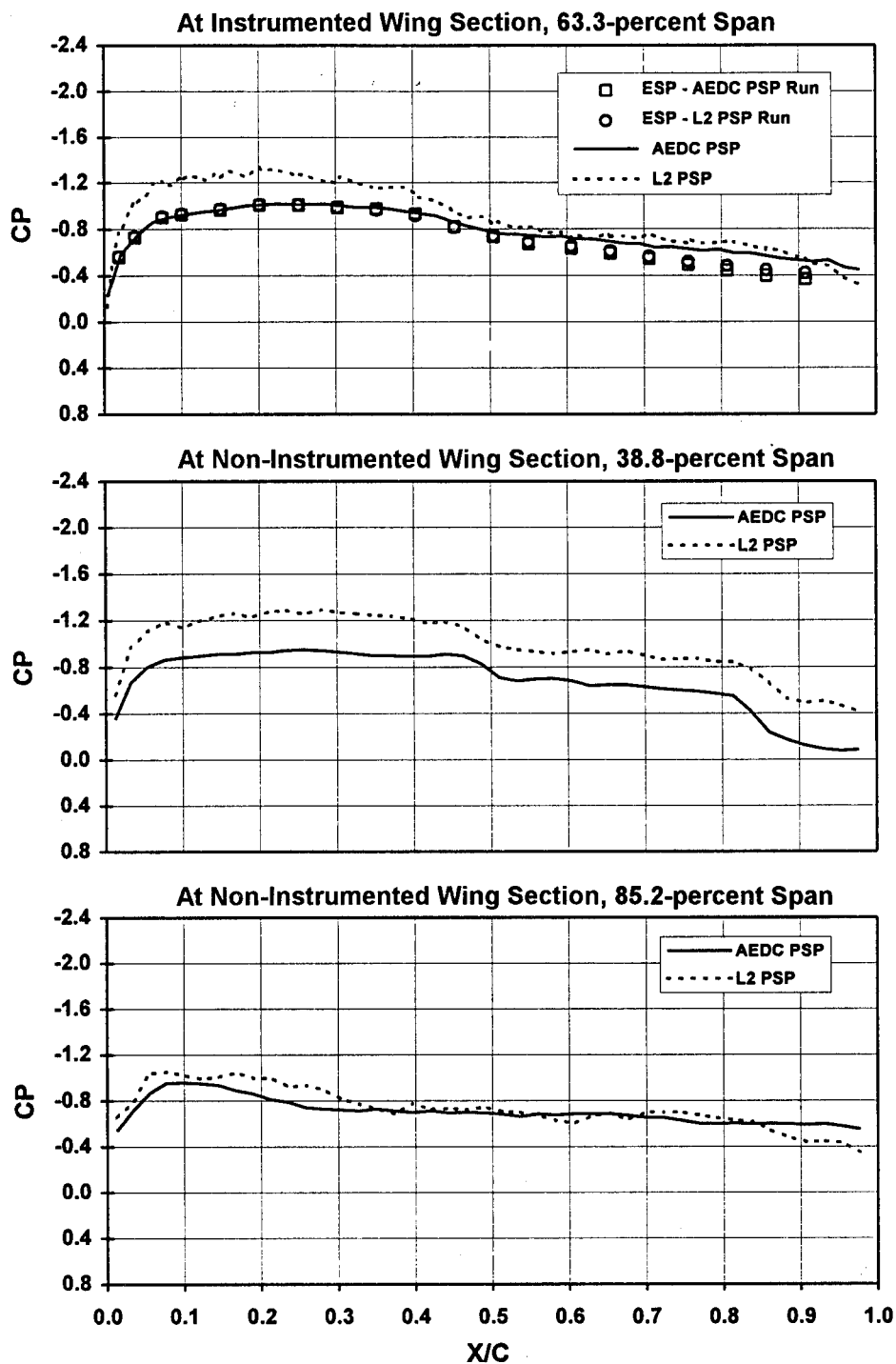
p. Mach = 0.95, Alpha = -8 deg, PT = 1,000 psfa, TT \approx 90°F

Figure 13. Continued.



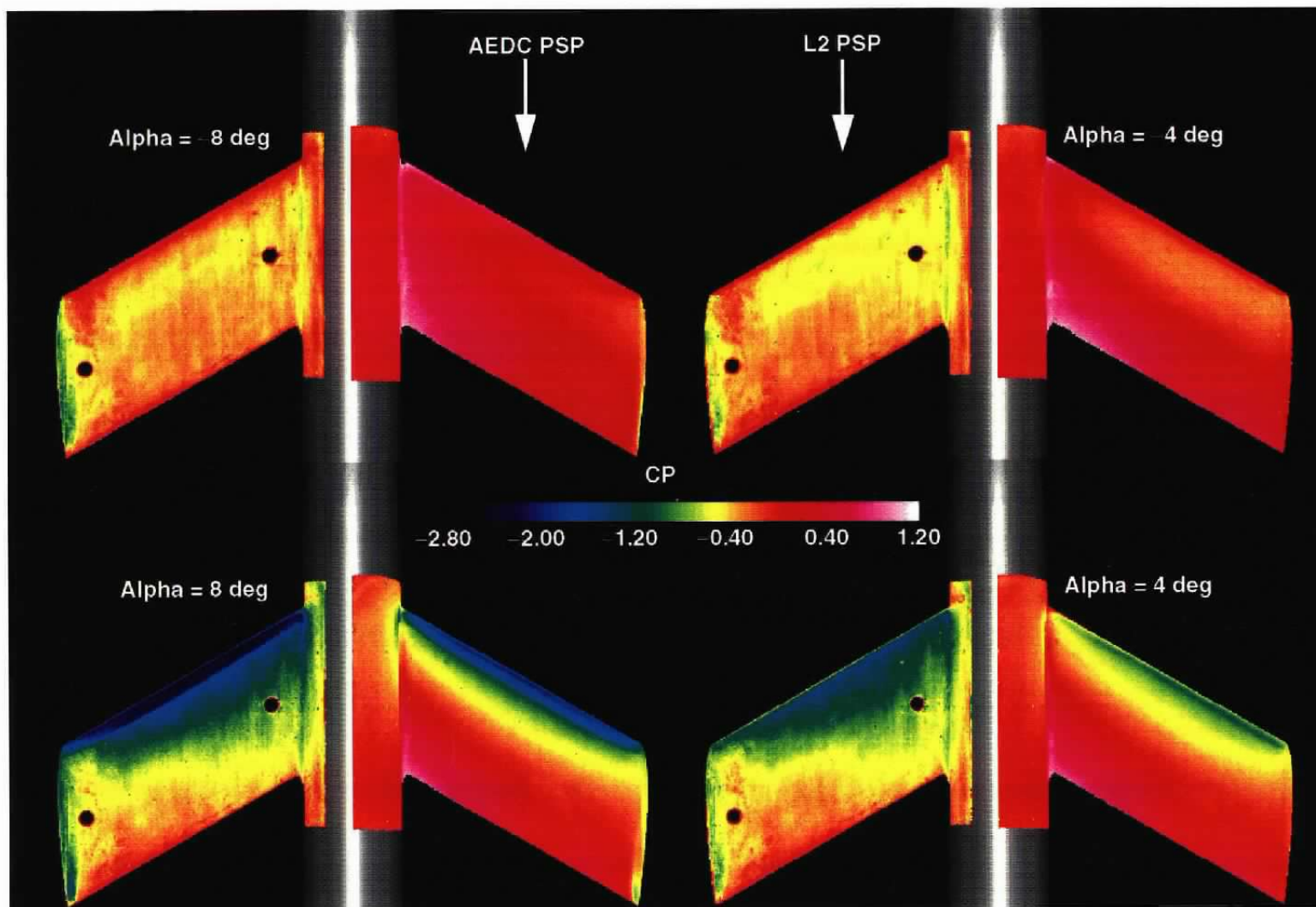
q. Mach = 0.95, Alpha = 0 deg, PT = 1,000 psfa, TT \approx 90°F

Figure 13. Continued.

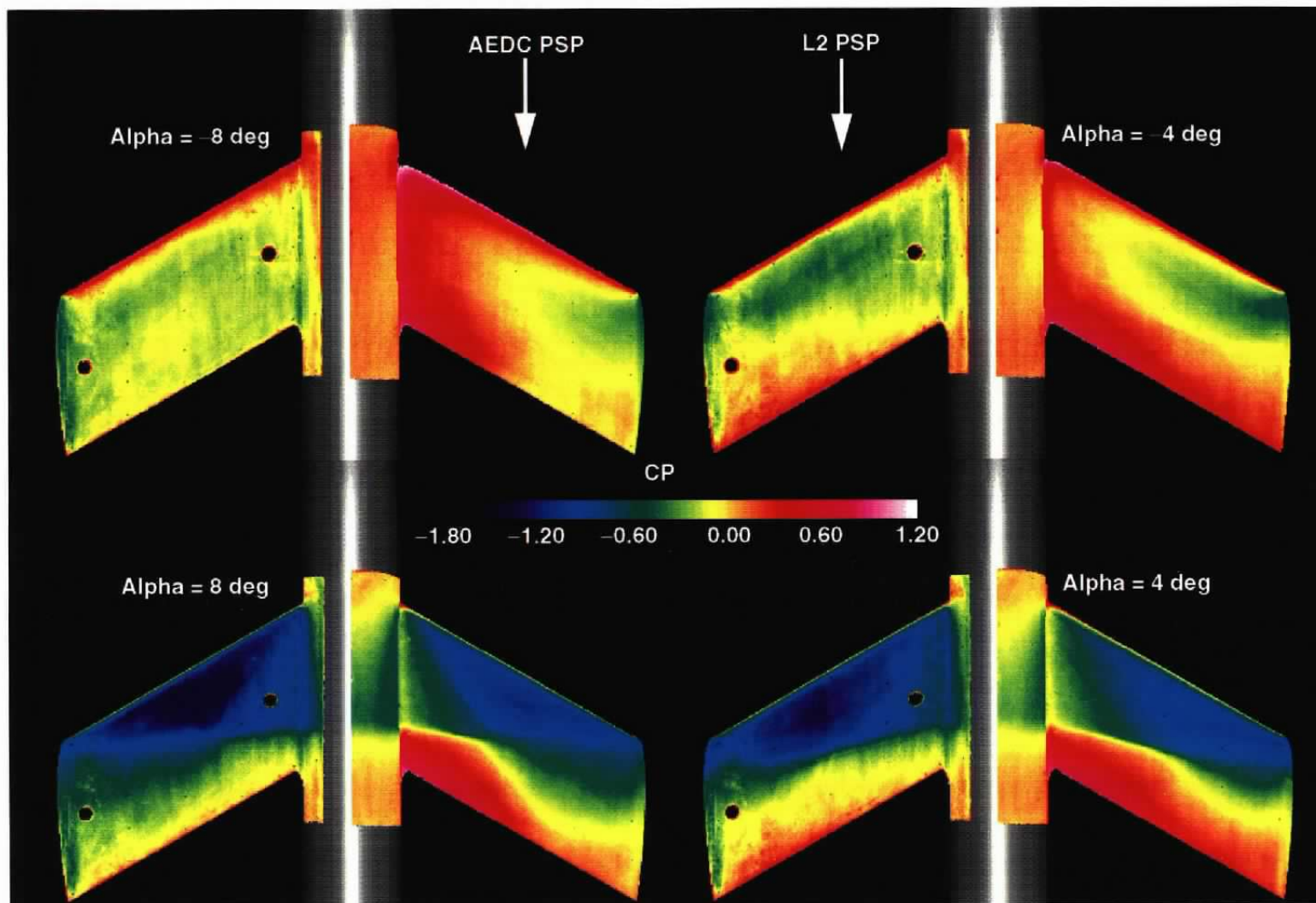


r. Mach = 0.95, Alpha = 8 deg, PT = 1,000 psfa, TT \approx 90°F

Figure 13. Concluded.

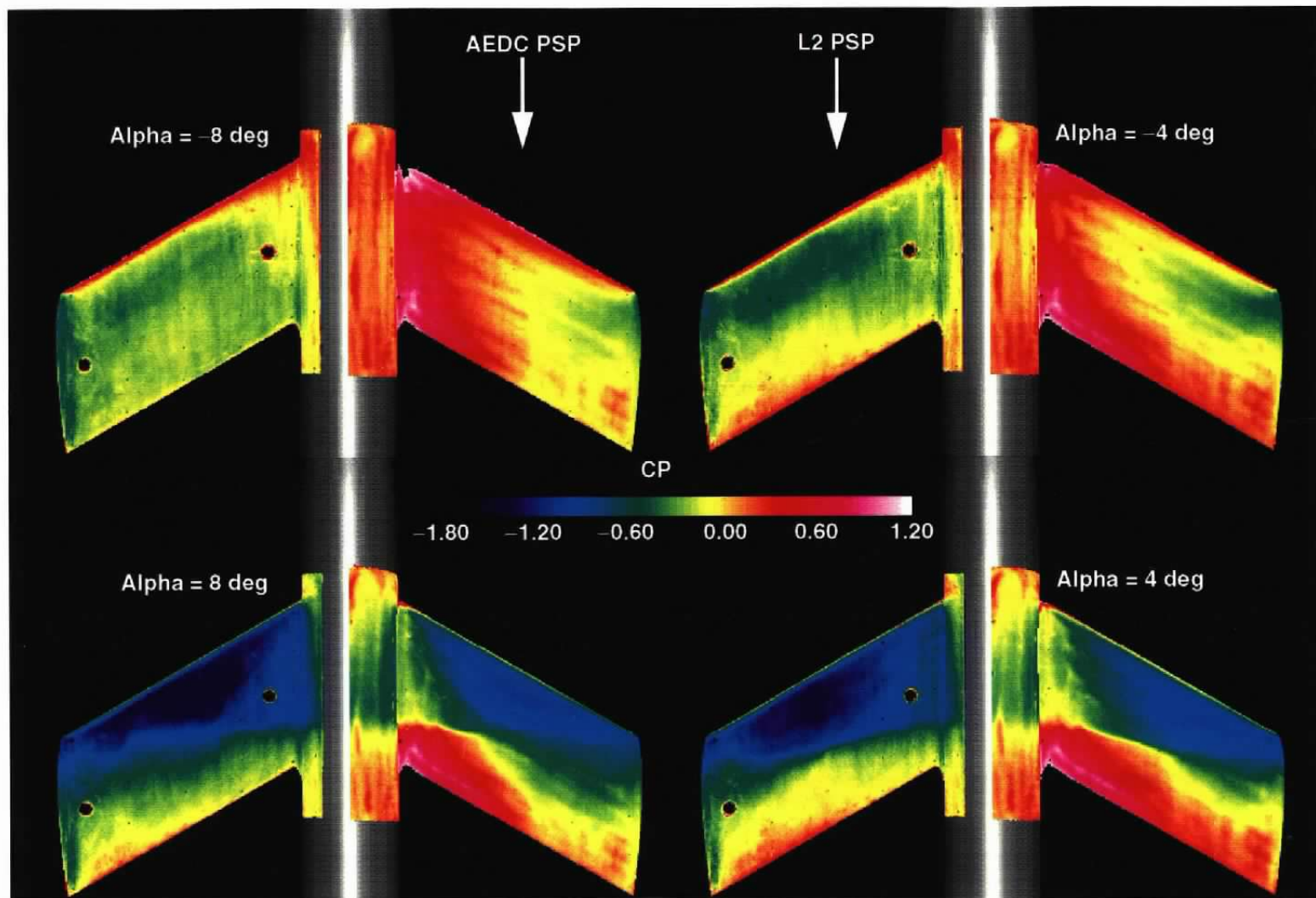


a. Mach = 0.6, PT = 1,000 psfa, TT \approx 90°F
 Figure 14. Pressure coefficient distribution comparison.



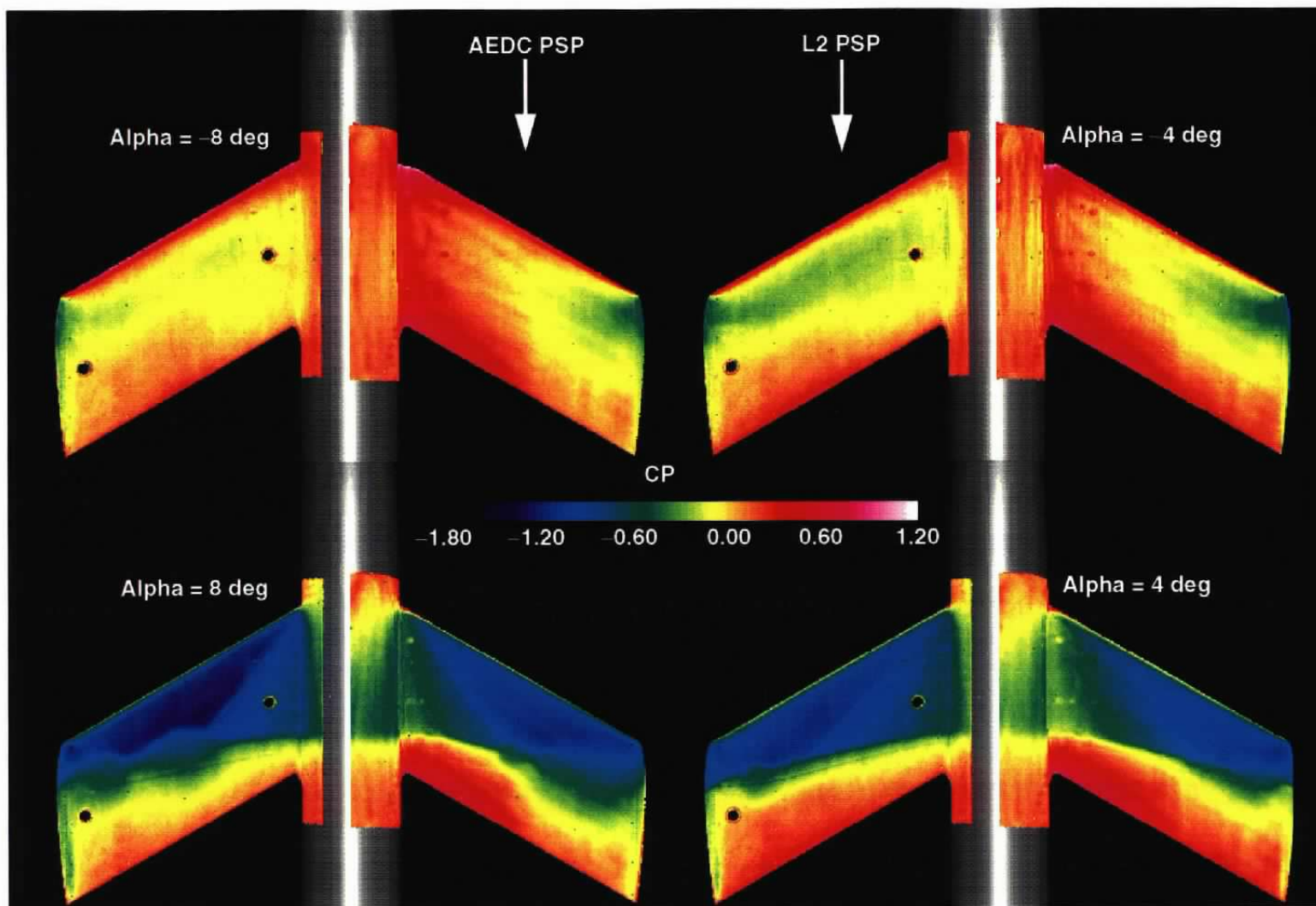
b. Mach = 0.85, PT = 1,000 psfa, TT \approx 90°F

Figure 14. Continued.



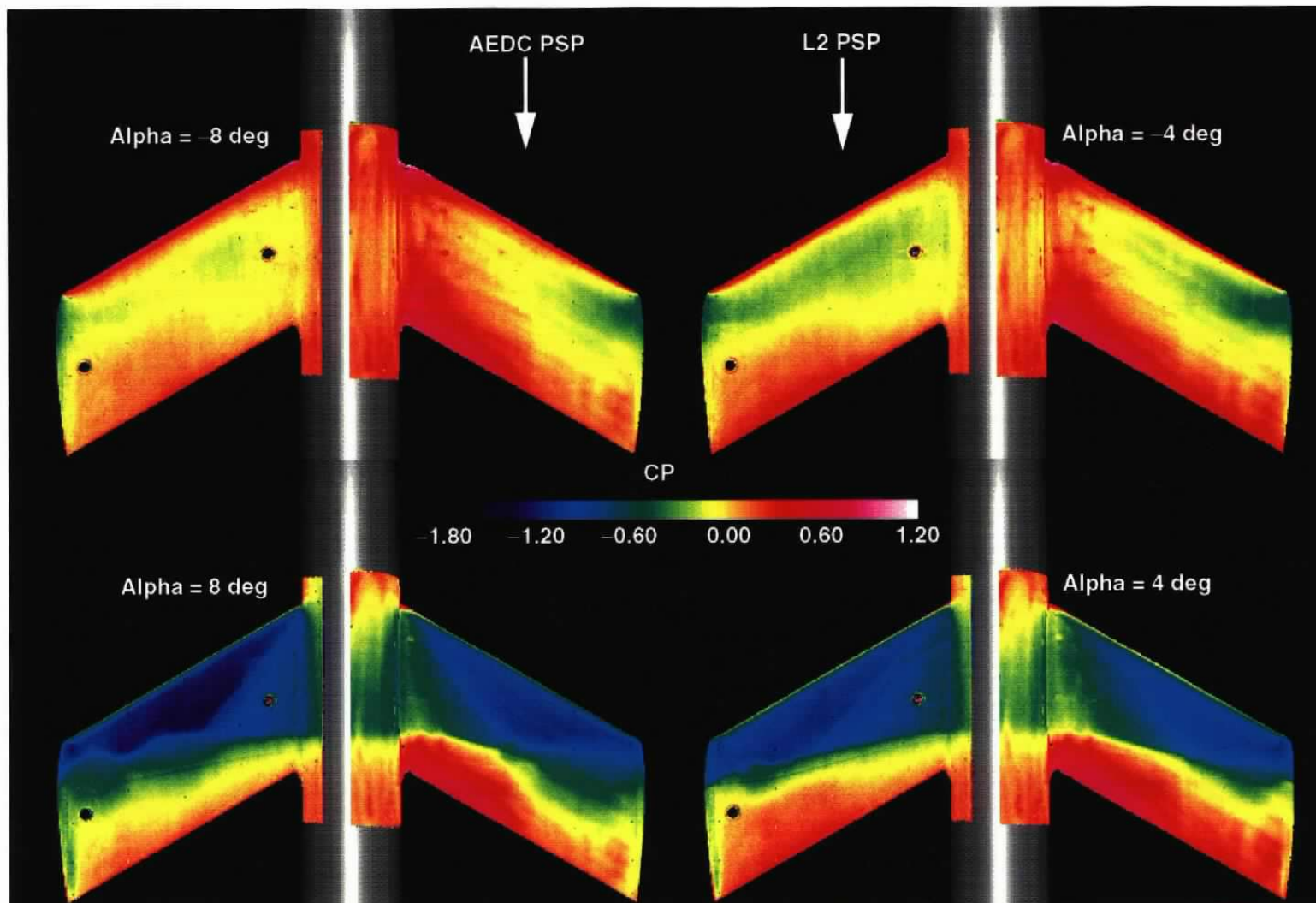
c. Mach = 0.85, PT = 1,000 psfa, TT \approx 120°F

Figure 14. Continued.



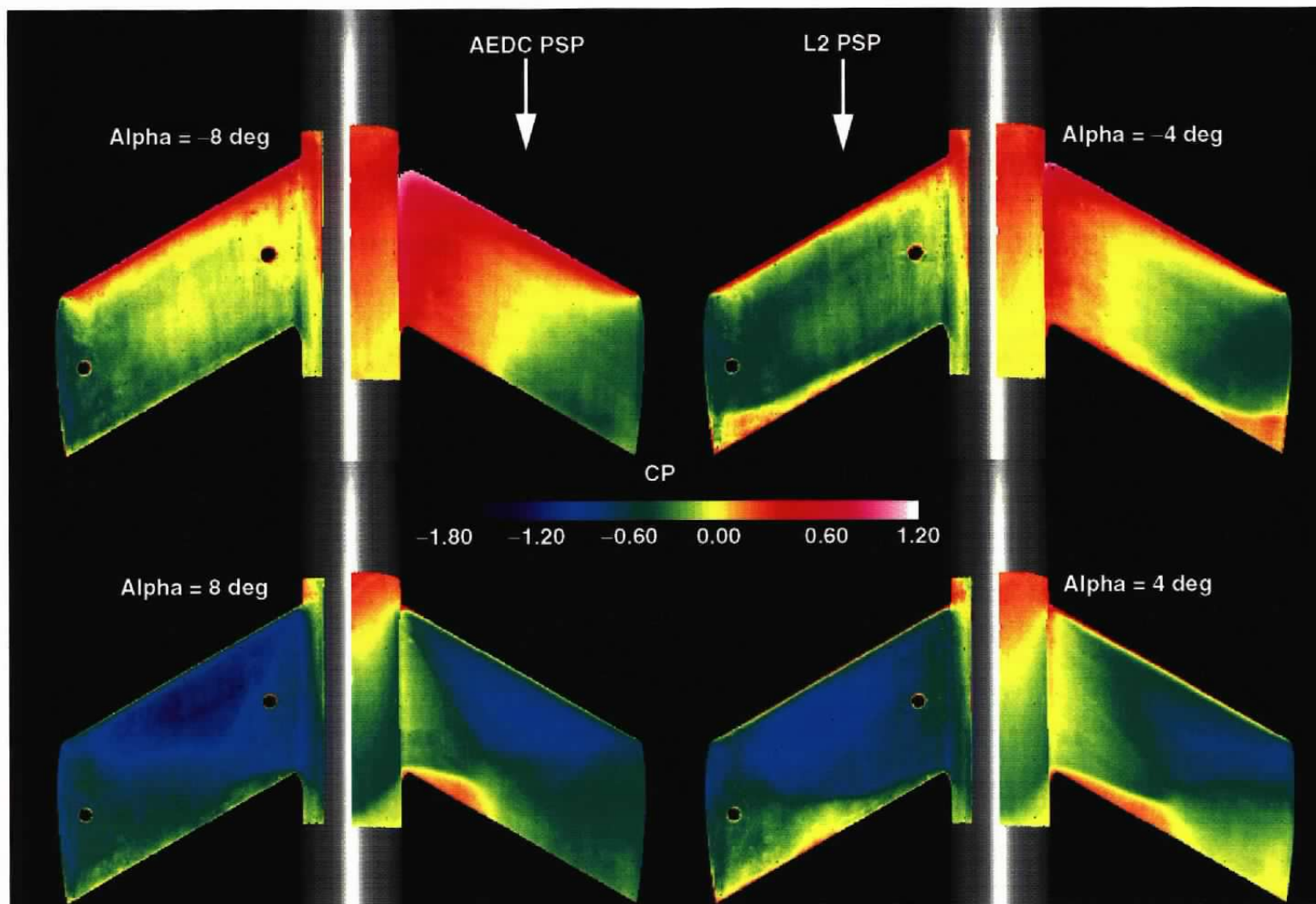
d. Mach = 0.85, PT = 2,000 psfa, TT \approx 90°F

Figure 14. Continued.



e. Mach = 0.85, PT = 2,000 psfa, TT ≈ 120°F

Figure 14. Continued.



f. Mach = 0.95, $P_T = 1,000$ psfa, $T_T \approx 90^\circ\text{F}$

Figure 14. Concluded.

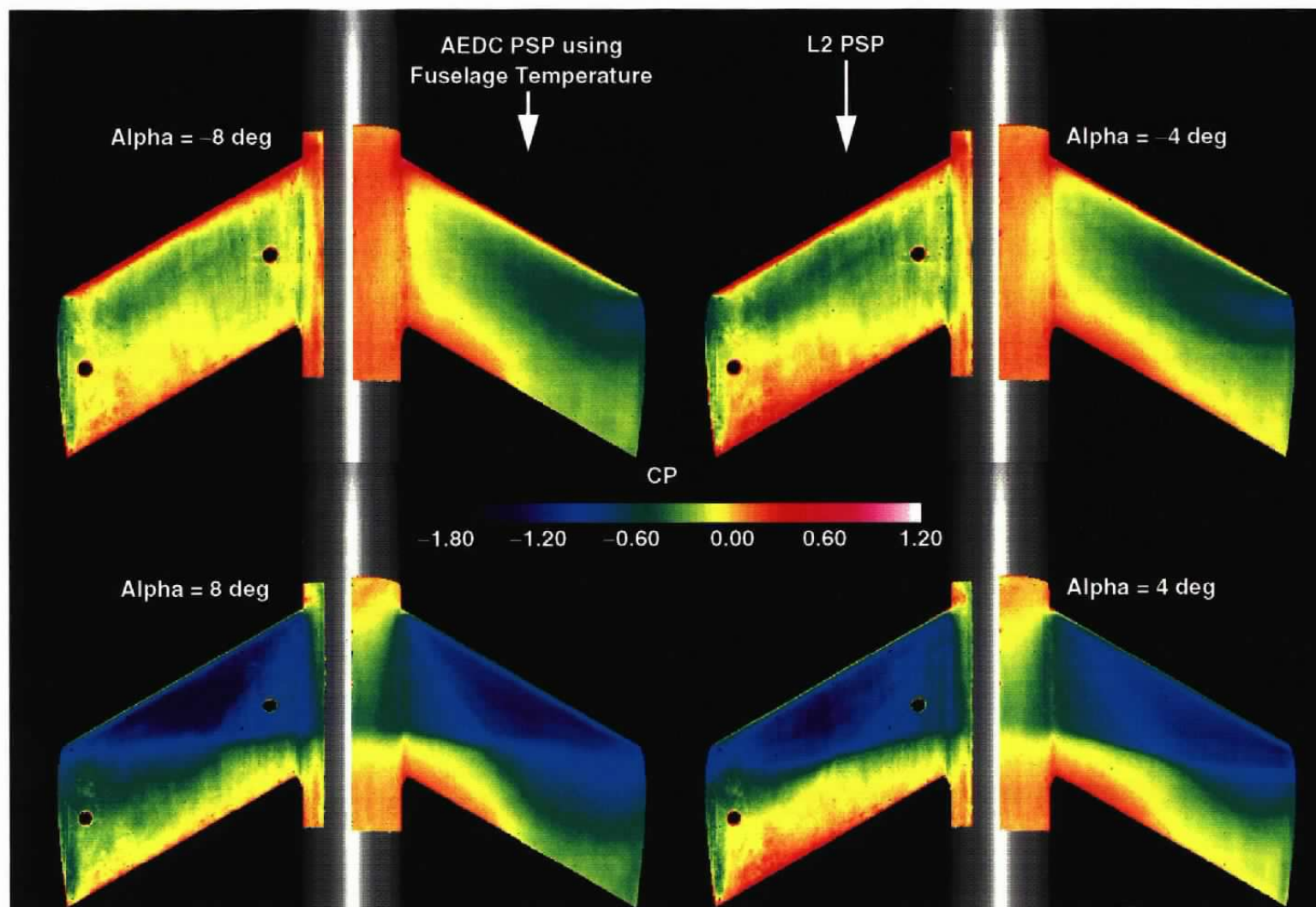


Figure 15. Comparison using fuselage temperature for the wing (AEDC PSP), Mach = 0.85, PT = 1,000 psfa, TT \approx 90°F.

Table 1. Pressure Orifice Designation and Location

Location	No.	F.S.	B.L.	W.L.
Fuselage	1	2.168	0.000	1.215
	2	4.332	0.000	1.864
	3	6.486	0.000	2.391
	4	8.661	0.000	2.866
	5	10.828	0.000	3.287
	6	12.991	0.000	3.636
	7	15.157	0.000	3.906
	8	17.322	0.000	4.122
	9	19.486	0.000	4.214
	10	21.650	0.000	4.275
	11	23.815	0.000	4.330
	12	25.975	0.000	4.330
	13	28.162	0.000	4.330
	14	30.326	0.000	4.330
	15	32.492	0.000	4.330
	16	34.655	0.000	4.330
	17	36.821	0.000	4.330
	18	38.988	0.000	4.330
	19	41.153	0.000	4.330
	20	43.319	0.000	4.330
	21	45.484	0.000	4.330
	22	47.644	0.000	4.330
	23	49.812	0.000	4.330
	24	51.974	0.000	4.330
	25	54.143	0.000	4.330
Wing	1	47.313	16.460	0.187
	2	46.520	16.425	0.279
	3	45.823	16.439	0.366
	4	45.080	16.445	0.446
	5	44.364	16.439	0.521
	6	43.632	16.450	0.590
	7	42.859	16.438	0.652
	8	42.154	16.432	0.709
	9	41.430	16.452	0.760
	10	40.685	16.470	0.802
	11	39.960	16.481	0.834

Location	No.	F.S.	B.L.	W.L.
Wing	12	39.213	16.478	0.856
	13	38.486	16.480	0.864
	14	37.744	16.489	0.855
	15	37.004	16.496	0.826
	16	36.277	16.478	0.769
	17	35.533	16.447	0.674
	18	35.174	16.476	0.608
	19	34.644	16.444	0.470
	20	34.337	16.444	0.335
	21	37.028	16.387	-0.826
	22	39.947	16.385	-0.834
	23	41.387	16.348	-0.760
	24	42.862	16.335	-0.652
	25	45.754	16.336	-0.366
Tail	1	71.217	9.947	0.081
	2	70.434	9.952	0.180
	3	69.993	9.958	0.221
	4	69.558	9.962	0.260
	5	69.115	9.964	0.298
	6	68.676	9.954	0.345
	7	68.250	9.956	0.381
	8	67.823	9.967	0.405
	9	67.381	9.970	0.437
	10	66.947	9.967	0.456
	11	66.489	9.960	0.469
	12	66.082	9.977	0.474
	13	65.190	9.973	0.448
	14	64.329	9.968	0.366
	15	63.630	9.945	0.174
	16	65.188	9.947	-0.488
	17	66.932	9.955	-0.489
	18	67.809	9.953	-0.446
	19	68.683	9.959	-0.389
	20	70.403	9.949	-0.225

Table 2. Nominal Test Conditions

Mach	PT, psfa	P _∞ , psfa	Q, psf	TT, °F	T _∞ , °F	Re × 10 ⁻⁶
0.60	1,000	784	198	90	54	1.60
0.85	1,000	624	315	90	32	1.96
0.85	1,000	624	315	120	48	1.83
0.85	2,000	1,247	631	90	22	3.92
0.85	2,000	1,247	631	120	48	3.66
0.95	1,000	560	353	90	7	2.05

Table 3. PSP Calibration Coefficients
a. AEDC PSP

a (V)	0	1	2	3
0	-2.4731E+02	-3.8429E+00	8.5561E-02	-3.5492E-04
1	3.1033E+03	2.9524E+01	-8.9414E-01	3.9988E-03
2	5.6287E+03	-1.5635E+02	1.4803E+00	-4.7194E-03

b. L2 PSP

a (V)	0	1	2
0	-1.1941E+03	5.4626E+00	-1.8030E-02
1	2.7159E+03	-7.9082E+00	2.4683E-03
2	1.5926E+03	-1.6064E+01	5.7678E-02

Table 4. Registration Mark Designation and Location
a. AEDC PSP Configuration

Number	F.S.	B.L.	W.L.
1	25.047	0.000	4.331
2	31.047	0.000	4.331
3	36.047	0.000	4.331
4	41.047	0.000	4.331
5	46.047	0.000	4.331
6	25.047	3.062	3.062
7	31.047	3.062	3.062
8	36.047	3.062	3.062
9	41.047	3.062	3.062
10	46.047	3.062	3.062
11	28.253	4.999	0.562
12	31.865	5.018	0.887
13	35.113	5.035	0.762
14	38.608	5.068	0.458
15	41.521	5.093	0.092
16	30.920	9.635	0.554
17	34.347	9.651	0.879
18	37.799	9.655	0.752
19	41.277	9.677	0.449
20	44.149	9.694	0.093
21	33.801	14.631	0.542
22	37.237	14.662	0.869
23	40.708	14.662	0.744
24	44.169	14.678	0.441
25	47.021	14.688	0.089
26	36.701	19.635	0.537
27	40.134	19.653	0.759
28	43.598	19.658	0.734
29	47.059	19.670	0.432
30	49.905	19.683	0.081
31	39.589	24.652	0.527
32	43.042	24.674	0.849
33	46.505	24.670	0.723
34	49.953	24.670	0.421
35	52.780	24.673	0.071

**Table 4. Concluded
a. L2 PSP Configuration**

Number	F.S.	B.L.	W.L.
1	26.047	3.062	3.062
2	31.047	3.062	3.062
3	36.047	3.062	3.062
4	41.047	3.062	3.062
5	46.047	3.062	3.062
6	28.253	4.999	0.562
7	31.665	5.018	0.887
8	35.113	5.035	0.762
9	38.608	5.068	0.458
10	41.521	5.093	0.092
11	30.920	9.635	0.554
12	34.347	9.651	0.879
13	37.799	9.655	0.752
14	41.277	9.677	0.449
15	44.149	9.694	0.093
16	33.801	14.631	0.542
17	37.237	14.662	0.869
18	40.708	14.662	0.744
19	44.169	14.678	0.441
20	47.021	14.688	0.089
21	36.701	19.635	0.537
22	40.134	19.653	0.759
23	43.598	19.658	0.734
24	47.059	19.670	0.432
25	49.905	19.683	0.081
26	39.589	24.652	0.527
27	43.042	24.674	0.849
28	46.505	24.670	0.723
29	49.953	24.670	0.421
30	52.780	24.673	0.071

NOMENCLATURE

a_{ij}	PSP calibration coefficients [see Eqs. (2) and (3)]
Alpha	Model angle of attack, deg
B.L.	Model buttock line, in.
CP	Surface pressure coefficient
F.S.	Model fuselage station, in.
I	Paint luminescence intensity at pressure, wind-on condition
I_0	Paint luminescence intensity in the absence of oxygen
I_{ref}	Paint luminescence intensity at reference pressure, wind-off condition
K_q	Stern-Volmer constant
Mach	Free-stream Mach number
P	Surface pressure at wind-on condition, psfa
P_{O_2}	Partial pressure of oxygen, psfa
P_{ref}	Surface pressure at wind-off condition, psfa
P_∞	Free-stream static pressure, psfa
PT	Tunnel stagnation pressure, psfa
Q	Free-stream dynamic pressure, psf
r	Temperature recovery factor [see Eq. (4)]
$Re \times 10^{-6}$	Free-stream unit Reynolds number, per foot
$T, T_{surface}$	Model surface temperature, °F

T_{∞}	Free-stream temperature, °F
TT	Tunnel stagnation temperature, °F
W.L.	Model water line, in.
X/C	Ratio of pressure orifice position (as measured from wing leading edge) to local chord
X/L	Ratio of pressure orifice position (as measured from fuselage orifice 12) to length between orifice 12 and 21